120
6-8-92 JS (2)

DOE/BC/14448-9
(DE92001045)

RESERVOIR HETEROGENEITY IN CARTER SANDSTONE, NORTH BLOWHORN CREEK OIL UNIT AND VICINITY, BLACK WARRIOR BASIN, ALABAMA

By
Ralph L. Kugler
Jack C. Pashin

May 1992

Performed Under Contract No. FG22-90BC14448

Geological Survey of Alabama
Tuscaloosa, Alabama

Bartlesville Project Office
U. S. DEPARTMENT OF ENERGY
Bartlesville, Oklahoma

DOE/BC/14448-9
Distribution Category UC-122

RESERVOIR HETEROGENEITY IN CARTER SANDSTONE, NORTH BLOWHORN CREEK OIL UNIT AND VICINITY, BLACK WARRIOR BASIN, ALABAMA

By
Ralph L. Kugler
Jack C. Pashin

DOE/BC/14448--9

DE92 001045

May 1992

Work Performed Under Contract No. DE-FG22-90BC14448

Prepared for
U.S. Department of Energy
Assistant Secretary for Fossil Energy

Chandra Nautiyal, Project Manager
Bartlesville Project Office
P. O. Box 1398
Bartlesville, OK 74005

Prepared by
Geological Survey of Alabama
Tuscaloosa, Alabama

CONTENTS

CONTENTS—CONTINUED

ILLUSTRATIONS

ILLUSTRATIONS—CONTINUED

ILLUSTRATIONS—CONTINUED

ILLUSTRATIONS—CONTINUED

EXECUTIVE SUMMARY

Additional oil remains to be produced from the Black Warrior basin using improved recovery strategies, such as waterflooding, injection, strategic well placement, and infill drilling. Characterizing heterogeneity provides information regarding how those strategies may be applied effectively. This report characterizes heterogeneity in the Mississippian (Chester) Carter sandstone reservoir in North Blowhorn Creek oil unit in Lamar County, Alabama, through sedimentologic, petrologic, and petrophysical analysis. In the first part of the report, a subsurface cross-section network is synthesized with lithofacies descriptions of cores to develop a depositional model for Carter sandstone in North Blowhorn Creek oil unit. In the second part, the detrital and diagenetic framework of the Carter reservoir is described and interpreted. This is followed by an evaluation of commercial porosity and permeability data and of the results of high-pressure mercury porosimetry. In the final part, results are synthesized with a five-level classification of reservoir heterogeneity in order to assess heterogeneities that may affect recoverability of oil in the Black Warrior basin.

North Blowhorn Creek oil unit currently is under waterflood and has 31 producing wells and 18 water-injection wells. Cumulative production through December 1990 was 4,832,247 bbls of oil, 2,781,598 Mcf of gas, and 4,488,217 bbls of water. This production represents 33 percent of the original oil in place and 67 percent of the total oil produced from the Black Warrior basin of Alabama. The Carter sandstone in North Blowhorn Creek oil unit is part of an isolated, northwest-southeast trending sandstone body that is enclosed in shale. The Carter oil reservoir in North Blowhorn Creek oil unit is contiguous with the Carter gas reservoir in the adjacent Armstrong Branch gas field to the northwest. The trapping mechanism for hydrocarbons in the combined North Blowhorn Creek oil unit/Armstrong branch gas field is stratigraphic, defined by pinchout of Carter sandstone.

Resistivity-log cross sections show that the Carter reservoir is internally complex, but varies systematically and predictably. The sandstone body has a sublinear northeast margin and an irregular southwest margin and is locally thicker than 40 feet along the axis of the body, near the northeast margin. The sandstone is not a single, homogeneous reservoir, but comprises a series of shingled, clinoformal lenses that dip southeast and decrease in size toward the southeastern terminus of the sandstone body. Downdip parts of the reservoir have a blocky signature with high resistivity, reflecting the highest quality reservoir. Along the axis of the sandstone body, near the downdip margin, lenses are commonly amalgamated. Updip, lenses have a serrate pattern and resistivity decreases toward the southwest, reflecting decreased reservoir quality.

Cores of Carter sandstone typically have a tripartite sequence, including from bottom to top, (1) a shale-and-siltstone facies, (2) a sandstone facies, and (3) a variegated facies. The shale-and-siltstone facies is interpreted to represent a storm-dominated shelf mud blanket that prograded across the Bangor carbonate platform. The sandstone facies, which is the principal Carter oil reservoir, represents a spectrum of beach and shoreface environments. The variegated facies, which contains lenticular sandstone, siltstone, and shale, was deposited in a suite of backshore environments which were dominated by storm surges. Sandstone-body geometry and depositional sequences indicate that the Carter sandstone in North Blowhorn Creek oil unit represents a southwestward-accreting spit complex that was part of a muddy strand plain that developed on a former carbonate platform, just beyond the limit of major delta progradation.

Carter sandstone dominantly is very fine-grained quartzarenite, containing locally abundant, intrabasinally derived shale fragments and skeletal debris. Because of the quartzose nature of the sandstone, provenance, based on petrographic criteria, is equivocal. Authigenic minerals in Carter sandstone include, in approximate order of formation, siderite, calcite, ferroan calcite, quartz, ferroan dolomite/ankerite, and kaolinite. Pressure-solution features include stylolites along shale laminae and wispy microstylolites on foresets of ripple laminae. Hydrocarbon migration postdated precipitation of kaolinite. Authigenic minerals in Carter sandstone reflect a diagenetic evolution that began shortly after burial and continued through deep burial (>10,000 ft) and subsequent uplift to present burial depths of about 2,300 feet.

The pore system of Carter sandstone consists of effective, intergranular macropores and ineffective micropores among detrital and authigenic clay particles. Authigenic carbonate minerals

occlude all pores only in the vicinity of accumulations of skeletal debris in shoreface sandstone and calcite cement is restricted to these accumulations, suggesting that carbonate-dissolution porosity is not widespread in the reservoir. Similarly, secondary pores formed by dissolution of aluminosilicate framework grains did not enhance effective porosity because products of dissolution were redistributed locally as kaolinite.

Commercial core analyses reveal poor correlations between porosity and permeability in Carter reservoir sandstone. Average porosity of reservoir sandstone is 12 percent, and average air permeability is 6.82 millidarcies. Capillary-pressure data derived from high-pressure mercury porosimetry show that pore-throat-distributions in Carter sandstone are polymodal owing to a mixture of pore types. Median pore-throat size and pore-throat size distributions are highly variable in nonreservoir sandstone and siltstone, but are relatively uniform in very fine-grained reservoir sandstone where the median pore-throat radius typically is between 0.7 to 2 μm. Fine-grained sandstone is not common, but occurs in some foreshore deposits where median pore-throat radius is between 3 and 7 μm. Fine-grained sandstone is more permeable, by an order of magnitude or more, than very fine-grained sandstone, even though porosity is similar. Petrographic observations and pore-throat size distributions indicate that fine-grained sandstone has fewer clays than very fine-grained sandstone, in addition to having larger pore throats.

Synthesis of sedimentologic, petrologic, and petrophysical observations with heterogeneity models indicates several levels of heterogeneity in the Carter sandstone reservoir in North Blowhorn Creek oil unit. At the highest level, the reservoir is vertically and laterally confined by impermeable shale, suggesting that improved recovery operations, such as injection, could utilize the margins of the reservoir to confine flow and direct migration of oil toward desired extraction points. Near the downdip margin of the sandstone body, amalgamated shoreface and foreshore sandstone lenses clearly join to form a single flow unit that is continuous among wells along the axis of the reservoir. Updip, where facies changes are most pronounced, separate lenses of reservoir sandstone typically do not extend between wells and merge into nonreservoir, backshore siltstone and shale. This fundamental facies anisotropy suggests fluids may be transmitted more easily along the axis of the sandstone body than perpendicular to the axis. Bedform distribution within reservoir sandstone is also affected by facies anisotropy. Shoreface and foreshore bars probably prograded shoreward only tens of feet, but extended hundreds or thousands of feet along depositional strike.

Lenses of fine-grained sandstone, although sparse and not laterally extensive, are more permeable than adjacent very fine-grained sandstone. These lenses form permeability contrasts that affect sweep efficiency by focusing flow into the most permeable intervals. Accumulations of skeletal debris localized zones of pervasive calcite and ferroan dolomite/ankerite cement that form barriers to vertical fluid flow that do not extend between wells. Within shoreface sandstone, convergence of anastomosing clay laminae and clay drapes on ripple foresets increases tortuosity of flow and impounds minor amounts of oil during enhanced recovery operations. Clay minerals in Carter sandstone have high ratios of surface area to volume and likely contain immobile water, which affects calculation of water saturation from resistivity logs. Well-log based interpretations of reservoir parameters should acknowledge the presence of both structural and dispersed clays in the sandstone. The distribution of kaolinite in Carter sandstone poses a potential migration-of-fines problem during improved-recovery operations.

The localized, lensoid nature of Carter sandstone reservoirs differs greatly from the widespread beach-barrier sandstone bodies that have formed the basis of previous sandstone-heterogeneity models. Therefore, results of this study provide a template for recognizing heterogeneity that will be useful in implementing improved-recovery strategies, not only for oil reservoirs in the Black Warrior basin, but in other sedimentary basins as well.

ABSTRACT

Additional oil remains to be produced from the Black Warrior foreland basin using improved recovery strategies, and characterizing reservoir heterogeneity provides information necessary to utilize these strategies effectively. This report characterizes heterogeneity in the Upper Mississippian (Chesterian) Carter sandstone reservoir in North Blowhorn Creek oil unit, the most productive oil reservoir in the Black Warrior basin of Alabama.

Sandstone-body geometry and depositional sequences determined from subsurface cross sections and cores indicate that the Carter sandstone in North Blowhorn Creek oil unit represents a spit system that was preserved as part of a muddy, delta-destructive strand plain. The Carter sandstone is not a homogeneous reservoir, but consists of a series of shingled, southeast dipping clinoformal lenses that decrease in size toward the southeastern terminus of the reservoir body. Near the downdip margin of the reservoir, amalgamated shoreface and foreshore sandstone lenses join to form a single flow unit that is continuous along the axis of the reservoir body. Updip lenses of reservoir sandstone are separated by shale and merge into nonreservoir, backshore siltstone and shale. As a result of this facies anisotropy, fluids may be transmitted more easily along the axis of the sandstone body than perpendicular to the axis.

Although Carter sandstone is quartzarenite, authigenic kaolinite and intrabasinal shale clasts and skeletal debris affect the quality of the reservoir. Accumulations of skeletal debris in shoreface sandstone localize zones of pervasive calcite and ferroan dolomite/ankerite cement that form barriers to vertical fluid flow and do not extend between wells. Pore-throat-size distributions determined by high-pressure mercury porosimetry are polymodal owing to a mixture of effective, intergranular macroporosity and ineffective microporosity between particles of detrital and authigenic clay. Median pore-throat size is relatively uniform in very fine-grained shoreface sandstone, but subtle interwell heterogeneity exists where local lenses of fine-grained foreshore sandstone occur. This sandstone is more permeable because clay is less abundant and pore throats are larger than those in adjacent very fine-grained sandstone. These lenses form permeability contrasts that affect sweep efficiency by focusing flow into the most permeable intervals. The abundance of detrital and authigenic clay in very fine-grained sandstone may affect interpretation of water saturation from resistivity logs and result in a migration-of-fines problem during improved-recovery operations.

Because the localized, lensoid nature of Carter sandstone reservoirs differs greatly from the widespread beach-barrier sandstone bodies that have formed the basis of previous sandstone-heterogeneity studies, results of this study provide a template for recognizing heterogeneity that will be useful for implementing improved-recovery strategies, not only for oil reservoirs in the Black Warrior basin, but in other sedimentary basins as well.

ABBREVIATIONS

API	-	American Petroleum Institute
bbls	-	Barrels
BOPD	-	Barrels of oil per day
BOPM	-	Barrels of oil per month
cm	-	Centimeters
ft	-	Feet
g	-	Grams
kV	-	Kilovolts
Mcf	-	Thousand cubic feet
ml	-	Milliliters
mm	-	Millimeters
nA	-	Nannoamps
psia	-	Pounds per square inch absolute
R	-	Correlation coefficient
µm	-	Micrometers
PN3150	-	Permit Number 3150
-1,750	-	Subsea true vertical depth
2,235	-	Measured depth

INTRODUCTION

OBJECTIVES

Oil production in the Black Warrior basin has declined in recent years although much additional oil may be producible utilizing improved recovery strategies, such as waterflooding, injection, strategic well placement, and infill drilling. High-quality reservoir characterization and reliable criteria for recognition of the types and scale of reservoir heterogeneity are crucial to development of effective enhanced recovery strategies, because reservoirs typically contain numerous features at megascopic, macroscopic, mesoscopic, and microscopic scales that affect fluid flow (Weber, 1986). The objectives of this project are to augment the National Reservoir Database (TORIS Database), to develop models of reservoir heterogeneity, and to identify oil resources that are producible at reasonable cost, thereby increasing recovery of hydrocarbons from Carboniferous sandstone reservoirs in the Black Warrior foreland basin. These objectives are being achieved through detailed geological, engineering, and geostatistical investigations of Carboniferous sandstone reservoirs in the basin. Such studies will be used to develop and test the effectiveness of geological and mathematical models for predicting the effects of reservoir heterogeneity on recovery of hydrocarbons.

This report presents accomplishments made in completing Task 3 of this project which involves development of criteria for recognizing reservoir heterogeneity in the Black Warrior basin. The report focuses on characterization of the Upper Mississippian Carter sandstone reservoir (fig. 1) in North Blowhorn Creek and adjacent oil units in Lamar County, Alabama (fig. 2). This oil unit has produced more than 60 percent of total oil extracted from the Black Warrior basin of Alabama. The Carter sandstone in North Blowhorn Creek oil unit is typical of the most productive Carter oil reservoirs in the Black Warrior basin of Alabama. The first part of the report synthesizes data derived from geophysical well logs and cores from North Blowhorn Creek oil unit to develop a depositional model for the Carter sandstone reservoir. The second part of the report describes the detrital and diagenetic character of Carter sandstone utilizing data from petrographic and scanning electron microscopes and the electron microprobe. The third part synthesizes porosity and pore-throat-size-distribution data determined by high-pressure mercury porosimetry and commercial core analyses with results of the sedimentologic and petrographic studies.

The final section of the report discusses reservoir heterogeneity within the context of the five-fold classification of Moore and Kugler (1990) (fig. 3). Although most heterogeneity classifications are based on observational scale, the classification of Moore and Kugler (1990) is particularly useful because each scale, or observational level, is related to practical reservoir and drilling parameters. According to this classification, the first and broadest level of heterogeneity (level-1) is the reservoir, namely a body of permeable reservoir rock surrounded by impermeable nonreservoir rock. Level-2 heterogeneity represents features within a reservoir rock body that restrict fluid flow and occur among two or more wells, whereas level-3 heterogeneity, or interwell heterogeneity, represents features that have an areal extent less than the average well spacing in an oil field. Level-4 heterogeneity represents variation that occurs at the scale of a core or wellbore, and level-5 heterogeneity occurs at the microscopic scale of pores and pore throats. The scales of observation used in this classification generally correspond to the megascopic, macroscopic, mesoscopic, and microscopic scales employed by Lake and others (1991).

Synthesis of sedimentologic, petrologic, and petrophysical data from this study and from investigations of outcrop exposures of reservoir units in the Black Warrior basin (Pashin and others, 1991) within the context of the heterogeneity classification (fig. 3) provides a basis for evaluating reservoir exploitation approaches necessary to recover the remaining mobile oil and of ongoing enhanced recovery projects in the basin to be completed in Tasks 5 and 6 of this project. The results also provide input data for mathematical methodologies to be used for reservoir modeling in Task 7.

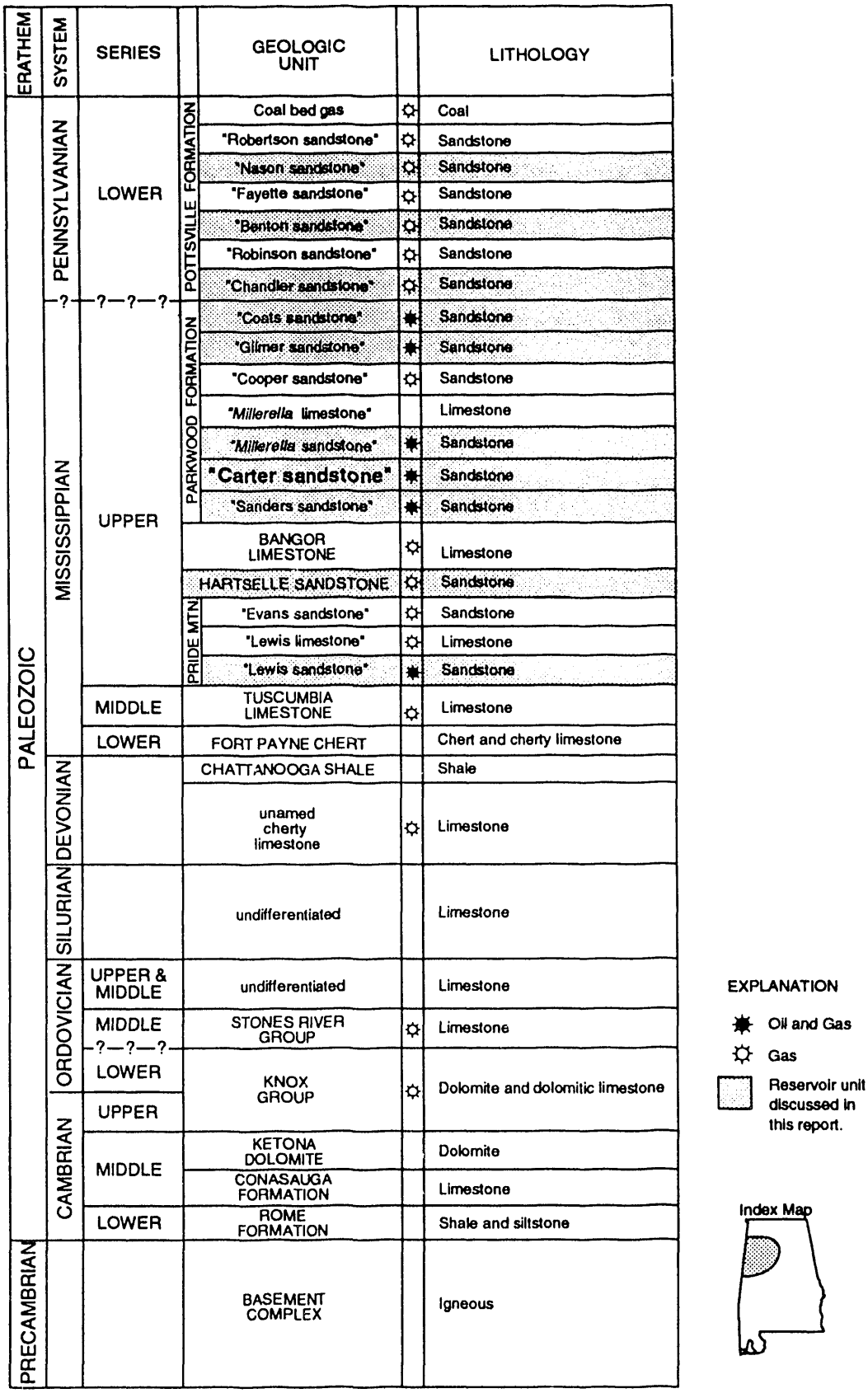

Figure 1.--Stratigraphic column showing petroleum reservoirs in the Black Warrior basin.

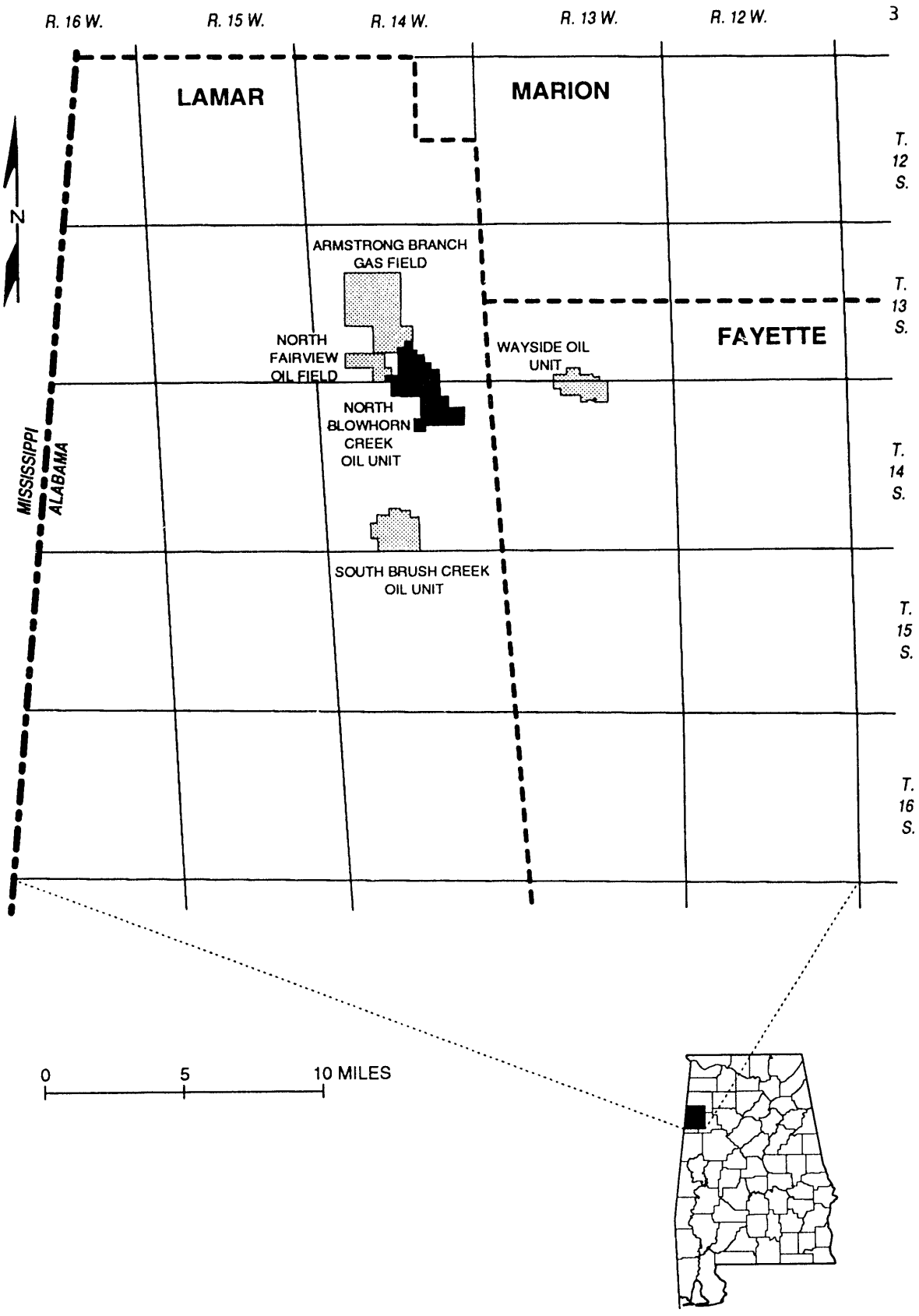

Figure 2.--Index map showing location of the North Blowhorn Creek oil unit and selected fields and units.

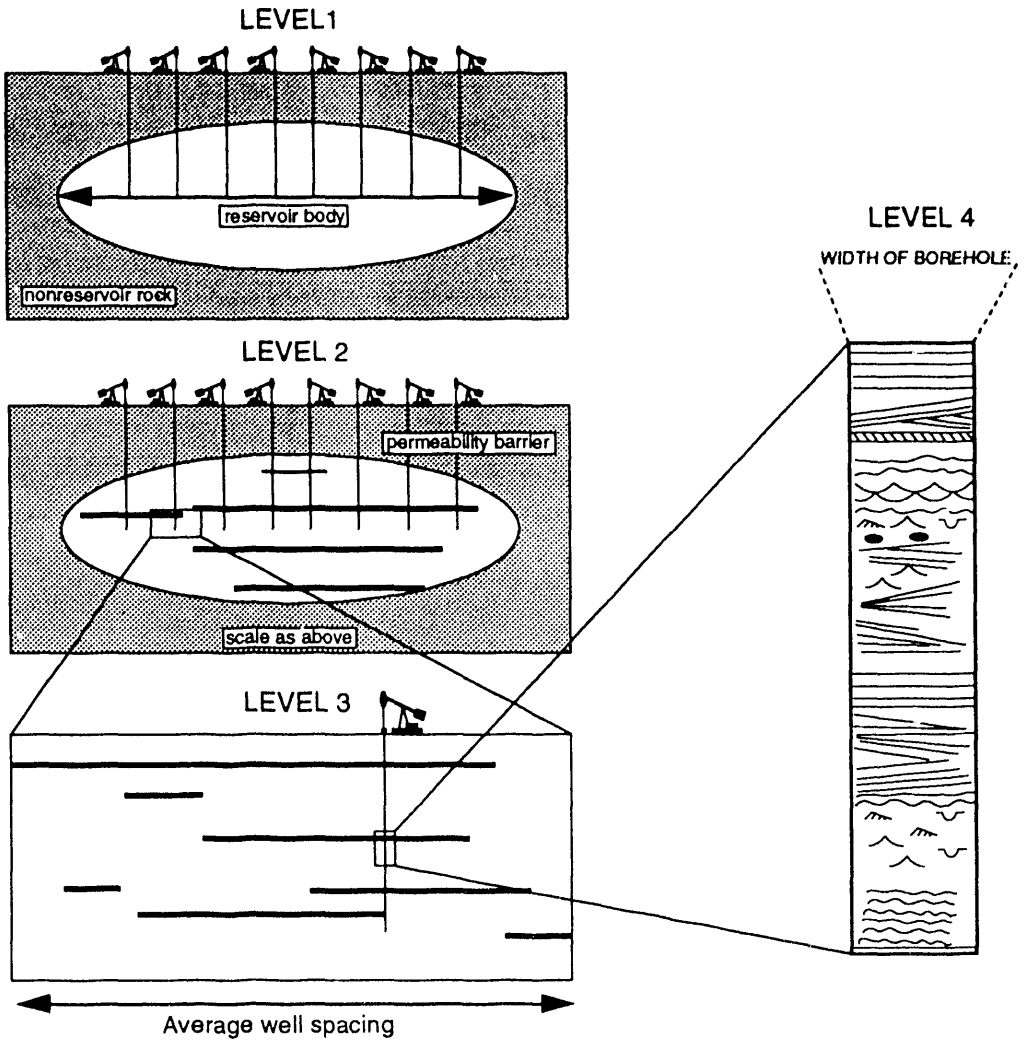

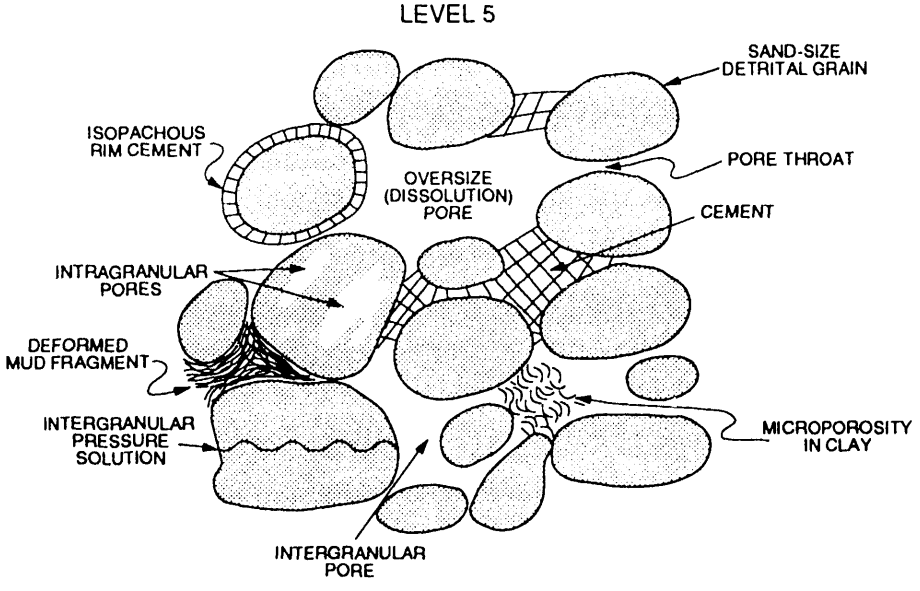

Figure 3.--Levels of heterogeneity (modified from Moore and Kugler, 1990).

REGIONAL GEOLOGIC SETTING OF THE BLACK WARRIOR BASIN

STRUCTURAL AND TECTONIC SETTING

The Black Warrior basin (fig. 4) is an asymmetric, triangular sedimentary basin in Alabama and Mississippi that is bounded on the north by the Nashville dome, on the southeast by the Appalachian orogen, and on the southwest by the Ouachita orogen (Mellen, 1947; Thomas, 1988a, b). The Black Warrior basin is separated from the Arkoma basin to the west by the Mississippi Valley graben, but is contiguous with the Appalachian basin to the northeast (Thomas, 1988b). The basin is located on the Alabama promontory, a pre-orogenic protuberance of the continental margin where tectonic activity was concentrated (Thomas, 1977, 1991). The Black Warrior basin is a Late Paleozoic foreland basin that formed as a flexural response to sediment and tectonic loading by Alleghanian thrust sheets in the Appalachian-Ouachita orogen (Beaumont and others, 1987, 1988; Hines, 1988).

Paleozoic strata crop out only in the eastern part of the Black Warrior basin in Alabama and northeastern Mississippi; two-thirds of the basin is buried beneath Cretaceous and younger strata of the Gulf Coastal Plain. Upper Cretaceous strata, chiefly the Coker and Gordo Formations of the Tuscaloosa Group, disconformably overlie Paleozoic strata. Adjacent to the deeply buried Ouachita orogen in Mississippi, Mesozoic and Cenozoic rocks are more than 6,000 feet thick.

Normal faults predominate throughout most of the Black Warrior basin and are closely spaced in Fayette and Lamar Counties, where the most productive oil reservoirs occur (fig. 5). These faults define a generally northwest-trending series of parallel, linear to arcuate horst-and-graben systems that turn westward in Mississippi. In eastern Pickens County, however, several contours turn sharply northward and mark a hinge zone to the east of several arcuate faults. The faults define a series of narrow grabens in Lamar and Pickens Counties that extend for tens of miles and locally have throw in excess of 1,000 feet.

Faults in the Black Warrior basin parallel the Ouachita orogenic belt, and displacement increases toward the orogenic front. The faults appear to have formed extensionally as a response to thrust loading in the Ouachita orogen and related subsidence of the foreland basin (Hines, 1988). Synsedimentary movement of the faults during the Carboniferous reflects sequential changes in basin geometry that occurred in response to episodic thrusting in the Appalachian and Ouachita orogens (Pashin, 1991).

The absence of Triassic and Jurassic strata in the Black Warrior basin makes the post-Alleghanian structural history of the basin uncertain. Extensional faulting may have continued during the Mesozoic, but clearly ceased before Late Cretaceous because normal faults do not displace Upper Cretaceous strata (Pashin, 1991). Southwestward tilting of the basin has occurred since the Late Cretaceous (Kidd, 1976; Klitgord and others, 1983; Thomas, 1985; Pashin, 1991). Extensional tectonics related to opening of the Gulf of Mexico and subsidence of the Mississippi Embayment are considered the major causes of tilting and burial of the western part of the Black Warrior basin.

STRATIGRAPHIC SETTING

The Paleozoic stratigraphic succession in the Black Warrior basin can be divided into two parts: a carbonate-dominated Cambrian to Lower Mississippian sequence and a clastic-dominated Mississippian-Pennsylvanian sequence. Cambrian to Lower Mississippian rocks were deposited on a shallow-marine shelf, reflecting deposition in a passive-margin setting (Thomas, 1988a). Strata of the younger, southwestward-thickening Mississippian to Pennsylvanian clastic wedge were deposited in a spectrum of terrestrial to open-marine environments as the Black Warrior foreland basin evolved.

Upper Mississippian strata are the most productive oil reservoirs in the Black Warrior basin of Alabama (fig. 6). Oil-producing units include the Lewis sandstone of the Pride Mountain Formation and the Sanders, Carter, Millerella, Gilmer, and Coats sandstones of the Parkwood Formation; other Mississippian reservoirs produce gas. Salient features of the Carter sandstone, which contains the most productive oil reservoirs, are discussed in the following section. Following this discussion, the sedimentological, petrological, and petrophysical framework of the Carter sandstone reservoir in

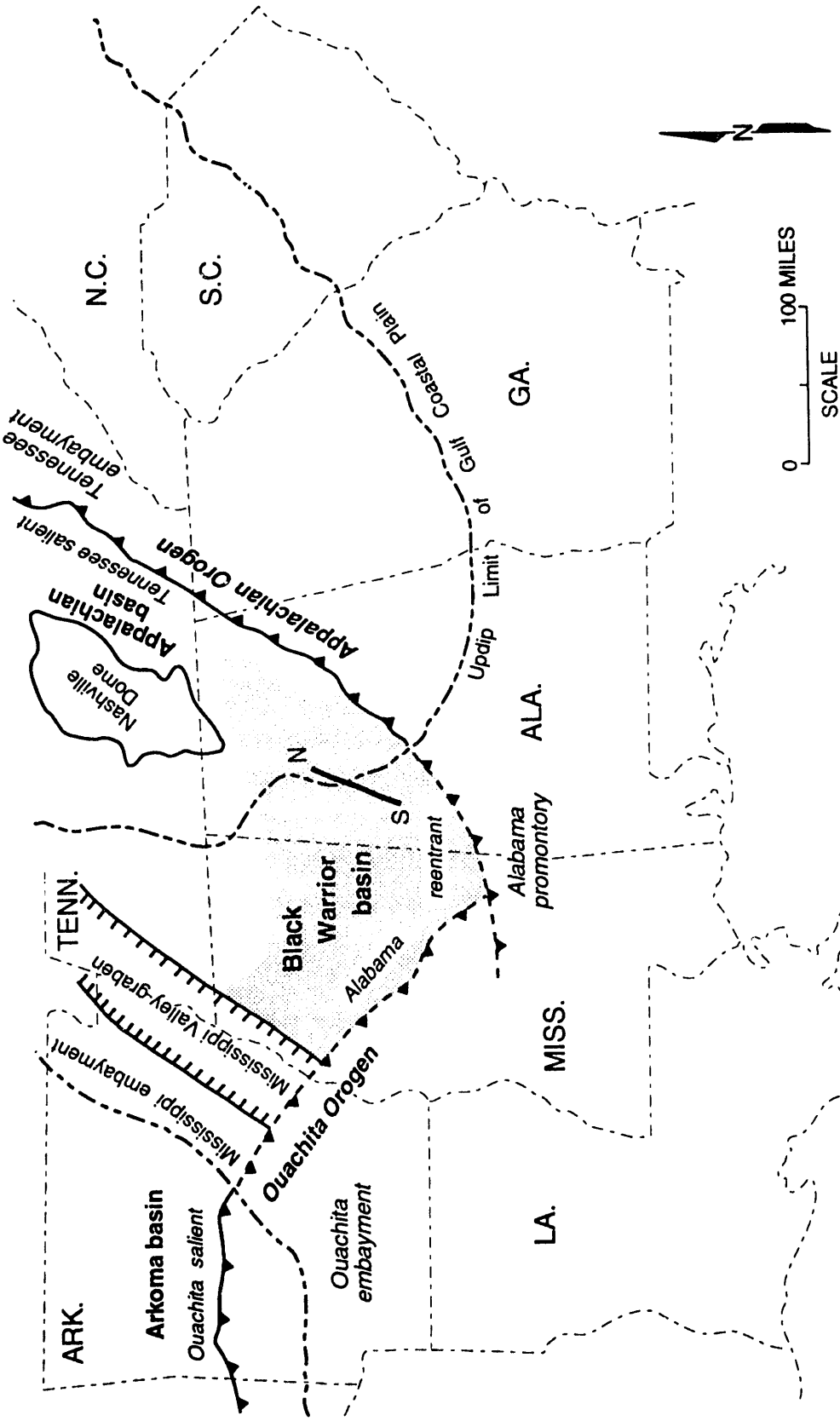

Figure 4.--Geologic setting of the Black Warrior basin (modified from Pashin and others, 1991).

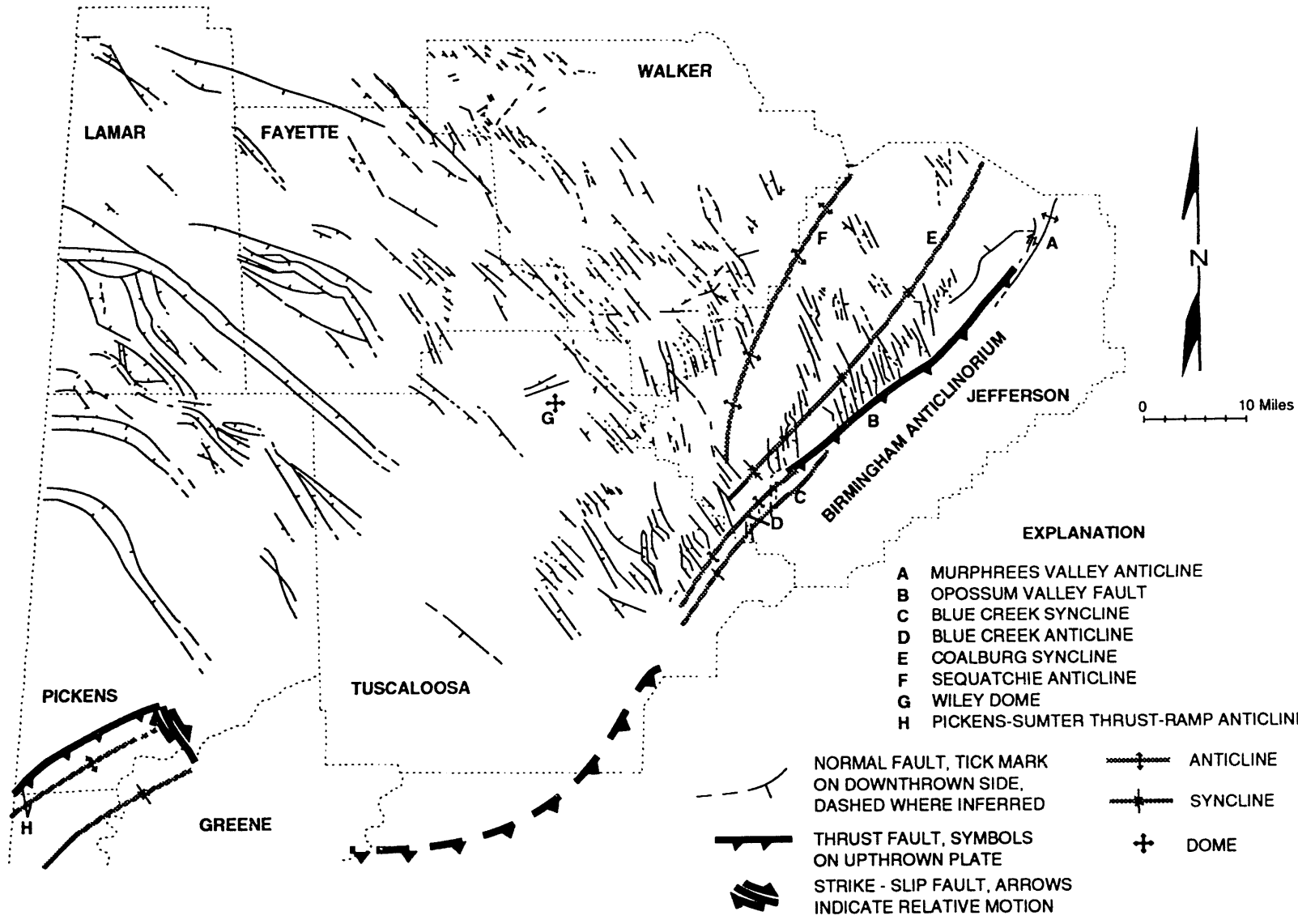

Figure 5.--Faults and folds in the Black Warrior basin of Alabama (modified from Pashin, 1991).

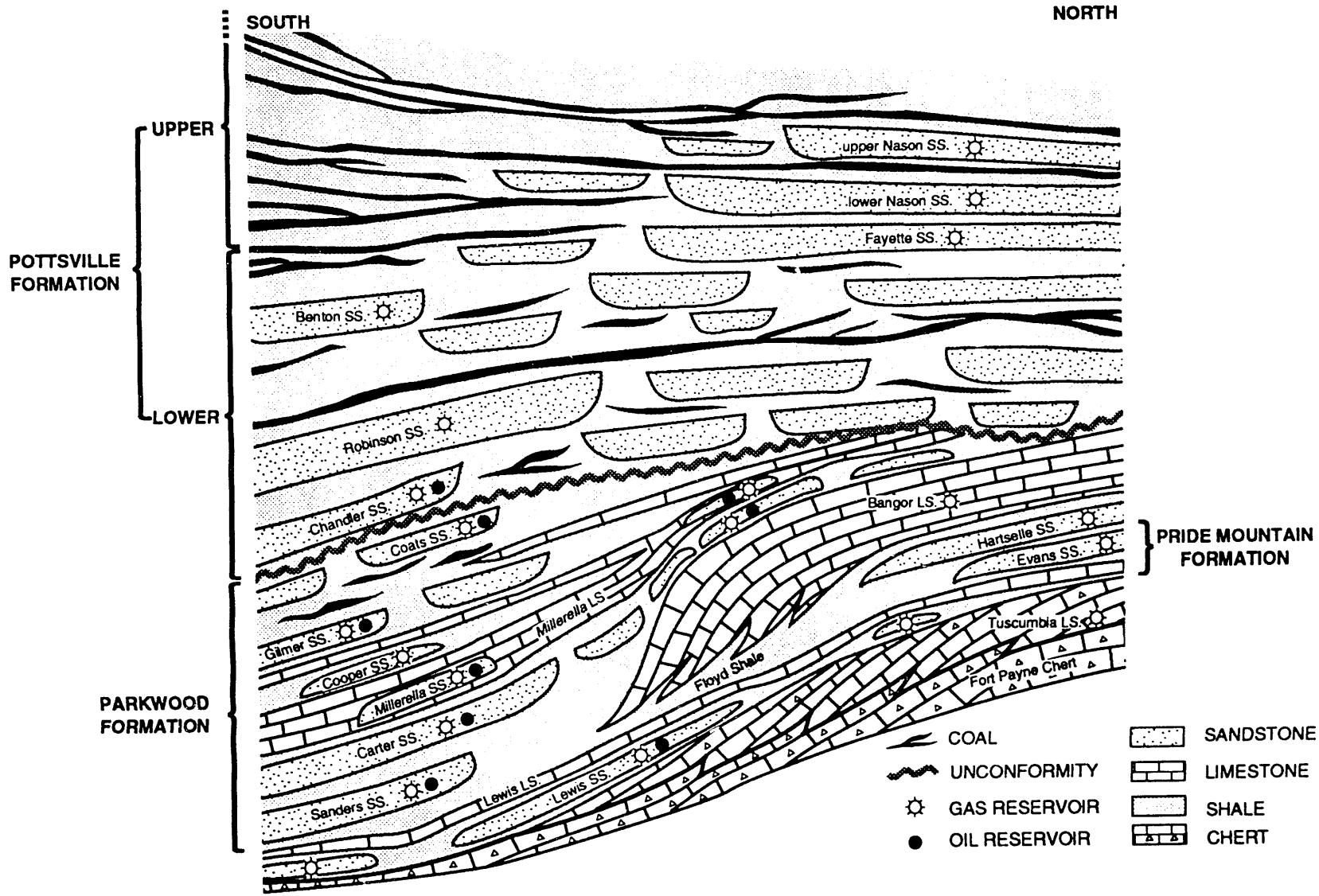

Figure 6.--Generalized structural cross section of the Black Warrior basin showing petroleum reservoirs. (See figure 4 for line of generalized cross section.)

North Blowhorn Creek oil unit, which is the most productive oil field in the Black Warrior basin of Alabama, is established.

The Parkwood Formation is commonly divided into upper and lower parts (Thomas, 1972; Cleaves, 1983). The lower Parkwood can further be divided into two parts, the Carter interval and the *Millerella* limestone interval. The Carter interval is dominantly a siliciclastic succession, whereas the *Millerella* interval caps the succession and contains numerous resistive markers. Above the *Millerella* interval, the upper Parkwood is a thick, siliciclastic dominated depositional sequence that is overlain by the Pottsville Formation.The Carter sandstone has been recognized only in the subsurface and is part of a thick progradational sequence that contains four named reservoir sandstone units in the Black Warrior basin of Alabama and Mississippi. These reservoir units are, in ascending order: (1) Rea; (2) Abernathy; (3) Sanders; and (4) Carter (Cleaves, 1981, 1983; Nix, 1986; Thomas, 1988a). Only Carter and Sanders reservoirs occur in Alabama.

The Carter interval in Alabama has a maximum thickness of nearly 400 ft in northwestern Pickens and southwestern Lamar Counties and thins markedly toward the northeast, where thickness scarcely exceeds 100 ft (Pashin and others, 1991). In Mississippi, the Carter interval is locally thicker than 1,000 ft (Mellen, 1947; Cleaves, 1981, 1983). However, the interval is generally thinner than 100 feet; the interval is absent throughout most of Tuscaloosa County (Pashin and others, 1991). Although the Carter interval commonly overlies the Bangor Limestone, in the southernmost part of the basin in Alabama, the interval overlies a resistive facies of the Floyd Shale. Carter sandstone is absent throughout the northern part of the basin in Alabama, but the Carter interval can be identified as a persistent shale marker that is typically thinner than 10 ft (Pashin and others, 1991).

The Carter interval represents the second siliciclastic basin-filling event during formation of the Black Warrior basin, thus signifying tectonism and subsidence along the southwest part of the Alabama promontory. On a regional scale the Carter interval is widely recognized to include deltaic, beach-barrier, and shelf-bar deposits (Cleaves and Broussard, 1980; Cleaves, 1981, 1983; Bearden and Mancini, 1985; Nix, 1986; Thomas, 1988a). One beach-barrier sandstone body in the Carter at North Blowhorn Creek oil unit has produced a majority of the oil from the Carter interval in Alabama (Moore and Kugler, 1990). The source area for Carter sandstone is a matter of controversy. One school of thought favors an orogenic Ouachita source in the southwest (Nix, 1986; Thomas, 1976, 1988a), whereas another school favors a cratonic source to the north or northwest (Welch, 1978; Shepard, 1979; Cleaves and Broussard, 1980; Cleaves, 1981, 1983; Bearden and Mancini, 1985).

The Bangor carbonate platform was a fundamental control on the nature and distribution of Carter sandstone in Alabama. Northeast of the Bangor platform margin, Carter sandstone occurs in a series of southeast-northwest trending bodies (fig. 7). In the basin to the southwest, the Carter was deposited in deltaic environments. Most production of oil from Carter reservoirs in Alabama is from beach-barrier and shelf-bar sandstone, concentrated near the Bangor platform margin.

CHARACTERISTICS OF THE CARTER SANDSTONE RESERVOIR IN NORTH BLOWHORN CREEK OIL UNIT

INTRODUCTION

North Blowhorn Creek oil unit is an ideal setting to develop criteria necessary to recognize reservoir heterogeneity and to evaluate strategies for improving oil recovery in Mississippian reservoirs in the Black Warrior basin because of the density of wells and the abundance of cores (fig. 8); well density is low and cores are scarce in other fields in the basin. In this part of the report, a sedimentological, petrological, and petrophysical framework for the Carter reservoir in North Blowhorn Creek oil unit is developed in order to establish criteria for recognizing reservoir heterogeneity that affects improved recovery strategies.

North Blowhorn Creek oil unit was discovered by Warrior Drilling and Engineering, Inc., in 1979 with the completion and testing of the Gordon 11-5 well (PN2751) (fig. 8). The well was drilled and cased to 2,921 ft and perforated from 2,285 to 2,303 ft in Carter sandstone. The well flowed 45 BOPD on initial test. Flowing tubing pressure was 10 psig (open choke), and gravity of the oil was 34° API.

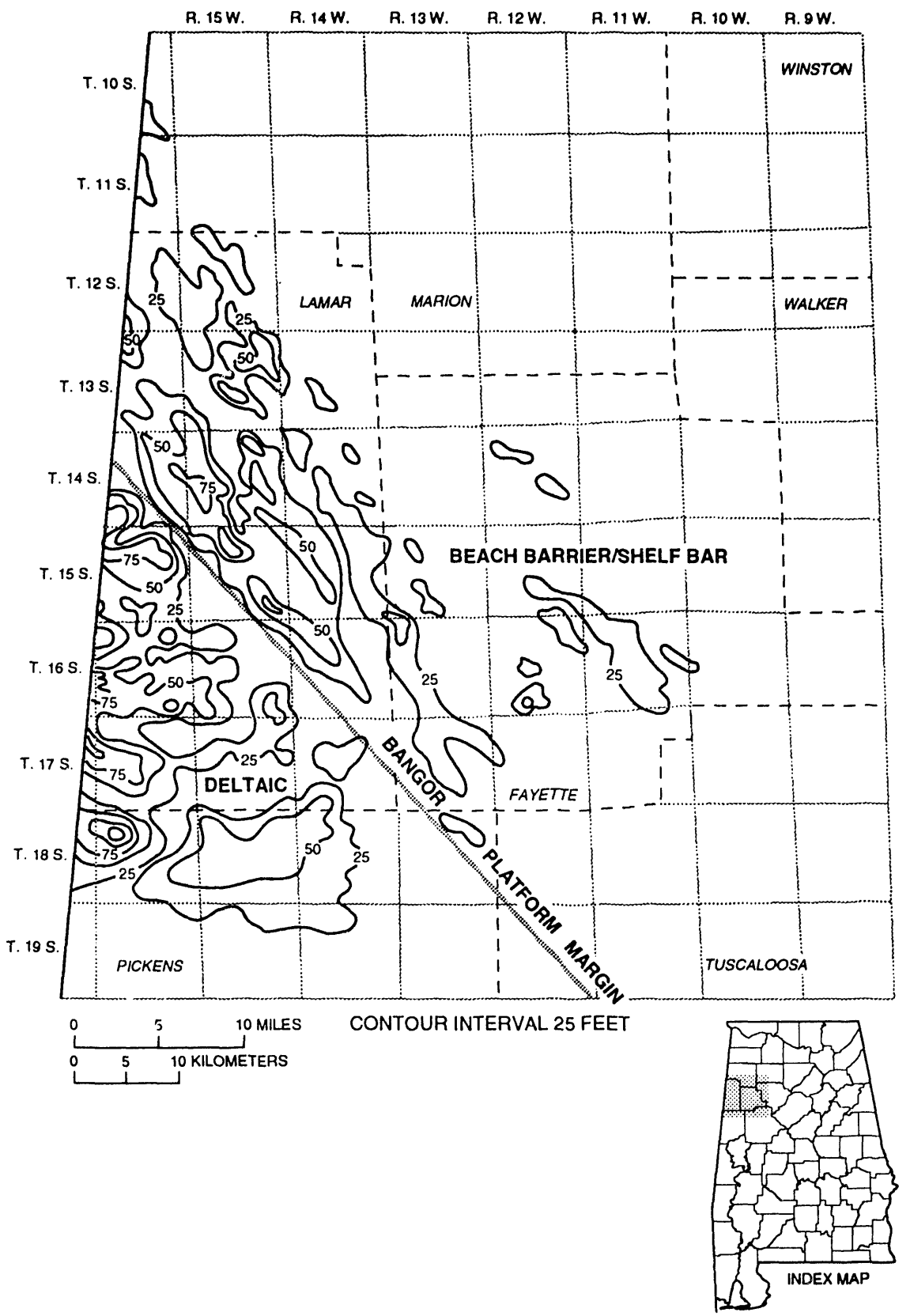

Figure 7.--Regional isolith map of Carter sandstone showing the Bangor Limestone platform margin (modified from Nix, 1991).

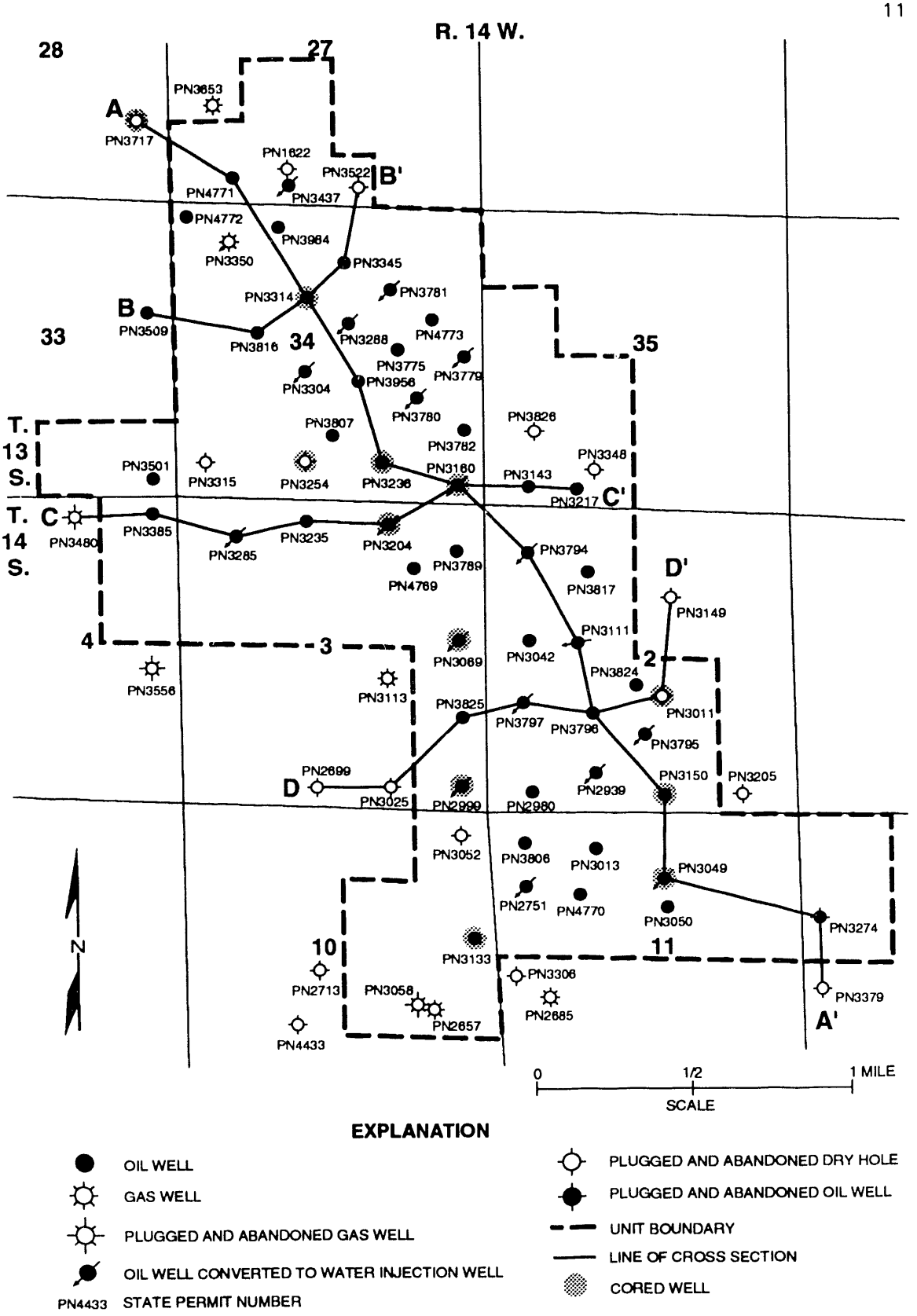

Figure 8.--Index map of North Blowhorn Creek oil unit.

The field was developed with an 80-acre well spacing. In February 1983, North Blowhorn Creek field was unitized and line-drive water injection began in June of that year. Prior to unitization, the field produced 601,007 bbls of oil, 888 MMcf of gas, and 887 bbls of water. The peak oil production rate of 86,341 BOPM was reached in 1985, 2 1/2 years after initiation of water injection. The oil unit currently has 31 producing wells and 18 injection wells.

Carter sandstone in North Blowhorn Creek oil unit is the most productive reservoir in the Black Warrior basin of Alabama. Cumulative production through December 1990 was 4,832,247 bbls of oil, 2,781,598 Mcf of gas, and 4,488,217 bbls of water. This production represents 33 percent of the original oil in place in the unit and 67 percent of the total oil produced from the Black Warrior basin of Alabama. Seven of the eight next most productive Carter oil fields in the Black Warrior basin of Alabama are located near North Blowhorn Creek oil unit.

Figures 9 and 10 are structure contour maps for North Blowhorn Creek oil unit that depict the base of the *Millerella* limestone and the top of the Carter sandstone, respectively. Structural dip of the base of the *Millerella* limestone (fig. 9) is approximately 50 ft/mi to the south. Structural dip of the top of the Carter sandstone is 25 to 60 ft/mi to the south. No closure is apparent on the top of the Carter sandstone. The Carter sandstone in North Blowhorn Creek oil unit is an isolated, elongate, northwest-southeast trending sandstone body that is enclosed in shale and pinches out to the northeast, southeast, and southwest (fig. 11). The Carter sandstone in North Blowhorn Creek is contiguous with the Carter reservoir in the adjacent Armstrong Branch gas field, to the northwest (Bearden, 1984, 1985; Epsman, 1987). The updip limit of the oil reservoir at North Blowhorn Creek oil unit is defined by the oil/gas contact at -1,724 ft. The updip limit of the Armstrong Branch gas field is defined by pinchout of porous Carter sandstone. Thus, the trapping mechanism for the combined North Blowhorn Creek oil unit/Armstrong Branch gas field is stratigraphic, defined by pinchout of Carter sandstone (Bearden, 1985).

The most productive Carter sandstone oil fields in the Black Warrior basin of Alabama are near North Blowhorn Creek oil unit, although the source for this oil is not well known. Possible source rocks include Upper Mississippian Floyd Shale, Upper Devonian Chattanooga Shale, and unnamed units of Silurian and/or late Ordovician age, all of which contain dark gray to black shale (Ryder, 1987). The Upper Mississippian Tuscumbia Limestone, Pride Mountain Formation, and Bangor Limestone also have been suggested as possible source rocks for bitumen in the Hartselle Sandstone, but the hydrocarbon-generating potential of these formations is not well established (Wilson, 1987). The Chattanooga Shale has an average organic-matter content of 16 weight percent, and the kerogen is intermediate between type I and type II (Rheams and Neathery, 1988).

Although woody kerogen is abundant, the Floyd Shale and Parkwood Formation contain sufficient amorphous and herbaceous kerogen to be source rocks for oil (Bearden and Mancini, 1985). Total organic carbon in these rocks ranges from 0.07 to 2.36 weight percent, with a mean of 0.58 weight percent and a standard deviation of 0.55 weight percent, indicating that these shales are moderate source rocks. Hydrogen indices, determined by Rock-Eval pyrolysis from samples in three wells in Lamar County, indicate that only the Chattanooga Shale and the Lewis limestone member of the Floyd Shale are potential source rocks. Geochemical comparison of Carter sandstone oil to extracts from the Lewis limestone and the Chattanooga Shale suggests that the Lewis limestone was the source rock for oil in the Carter sandstone (Robertson Research, 1985). Clearly, additional research would be valuable for identifying hydrocarbon source-rock potential in the Black Warrior basin.

METHODS

One axial stratigraphic and three sagittal stratigraphic cross sections were constructed for the Carter sandstone in North Blowhorn Creek oil unit using resistivity logs (figs. 8, 12, 13). Lithology, grain-size trends, stratification type, and sedimentary structures, were described for 13 cores of Carter sandstone from North Blowhorn Creek, Fairview, and Wayside fields.

Framework-grain composition and diagenetic character of Carter sandstone from North Blowhorn Creek and Wayside oil units were determined by modal analysis with a standard petrographic microscope. Approximately 300 points were identified in each of 50 thin sections.

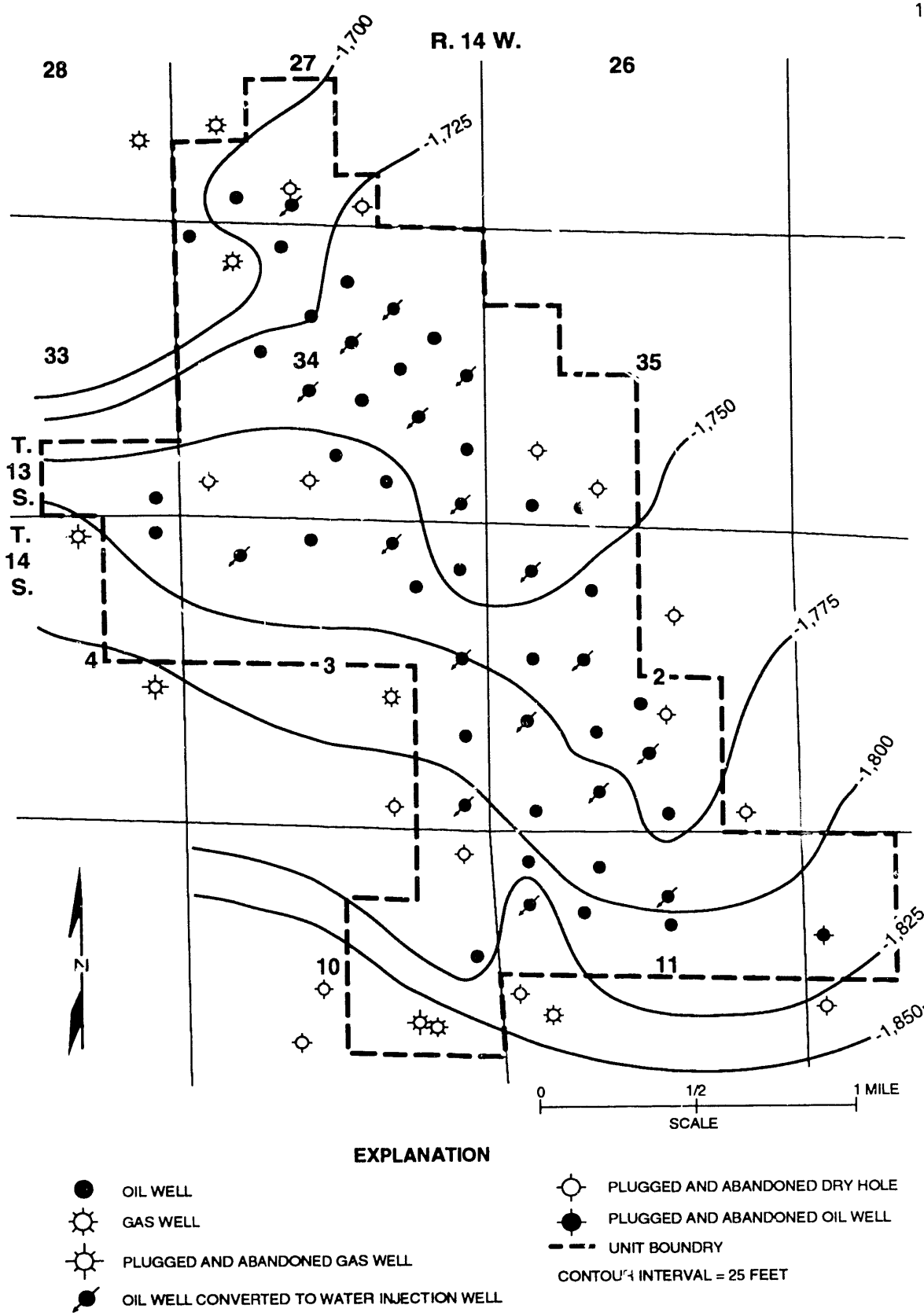

Figure 9.--Structure contour map on base of *Millerella* limestone in North Blowhorn Creek oil unit (modified from Moore and Kugler, 1990).

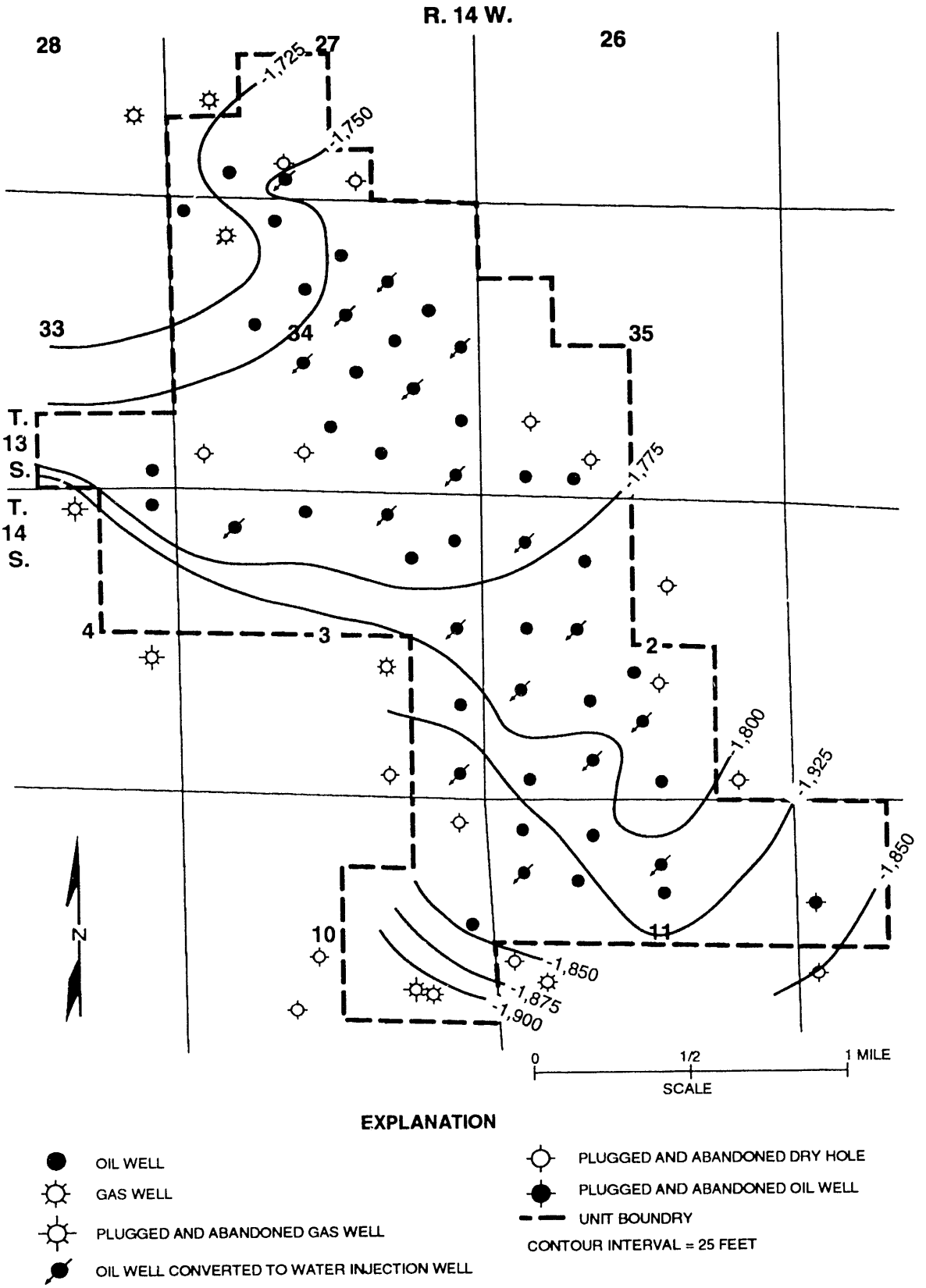

Figure 10.--Structure contour map on top of Carter sandstone in North Blowhorn Creek oil unit (modified from Moore and Kugler, 1990).

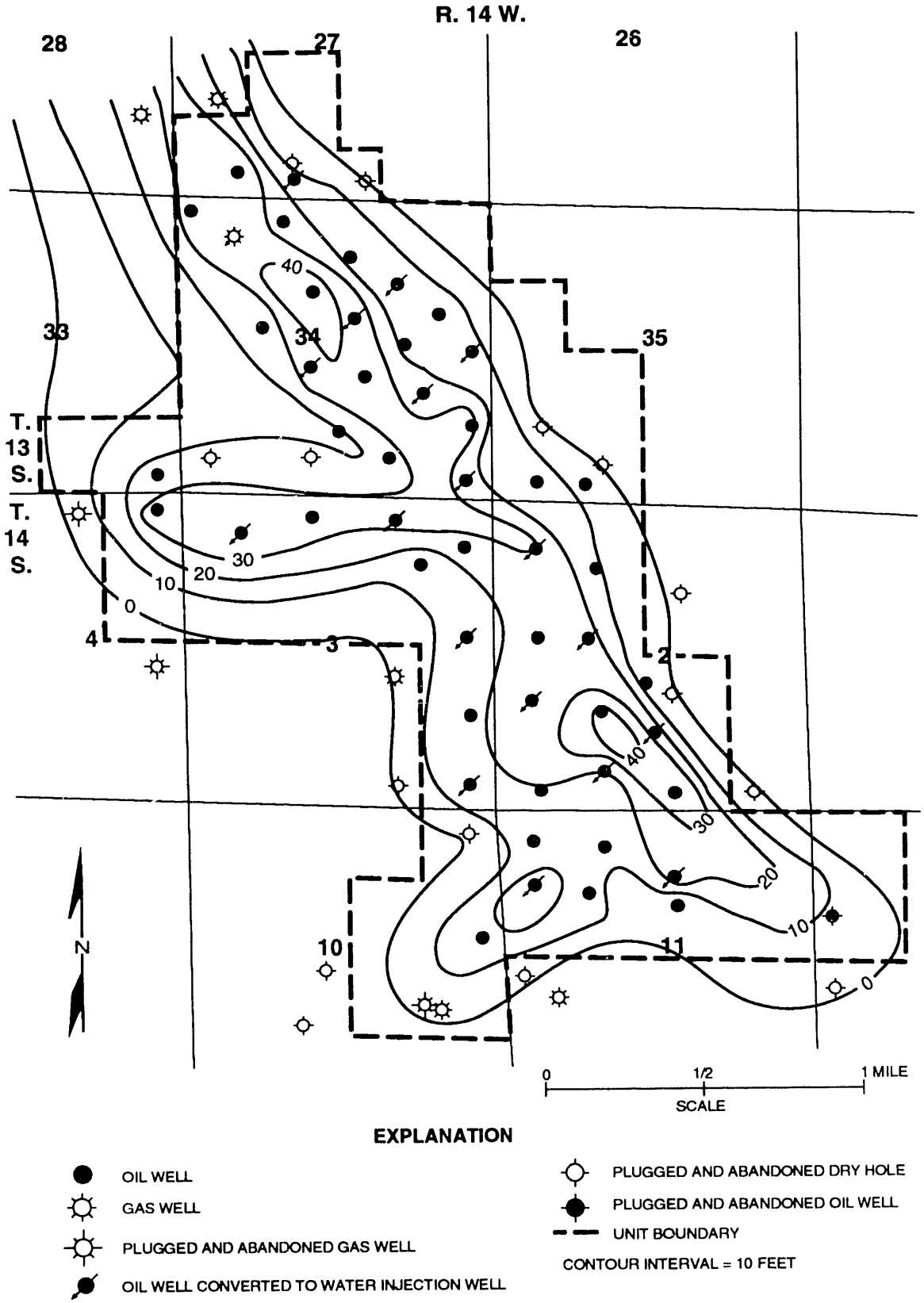

Figure 11.--Sandstone isolith map of total Carter sandstone in North Blowhorn Creek oil unit (modified from Moore and Kugler, 1990).

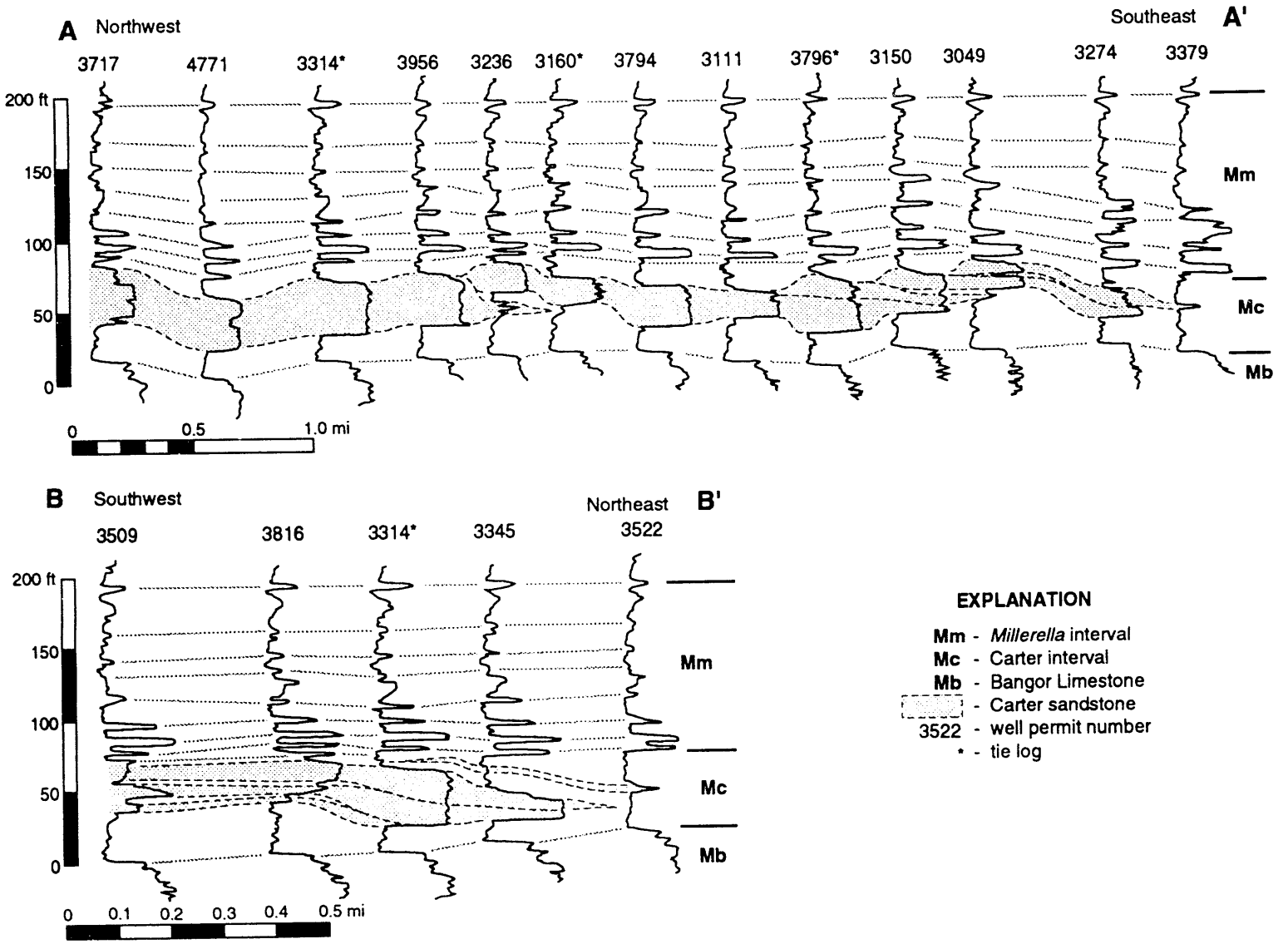

Figure 12.--Resistivity log stratigraphic cross-sections A-A' and B-B', North Blowhorn Creek oil unit. (See figure 8 for lines of cross section.)

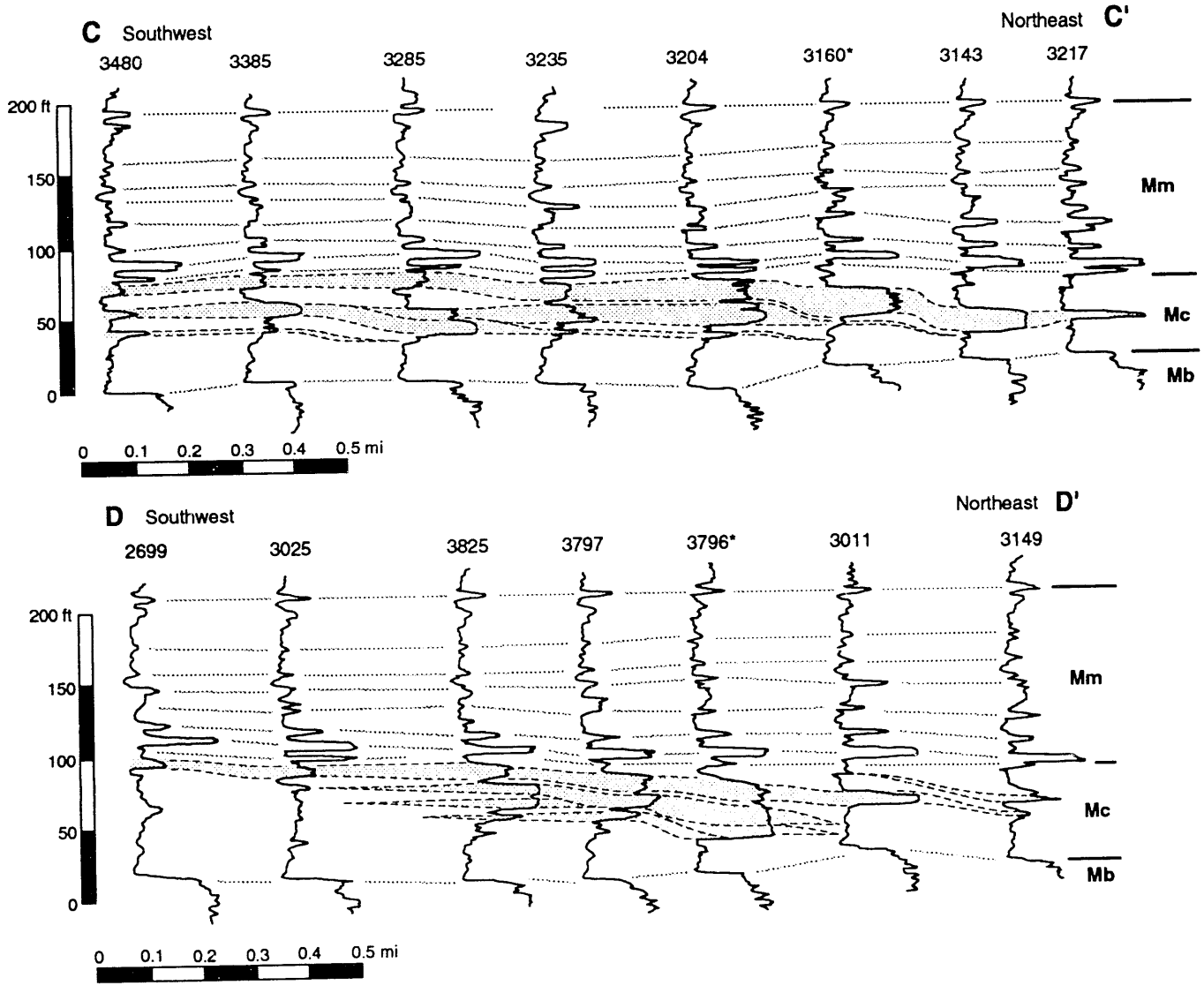

Figure 13.--Resistivity log stratigraphic cross-sections C-C' and D-D', North Blowhorn Creek oil unit. (See figure 8 for location of lines of cross section and figure 12 for explanation.)

Generally, the composition of more than 200 framework grains in each sample was determined using this procedure. Three hundred thin sections were examined qualitatively. Particular attention was given to relationships between authigenic minerals and pores. All thin sections were back-pressure impregnated with blue-dyed epoxy to facilitate identification of pore type. Thin sections also were stained with alizarin red-S and potassium ferricyanide according to the method of Evamy (1963) to aid identification of carbonate minerals. X-ray diffraction analyses of selected, unoriented whole-rock powders corroborated mineral identification.

The morphology, composition, and distribution of authigenic minerals and pores were evaluated with a Hitachi 2500B scanning electron microscope equipped with a Robinson backscattered-electron detector and Tracor-Northern energy-dispersive X-ray analysis and image-analysis systems. Gold-palladium-coated, freshly broken rock surfaces were viewed in secondary-electron mode to examine detrital grain morphology, pore types, pore throats, and cement-stratigraphic relationships. Images of carbon-coated, polished thin sections were viewed in backscattered-electron mode to determine chemical composition and variation in authigenic minerals, cement-stratigraphic relationships, and pore types. Qualitative energy-dispersive X-ray (EDX) analyses and digital EDX maps of polished thin sections were used in mineral identification, in characterization of compositional variation in authigenic minerals, and in characterization of porosity.

A JEOL superprobe-8600 electron microprobe equipped with five automated wavelength-dispersive spectrometers, a solid-state backscattered-electron detector, and Tracor-Northern EDX and image-analysis systems was used to quantitatively determine the chemical composition of authigenic carbonate minerals, using carbonate-mineral standards. Standard operating conditions were 15 kV primary-beam acceleration potential, 10 nA sample current, and 5-10 μm beam diameter. Concentrations of calcium, iron, magnesium, manganese, and strontium were determined. Bence-Albee routines were used to reduce microprobe data.

Porosity and permeability data from all available commercial core analyses from North Blowhorn Creek oil unit were compiled for comparison with core descriptions, petrographic data, and high-pressure mercury porosimetry data. Capillary-pressure data obtained from high-pressure mercury porosimetry were used to characterize pore-throat size distributions and their relationships to pore types. A Micromeritics Autopore II 9200 was used for these analyses following procedures outlined by Kopaska-Merkel (1991). Mercury intrusion volume was monitored from 1.5 to 20,000 psia. Thin sections were made from the ends of plugs used for porosity measurement. All porosimetry samples were cleaned by refluxing toluene in a Soxhlet extractor. Samples were also cleaned with chloroform when necessary.

SEDIMENTOLOGY

Sedimentologic analysis determines reservoir architecture and provides a conceptual framework for characterizing sandstone heterogeneity in North Blowhorn Creek oil unit. The Carter sandstone of North Blowhorn Creek is interpreted to represent a spit system that was preserved as part of a muddy, delta-destructive strand plain. Similar deposits are common in other Upper Mississippian strata of the Black Warrior basin (Pashin and others, 1991), but morphodynamic variation of the beach systems is great and reflects a spectrum of wind, wave and tide regimes. The localized, lensoid nature of Carter sandstone reservoirs differs greatly from the widespread beach-barrier sandstone bodies that have formed the basis of previous sandstone heterogeneity studies (Sharma and others, 1990 a, b). Hence, detailed modeling of Carter reservoirs will provide information that is useful in implementing improved-recovery strategies not only in the Black Warrior basin, but in other sedimentary basins as well.

STRATIGRAPHIC ARCHITECTURE

Resistivity-log cross sections from North Blowhorn Creek oil unit establish that reservoir architecture is internally complex but varies systematically and predictably (figs. 8, 12, 13). Below the Carter interval is the Bangor Limestone. Using a resistive marker that defines the top of the Millerella

limestone interval, the top of the Bangor is sharp, is readily correlated throughout the oil unit, and defines a surface that rises toward the northeast. Above the Bangor is a shale that extends throughout the oil unit. Although the basal contact of the shale is sharp and continuous, the upper part of the shale unit intertongues with the Carter sandstone.

The net-sandstone isolith map (fig. 11) demonstrates that the Carter sandstone in North Blowhorn oil unit is a northwest-southeast trending body that extends northwest of the oil unit and terminates in the southeast part of the unit. The sandstone body has a sublinear northeast margin and an irregular southwest margin. Sandstone is locally thicker than 40 ft along the axis of the body; the axis lies close to the northeast margin of the reservoir. However, isolith patterns become increasingly irregular toward the southeast, and the thickest sandstone defines a series of hooklike forms that project westward from the sandstone-body axis.

In North Blowhorn Creek, the Carter sandstone is not a single, homogeneous reservoir but comprises several sandstone lenses. The axial cross section, A-A' (fig. 12), indicates that the sandstone body contains a series of imbricate, clinoformal lenses that dip southeast and decrease in size toward the terminus of the sandstone body. Similarly, the sagittal cross sections, B-B', C-C , and D-D' (figs. 12, 13), depict imbricate, clinoformal lenses that dip northeast. Within the sagittal sections, however, the sandstone lenses contain distinctive changes in log signature, and hence, facies architecture.

The depositionally downdip parts of the lenses tend to have a blocky log signature with high resistivity, reflecting the best reservoir quality, although a serrate pattern is locally apparent (figs. 12, 13). Lenses are typically amalgamated along the sandstone-body axis, forming a single, blocky reservoir-sandstone unit. In contrast, the depositionally updip parts of the lenses tend to have a serrate log pattern, and resistivity decreases toward the southwest, reflecting decreased reservoir quality.

The *Millerella* interval contains a series of laterally extensive carbonate and shale markers (figs. 12, 13). In general, limestone units thin upward, and carbonate content increases slightly toward the northeast and markedly toward the southeast. Moreover, limestone markers tend to follow irregularities in the upper contact of the sandstone, descending stratigraphically northeast across the Carter reservoir.

LITHOFACIES ANALYSIS

Cores of Carter sandstone from North Blowhorn Creek oil unit typically contain a tripartite lithofacies sequence, including from bottom to top, (1) shale-and-siltstone facies, (2) sandstone facies, and (3) variegated facies (fig. 14). Cores from the nearby South Brush Creek oil unit and North Fairview oil field exhibit a similar sequence.

SHALE-AND-SILTSTONE FACIES

Characteristics

The shale-and-siltstone facies forms the base of the Carter interval and is composed of medium gray to very dark gray, organic-rich shale and light gray siltstone (fig. 14). In well logs, the facies has low resistivity and an irregular signature; facies thickness typically ranges from 20 to 75 ft In core, the facies contains several bedding styles and sedimentary structures. The contact with the Bangor Limestone was not observed in core, but the contact with the overlying Carter sandstone is gradational.

Wavy, lenticular, and flaser bedding predominate in the shale-and-siltstone facies; shale is generally silty and poorly fissile, whereas siltstone occurs in laminae to thin beds with sharp upper and lower contacts (figs. 15 through 17). Load casts and associated convolute laminae are abundant at the base of the siltstone layers, particularly the thickest beds, and wave ripples and horizontal laminae abound within the layers. Locally, current ripple-drift cross laminae occur in the siltstone beds. Biogenic structures are scarce in the shale-and-siltstone facies, although horizontal feeding burrows are locally common, and some resting traces were observed.

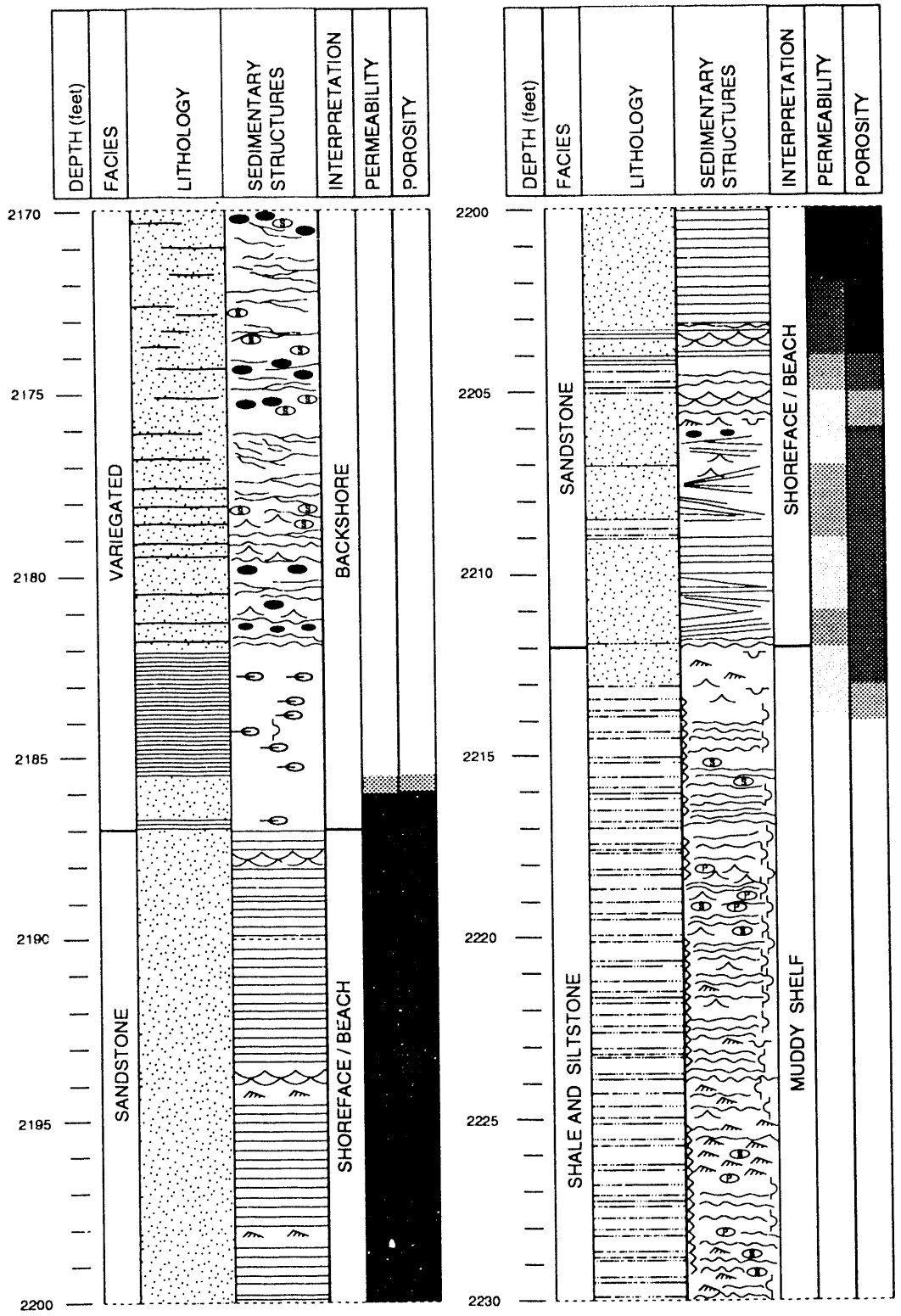

Figure 14.--Core log for well PN2999 illustrating sedimentary structures, porosity and permeability variation, and facies interpretations. (See following page for explanation.)

EXPLANATION

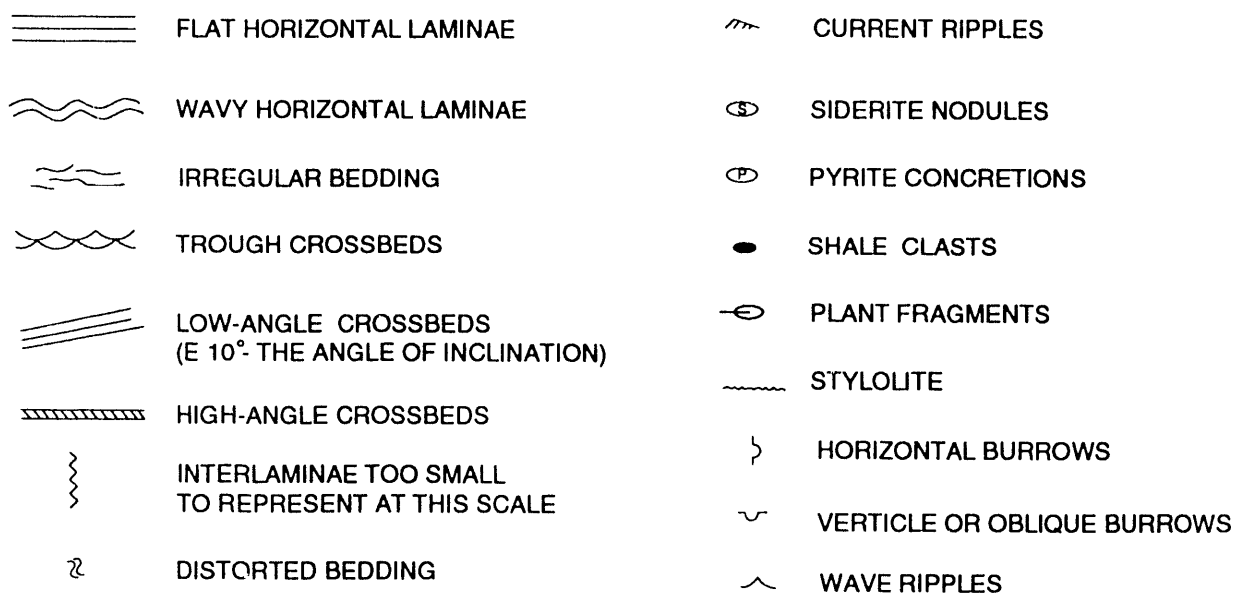

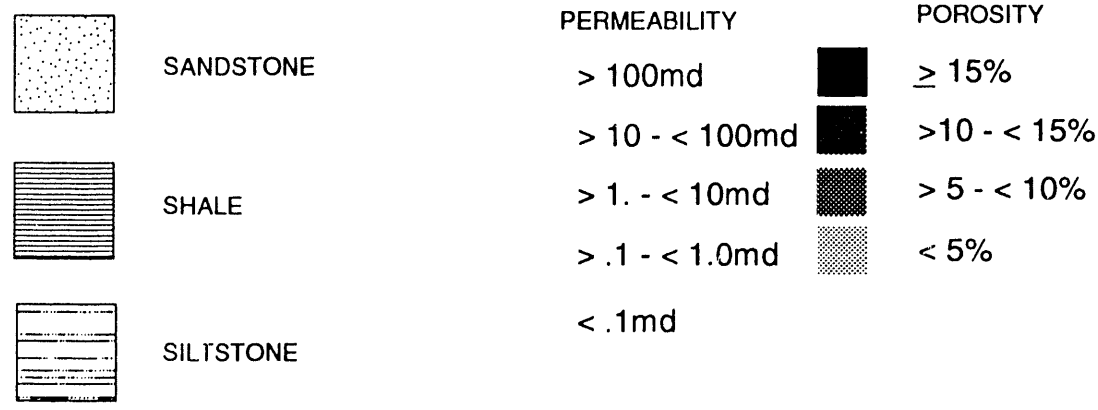

Figure 14.--Core log for well PN2999 illustrating sedimentary structures, porosity and permeability variation, and facies interpretations-Continued.

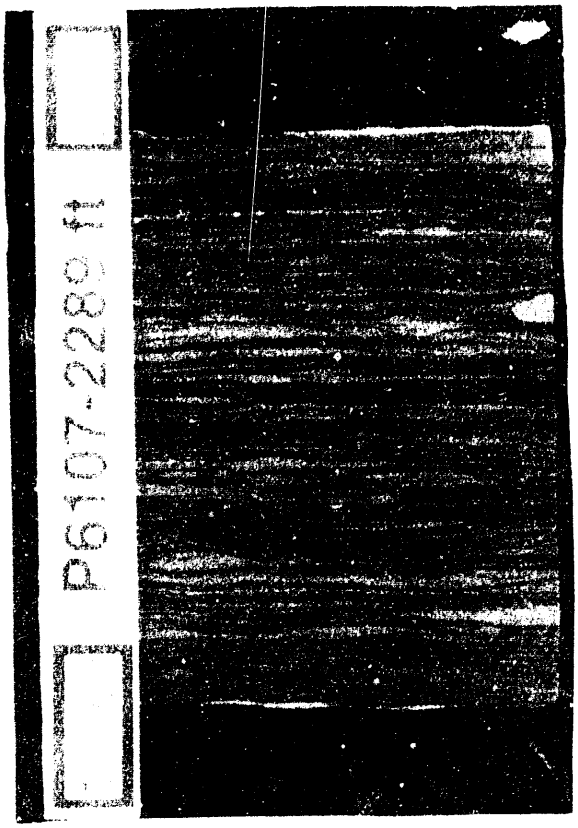

Figure 15.--Core photograph of lenticular sandstone and shale (Carter sandstone, North Fairview oil field, well PN6107, 2,289 ft). Note current ripple-drift cross laminae and horizontal feeding burrows.

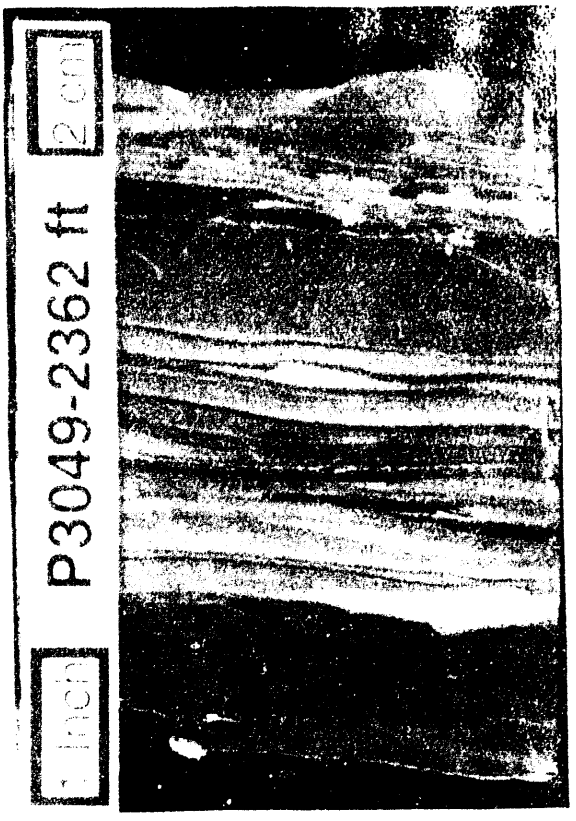

Figure 16.--Core photograph of wavy-bedded shale and siltstone (Carter sandstone, North Blowhorn Creek oil unit, well PN3049, 2,362 ft). Note graded laminae and poorly developed casts.

Shale-to-siltstone ratio varies from 0.2 to 0.8. Siltstone beds tend to be thickest in parts of the cores with low shale-to-siltstone ratio. Generally, the siltstone beds define a thickening- and coarsening-upward sequence. Sideritic concretions occur in all cores and generally form discoid to oblate masses ranging in size from pebbles to cobbles. The concretions commonly displace laminae in the host strata and locally contain septaria. Moreover, discoid to irregular, sand- to pebble-size marcasite nodules occur in some cores.

Interpretation: Muddy Shelf

The shale-and-siltstone facies is interpreted to represent a storm-dominated shelf mud blanket that prograded across the Bangor carbonate bank (fig. 18). Occurrence of thin siltstone beds with wave ripples indicates that mud deposition was interrupted by episodic wave events. Wavy, lenticular, and flaser-bedded siltstone with abundant load casts and wave ripples (figs. 15 through 17) are widespread in the Appalachian region and have been interpreted to represent distal storm deposits (Pashin and Ettensohn, 1987). Indeed, similar sand-rich deposits are now forming on the storm-dominated shelf of the North Sea (Aigner and Reineck, 1982) and have been recognized in the Lewis interval of the Black Warrior basin (Pashin and others, 1991).

Abundant load casts, some of which are clearly syndepositional (figs. 16, 17) indicate that the muddy substrate was soft, fluid and could be deformed with only minimal accumulation of quartz-rich sediment. Lack of body fossils and presence of marcasite nodules in the facies suggests that the substrate was too fluid and foul to accommodate a diverse fauna. However, feeding burrows and

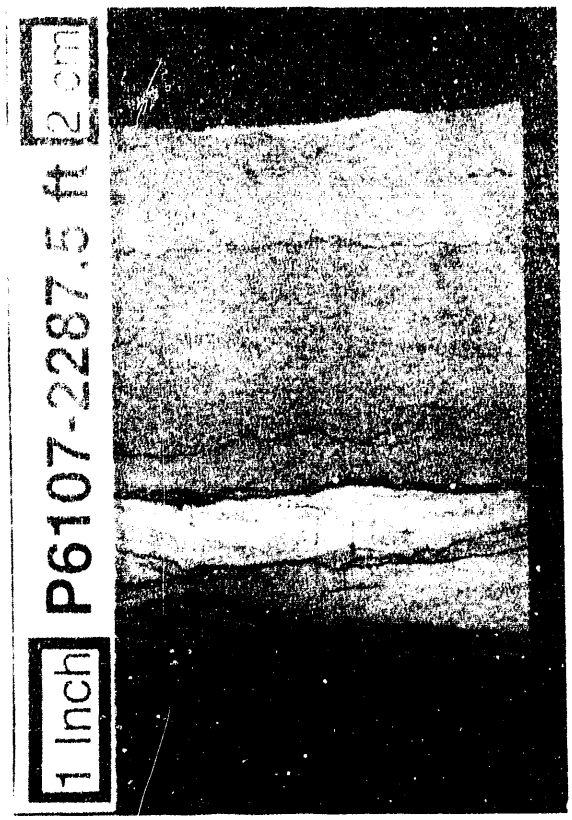

Figure 19.--Core photograph of contact of sandstone facies with underlying shale and siltstone facies (Carter sandstone, North Fairview oil field, well PN6107, 2,287.5 ft). Note the pressure-solution seams along clay laminae. Note the lack of oil stain below the clay laminae in the lower half of the photograph.

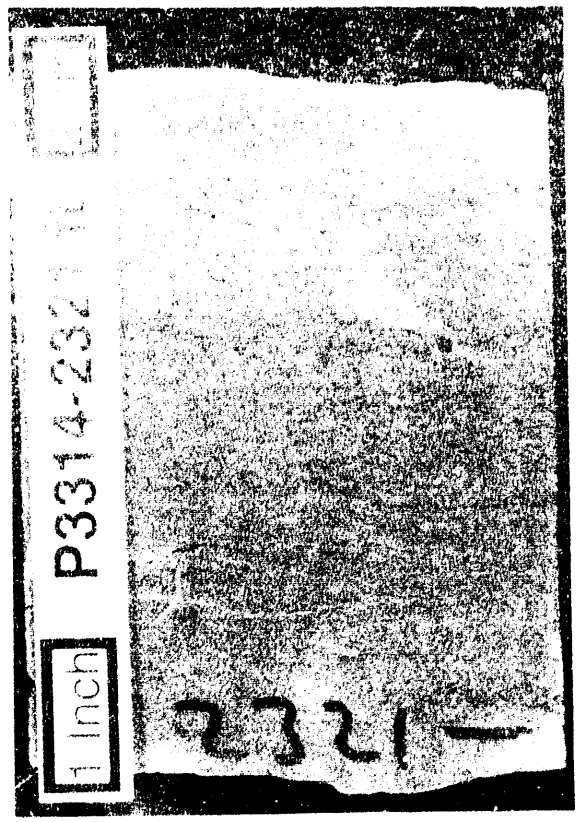

Figure 20.--Core photograph of lunate-ripple cross laminae (Carter sandstone, North Fairview oil field, well PN3314, 2,321 ft).

26). In well PN3236, amalgamated shell accumulations make up an interval 4.0 ft thick. Brachiopod shells generally are poorly oriented but are most commonly preserved convex-side up. Concentrations of skeletal debris localize zones of pervasive concretionary calcite and ferroan dolomite ankerite cement within the sandstone facies. Aside from skeletal material, biogenic structures in the sandstone facies are few, save for isolated feeding, resting, and escape burrows.

Interpretation: Beach and Shoreface

The sandstone facies, the principal Carter oil reservoir, is interpreted to represent sedimentation in a spectrum of shoreface and beach environments (fig. 18). Similar beach and shoreface deposits are common in asphaltic facies of the Lewis sandstone and the Hartselle Sandstone in Alabama (Pashin and others, 1991). The thin zone of gradation from the shale-and-siltstone facies into the sandstone facies indicates that the transition from shelf to shoreface was well defined. The general sequence of sedimentary structures in the sandstone lithofacies, specifically (1) lunate-ripple cross laminae (figs. 20, 21), (2) high-angle planar and tangential crossbeds (fig. 23), and (3) low-angle, planar crossbeds (fig. 22), is characteristic of shoreface-beach systems and reflects progressive deformation of waves as they approach shore (Clifton, 1976).

Dominance of lunate-ripple cross laminae (figs. 20, 21) over wave ripples suggests that waves were supplanted by unidirectional currents in the lower shoreface, perhaps in response to

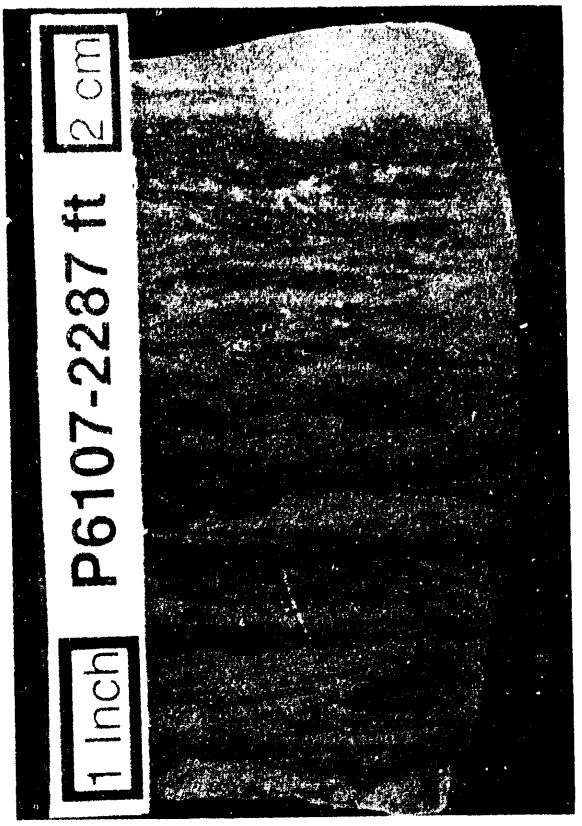

Figure 21.--Core photograph of lunate-ripple cross laminae defined by discontinuously distributed hydrocarbon residue (Carter sandstone, North Fairview oil field, well PN6107, 2,287 ft).

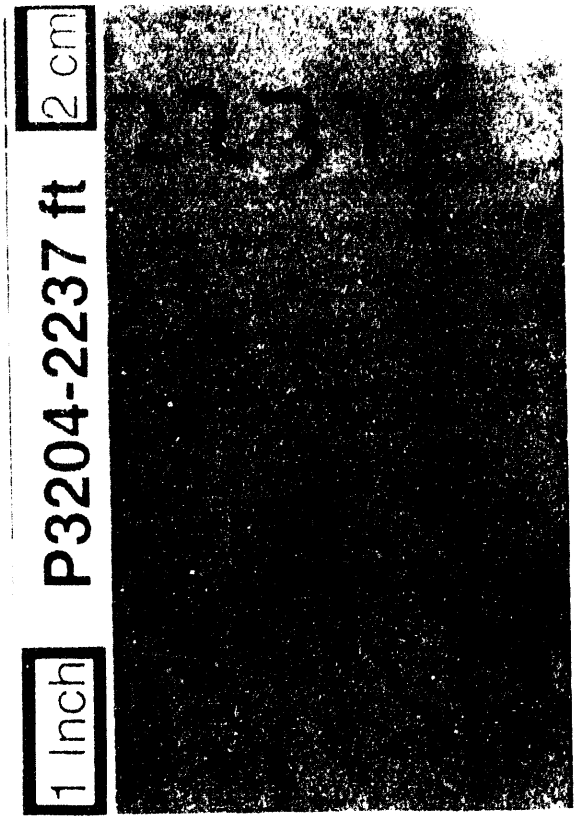

Figure 22.--Core photograph of low-angle planar crossbeds (Carter sandstone, North Blowhorn Creek oil unit, well PN3204, 2,237 ft.)

geostrophic flows and rip currents. Thin intervals of high-angle crossbedding (fig. 23) are characteristic of shoreface bars and ridge-and-runnel systems, which occur in the breaker zone and the lower foreshore of modern beach systems (Davis and others, 1972; Davidson-Arnott and Greenwood, 1976). Low-angle, planar crossbedding (fig. 22), furthermore, is the characteristic sedimentary structure of the breaker, surf and swash zones of beaches (Thompson, 1937; Clifton, 1976). Deviation of sequences in the sandstone facies from an idealized succession of sedimentary structures owes to several sources including amalgamation of sandstone lenses (figs. 12, 13), reworking during storm surges (fig. 18), multiple shoreface-bare systems, and instability of the beach-shoreface system caused by daily, monthly, and seasonal tidal cycles.

Shale-clast conglomerate layers (figs. 24, 25) indicate that shoreface erosion was a significant process. Some conglomeratic intervals apparently signify episodes when muddy intervals were reworked, thereby forming amalgamated lenses along the main sandstone body axis. Shale clasts may have also been eroded from the innermost shelf, transported by geostrophic flows, and deposited on the shoreface. Moreover, isolated shale clasts may simply represent mud drapes reworked from shoreface sediment.

Scarce bioturbation indicates that the sandy substrate was, in contrast to the organic-rich mud of the shale-and-siltstone facies, a poor food source for soft-bodied infauna. Poor orientation and disarticulation of crinoids and brachiopods (fig. 26) indicates transport, but it is doubtful that the skeletal material was transported from the adjacent shelf which lacked calcified faunas or from back barrier environments which may have had reduced salinity. One interpretation is that the sandy substrate was firm enough to support suspension-feeding epifauna. Perhaps these organisms lived at the foot of the shoreface where substrates were most stable.

Figure 23.--Core photograph of high-angle cross-beds (Carter sandstone, North Blowhorn Creek oil unit, well PN2999, 2,206 ft).

Figure 24.--Core photograph of shale clasts and anastomosing clay laminae (Carter sandstone, North Blowhorn Creek oil unit, well PN3058, 2,291 ft).

As with shale clasts, shell accumulations apparently formed in more than one manner. Some thin accumulations, particularly those in low-angle crossbedded sandstone, are interpreted to represent shells washed up on the beach, whereas other accumulations, particularly those in rippled sandstone, were concentrated by shoreface currents. The thickest shell accumulations, like that in well PN3236, ostensibly formed in rip channels or are thick lower shoreface storm deposits.

VARIEGATED FACIES

Characteristics

The variegated facies contains shale, siltstone, and sandstone, and is so named because these strata contain the most diverse colors in the Carter interval (fig. 14). The facies has a serrate to blocky log signature with resistivity intermediate between that of the shale-and-siltstone and sandstone facies. Cores establish that the variegated facies generally occurs in the upper part of the Carter interval and is restricted to the depositionally updip end of the sandstone lenses that make up the reservoir rock body in North Blowhorn Creek oil unit. Within the lenses, the sandstone facies grades depositionally updip into lenticular sandstone, siltstone, and shale, which, in turn, grade into medium gray siltstone and dark gray to brownish-gray shale and mudstone.

Lenticular-bedded sandstone, siltstone, and shale predominate in the variegated facies (fig. 14). Sandstone and siltstone occur as irregular, yellowish-brown, calcareous lenticles that typically range in thickness from 0.5 to 4.0 inches and are separated by anastomosing clay laminae. Most of the lenticles appear structureless, but some sandstone and siltstone contains deformed ripple cross

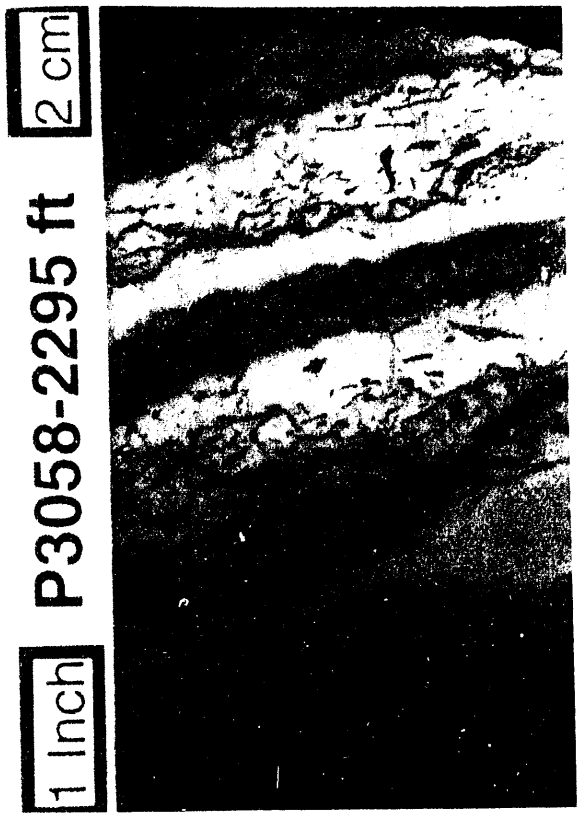

Figure 25.--Core photograph of kaolinite-cemented sandstone containing abundant clay laminae and shale clasts (Carter sandstone, North Blowhorn Creek oil unit, well PN3058, 2,295 ft).

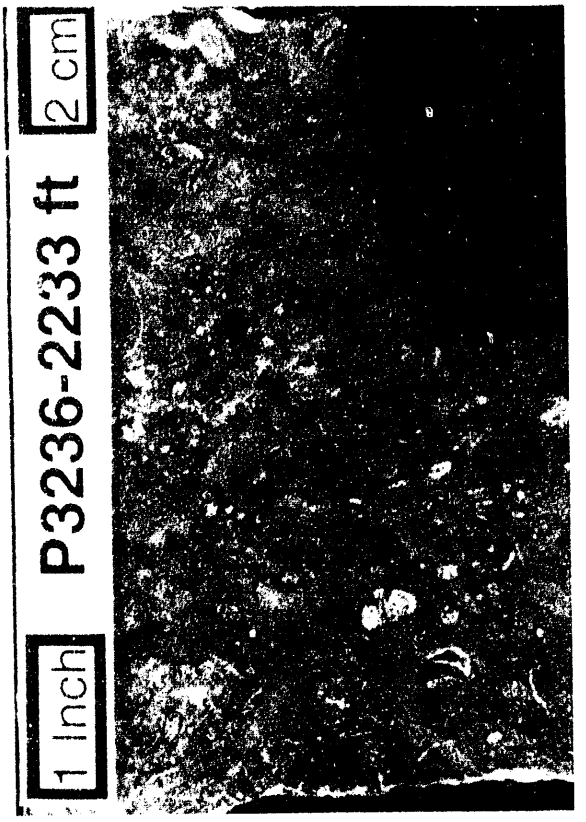

Figure 26.--Core photograph of accumulation of skeletal debris, consisting of poorly oriented brachiopod shells and echinoderm ossicles (Carter sandstone, North Blowhorn Creek oil unit well PN3236, 2,233 ft).

laminae which reveal that the lenticles represent pebble- to cobble-size rip-up clasts. The lenticles contain few biogenic structures, although branching, dark reddish-brown siderite rhizoids, or root structures, are locally abundant (fig. 27). Sandstone in the variegated facies is cemented pervasively with kaolinite, siderite, and ferroan dolomite/ankerite, which impart a yellowish- to reddish-brown color mottling to much of the facies

Farther updip depositionally, lenticular-bedded units grade into relatively homogeneous medium- to thick-bedded shale and siltstone. The siltstone contains well-developed laminae that are disrupted by abundant feeding and escape burrows as well as siderite rhizoids. Dark gray shale, in contrast, is locally laminated and contains plant fragments. Most of the shale is root mottled or contains abundant slickensides. Sand- to granule-size caliche nodules are also present in the shale. Medium to thick beds of red (brownish-gray) shale have gradational contacts with the dark gray shale and are also root mottled and contain caliche nodules. In well PN3160, red mudstone contains caliche nodules that are up to pebble size.

Interpretation: Backshore

The variegated facies is interpreted to represent a suite of backshore environments in which sedimentation was dominated by storm surges and soil formation (fig. 18). The depositionally updip position of the serrate, moderately resistive variegated facies relative to the blocky, highly resistive sandstone facies (figs. 12, 13) indicates that beach topography sloped uniformly offshore and that eolian dune ridges, which are so prevalent in modern beach-barrier systems (McCubbin, 1982; Elliott,

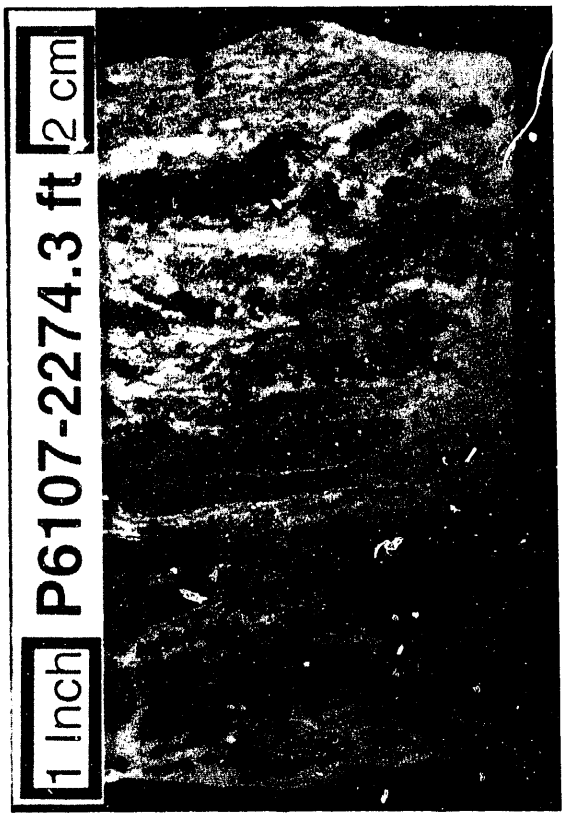

Figure 27.--Core photograph of siderite rhizoids in variegated facies (Carter sandstone, North Fairview oil field, well PN6107, 2,274.3 ft).

1986) were not present. Facies analysis of the Carter sandstone in North Blowhorn Creek oil unit suggests that washover fans, which develop as dune ridges are breached by a surging sea, also were not developed in the unit. Instead, unusual structures herein designated as storm-surge aprons are interpreted to have been the major lower backshore deposit.

Occurrence of root structures and abundant rip-up clasts immediately landward of the foreshore indicate episodes of high-energy sedimentation in the supratidal zone. Although no clear analogs for these deposits have been identified, intermittent flooding of the supratidal zone occurs on wind-tidal flats (Miller, 1975; Reineck and Singh, 1980). However, modern wind-tidal flats form in protected lagoons and embayments and are thus dominated by low-energy sedimentary structures. In contrast, the Carter rip-up clasts formed immediately behind an unprotected foreshore and are thus interpreted to have been deposited by major storm surges which can raise water level more than 20 feet during hurricanes (Hayes, 1967).

Although sedimentation in the lower backshore was dominated by vigorous, storm-induced flows, low-energy processes prevailed in the upper backshore. Root structures and caliche nodules provide evidence for exposure in an evaporative setting. Gray paleosols probably formed in marshy areas that favored reduction and preservation of organic matter, whereas red paleosols probably formed on topographic highs that favored oxidation and caliche formation. Laminated or burrowed shale and siltstone is interpreted to have formed in paludal environments, and some of these deposits may represent saline slackwater ponds that remained after storm-surge floods.

DEPOSITIONAL MODEL

Sandstone-body geometry and depositional sequences indicate that the Carter sandstone in North Blowhorn Creek oil unit represent a spit complex (fig. 28). Spits form at the down-drift ends of barrier islands and are characterized by a fanlike arrangement of beach ridges that curve shoreward and accrete in the direction of geostrophic flow. Spit-type systems occur in several depositional settings, including tidal inlets (Boothroyd, 1985), estuary mouths (Fairbridge, 1980; Smith, 1986), and chenier plains (Gould and McFarlan, 1959).

The sublinear northwest boundary of the sandstone body marks the seaward spit margin, whereas the irregular southeast margin delineates several spit arms (figs. 11, 28). The most compelling evidence for a spit complex in North Blowhorn Creek is the shingling of successively smaller sandstone lenses toward the southeast terminus of the sandstone body in cross-section A-A' (fig. 12). Each sandstone lens is interpreted to represent a spit arm, and the largest arms are in the west-central and southeastern parts of the oil unit.The arrangement and internal facies architecture of the sandstone lenses provides increased understanding of current systems and the resulting beach morphodynamics in Upper Mississippian rocks of the Black Warrior basin. Evidence for storm surges in a northeast-facing beach system establishes that the dominant wind direction was onshore and had a major south to southwest component (figs. 18, 28). Southeastward spit accretion indicates that significant geostrophic flows were directed southeast during Carter deposition. The acute, westward curving of some spit arms indicates that geostrophic flows had a strong onshore component and thus veered sharply at the end of the spit complex, perhaps even during fair weather.

Although the lensoid nature of the Carter sandstone in North Blowhorn Creek superficially resembles reservoirs in the Lewis sandstone, the morphodynamics of the beach systems differed markedly. Some Lewis beaches were intertidal structures and were therefore active only during parts of the tidal cycle (Pashin and others, 1991). In contrast, Carter beach deposits lack evidence for tidal processes and were essentially reflective systems dominated by varying meteorology and wave climate.

The North Blowhorn Creek spit had characteristics of cheniers and delta-destructive barrier-island arcs. Cheniers and barrier-island arcs form linear to arcuate sand bodies in muddy depositional systems and form on or at the margin of abandoned delta lobes (Gould and McFarlan, 1959; Wells and Coleman, 1981; Penland and Boyd, 1985). However, the Carter spit was part of a muddy strand plain that developed on a former carbonate platform; that platform lay just beyond the limit of major delta progradation (figs. 6, 7).

One way to interpret Carter beach systems is as delta-destructive elements that accumulated immediately beyond abandoned and exposed delta lobes; the beach systems were fed ostensibly by younger, active delta lobes in the northwest. Cross-sections B-B' and D-D' (figs. 12, 13) demonstrate that blocky beach-shoreface sandstone occurs farther above the Bangor Limestone in each successive sandstone lens. This configuration suggests that spit deposition occurred as soft, fluid shelf mud compacted and also suggests that deposition occurred during an episode of net relative sea-level rise. As relative sea level continued to rise and nearby deltaic sand sources waned, the North Blowhorn Creek spit was inundated, and shallow-water carbonate deposition represented by the Millerella limestone occurred across the area.

PETROLOGY

Knowledge of the detrital and authigenic mineral composition of sandstones is important to recognizing reservoir heterogeneity and planning enhanced oil recovery operations for several reasons. Experimental and empirical studies have demonstrated the dependence of reservoir quality on sandstone composition (for example, Bloch, 1991; Selley, 1978; Scherer, 1987). The degree of mechanical and chemical stability of the detrital framework affects porosity and permeability evolution during burial. Understanding the evolution of detrital grain replacing and pore filling authigenic minerals contributes substantially to understanding the nature of the pore network in sandstone reservoirs and its relationship to petrophysical properties. Additionally, knowledge of the

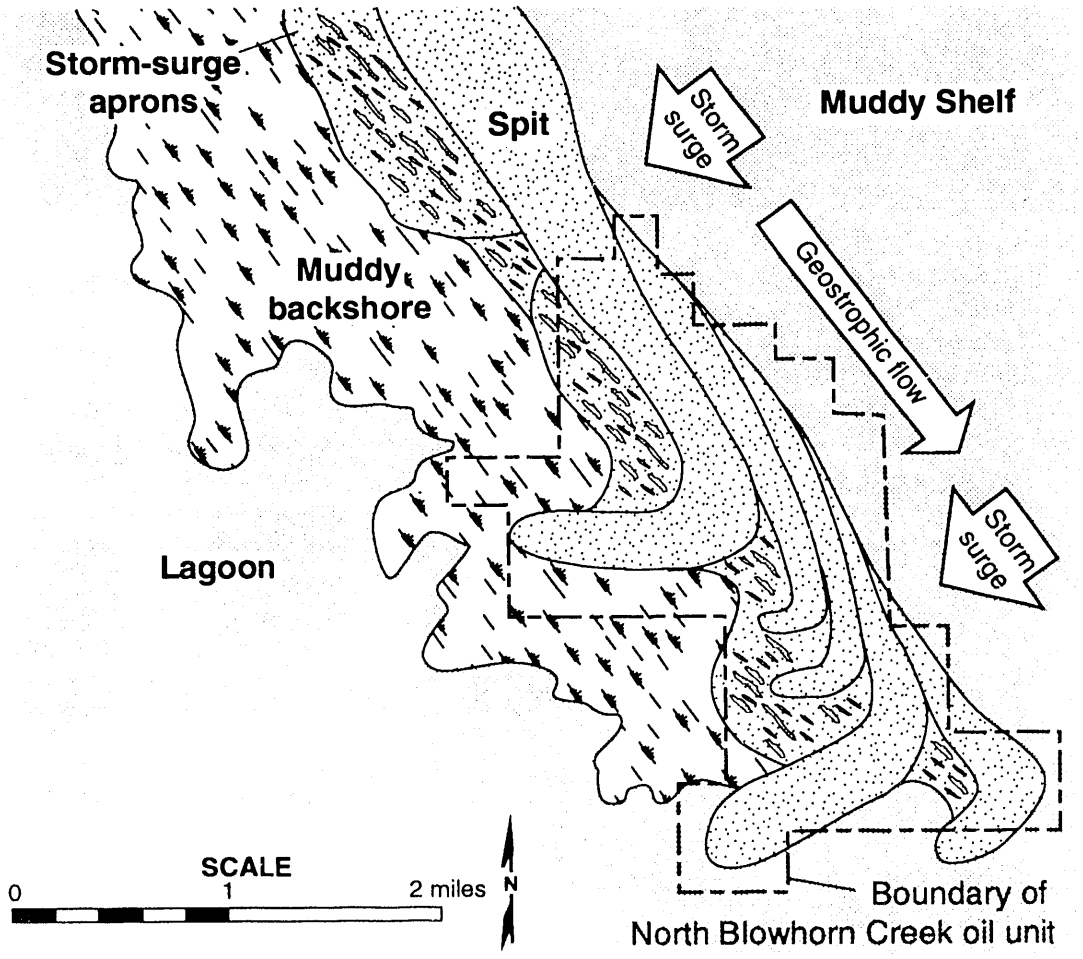

Figure 28.--Paleogeographic reconstruction of North Blowhorn Creek spit complex.

diagenetic character of a sandstone can be used to avoid formation damage during drilling, completion, stimulation, and production (Almon and Davies, 1981; Harper and Buller, 1986; Hurst and Archer, 1986; Kantorowicz and others, 1986; Krueger, 1986). Detailed characterization of the mineral composition of a reservoir sandstone is necessary at all stages of field development (Kantorowicz and others, 1986). In order for this knowledge to be useful in field development, however, it must be related to engineering performance (Harper and Buller, 1986).

This section discusses the detrital framework composition and diagenetic character of Carter sandstone in North Blowhorn Creek oil unit in order to delineate factors that contribute to levels 4 and 5 reservoir heterogeneity. The detrital and diagenetic character of Carter sandstone in this reservoir is similar to that of Mississippian sandstone oil reservoirs elsewhere in the Black Warrior basin of Alabama and Mississippi (Shepard, 1979; Bearden, 1984; Bat, 1987; Cleaves and Bat, 1988; Hughes and Meylan, 1988). Therefore, generalizations made in this report regarding aspects of detrital-framework composition and diagenesis that influence reservoir heterogeneity are likely to have application to Mississippian sandstone reservoirs throughout the basin, although attention should be paid to the effects of variation among depositional and early geochemical environments. Generalizations made in this report probably are not applicable to overlying Pottsville sandstones because of a significant increase in the percentage of unstable lithic detrital framework grains (Mack and others, 1981, 1983; Raymond, 1990).

DETRITAL FRAMEWORK

Carter sandstone is dominantly very fine-to medium-grained, moderately to well-sorted quartzarenite, according to the classification of Folk (1980) (fig. 29) if intrabasinally derived shale clasts are excluded from the detrital framework for classification. If intrabasinal clasts are included, some Carter sandstone can be classified as sublitharenite. Nevertheless, Carter sandstone is quartzose (fig. 30). This composition is compatible with that determined by other workers (Shepard, 1979; Bearden, 1984; Hughes and Meylan, 1988) for Carter sandstone in much of the Black Warrior basin. Despite the quartzose nature of the sandstone, the reservoir in North Blowhorn Creek oil unit is heterogeneous owing to the geometry and facies variation of sandstone lenses, but also to the presence of intrabasinally derived framework grains and to diagenesis.

QUARTZ

Subangular to well-rounded quartz composes more than 97 percent of the detrital framework of most Carter sandstone in North Blowhorn Creek oil unit. More than 90 percent of detrital quartz in North Blowhorn Creek oil unit is monocrystalline; more than 95 percent of this quartz has nonundulose to slightly undulose extinction. Only two monocrystalline quartz grains containing inclusions of vermicular chlorite were found. Although an extremely minor component of the sandstone, this interesting type of quartz is indicative of a hydrothermal vein provenance (Folk, 1980). Polycrystalline quartz is present (fig. 31), but generally comprises less than 10 percent of total quartz. Polycrystalline quartz grains contain both stable and unstable textures (Young, 1976), including textures indicating metamorphic provenance.

FELDSPAR

Feldspar is scarce in Carter sandstone, typically composing less than one percent of total rock volume. Feldspars present in the sandstone include orthoclase, microcline, plagioclase, and perthite. This feldspar assemblage is generally indicative of a plutonic provenance. However, the present feldspar composition of Carter sandstone likely is not representative of feldspar composition at the time of deposition because of the effects of diagenesis. Most Carter sandstone in the reservoir interval contains kaolinite within detrital grain size and shape areas that occupies several volume percent of the sandstone. Much of this kaolinite likely originated by alteration of detrital feldspar. Additional evidence for diagenetic alteration of feldspar includes scarce skeletal feldspars that contain intragranular porosity.

ROCK FRAGMENTS

Rock fragments in Carter sandstone are both extrabasinal and intrabasinal. Extrabasinal rock fragments were transported to the site of deposition from outside the sedimentary basin and are useful for determining provenance, whereas intrabasinal rock fragments are locally derived within the depositional basin (Zuffa, 1985). Intrabasinal rock fragments are not useful for provenance determination but strongly affect reservoir quality and are a major source of heterogeneity in Carter sandstone. Both types of rock fragment together account for in excess of 20 percent of total rock volume in some Carter sandstones in the North Blowhorn Creek oil unit. However, extrabasinally derived rock fragments are a minor component of Carter sandstones and account at most for only a few percent of the total detrital framework. The most common type of extrabasinal rock fragment is chert, which accounts for as much as three percent of framework volume in a few samples. Chert fragments imply a sedimentary source for Carter sandstone. The amount of chert in Carter sandstone may have been overestimated by workers in the past because chert has a similar appearance to authigenic kaolinite that typically occupies detrital grain-size volumes in Carter sandstone. Correct identification of chert has obvious implications for provenance determination, whereas correct identification of kaolinite has implications, both for provenance determination if kaolinite replaces

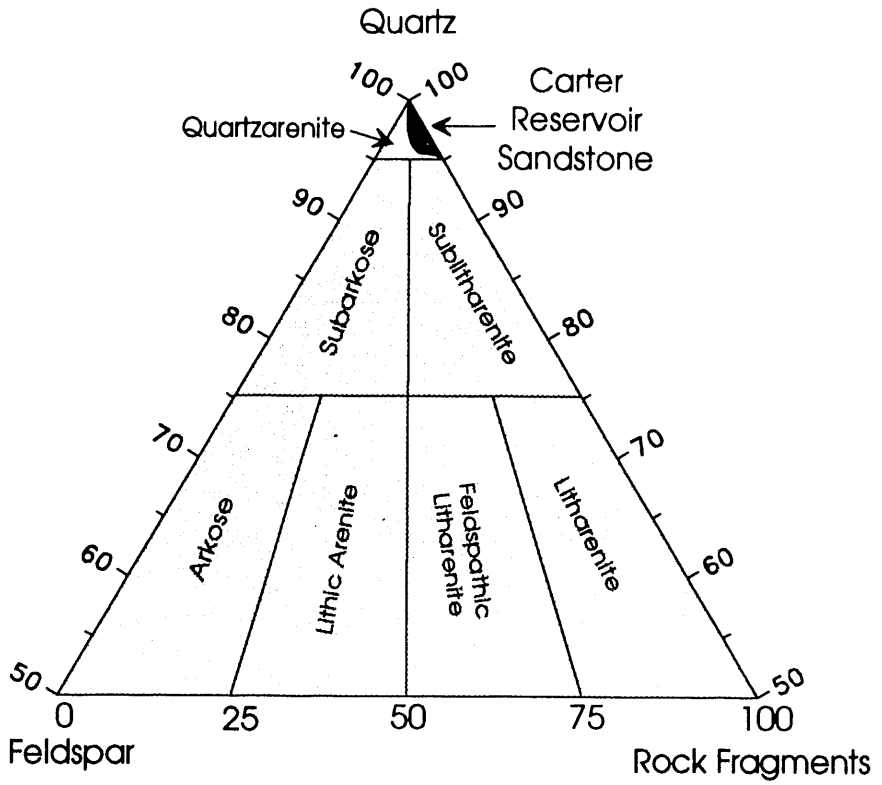

Figure 29.--Detrital framework composition of Carter sandstone (classification diagram of Folk (1980).

feldspar, and for reservoir quality because of production problems and correct determination of water saturation from well logs. Phyllitic rock fragments derived from low-rank metamorphic sources are present but scarce. Some foliated, clay-rich rock fragments have equivocal textures which suggest derivation either from shale or from slate.

Intrabasinal rock fragments most commonly are rip-up clasts. These clasts range in size from the average grain size of the sandstone to clasts several times larger than average grain size. The composition of intrabasinal clasts is variable. Most are clay-mineral rich; however, others are sideritic mud. Clay-mineral-rich shale fragments have a detrimental effect on the quality of Carter reservoirs because they deform plastically during compaction to form pseudomatrix that occludes porosity (figs. 32 through 34). This type of fragment also provides an optimal site for pressure solution. The dominant clay mineral in most fragments is kaolinite (fig. 35), but chlorite (fig. 36) is also abundant in some fragments. Illite and quartz are less abundant components. The kaolinite in these fragments has large surface area, contains major microporosity, and typically contains irreducible water, thus creating a potential migration-of-fines problem and difficulty in interpreting water saturation using well logs (Almon and Davies, 1981).

OTHER DETRITAL FRAMEWORK COMPONENTS

Fossil fragments, micas, and heavy minerals are minor framework components in Carter sandstone. Fossil fragments occur in most Carter sandstone in minor amounts and are localized only in shell lags in beach and shoreface deposits where they may account for more than 20 percent of total rock volume. Fossils include abraded fragments of brachiopods, bryozoans, echinoderms, and gastropods. These fossil fragments have lost their original internal structure; most have been

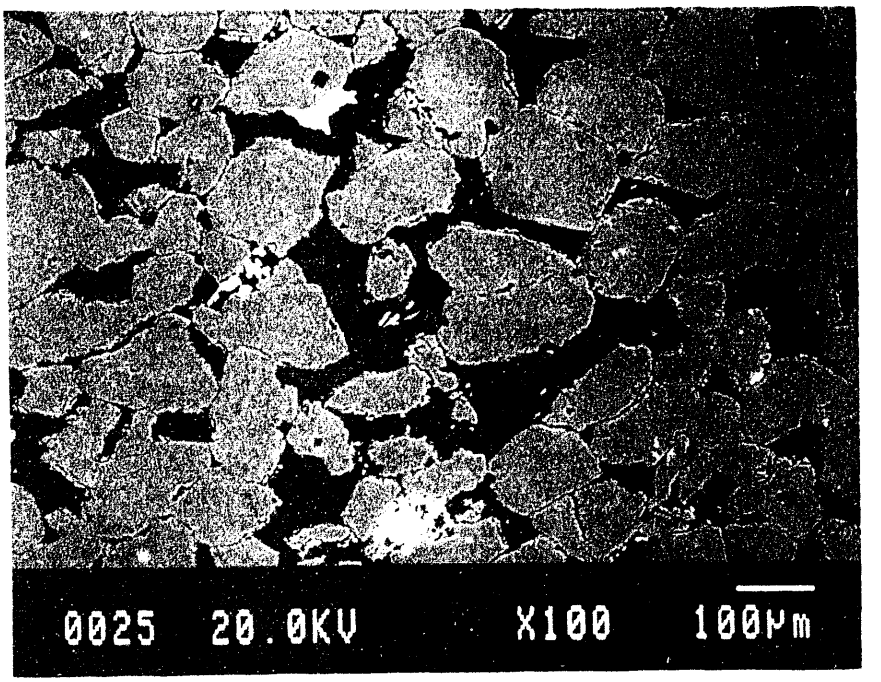

Figure 30.--Backscattered-electron micrograph showing detrital framework grain composition of Carter sandstone (Carter sandstone, North Blowhorn Creek oil unit, PN2999, 2,194 ft; scale is on photograph). All detrital grains in the field of view are quartz (medium gray areas). Kaolinite (dark gray), which may have replaced detrital feldspar, occupies two grain-size areas in the center of the micrograph. White areas are authigenic ferroan dolomite/ankerite and siderite. Black areas are pores.

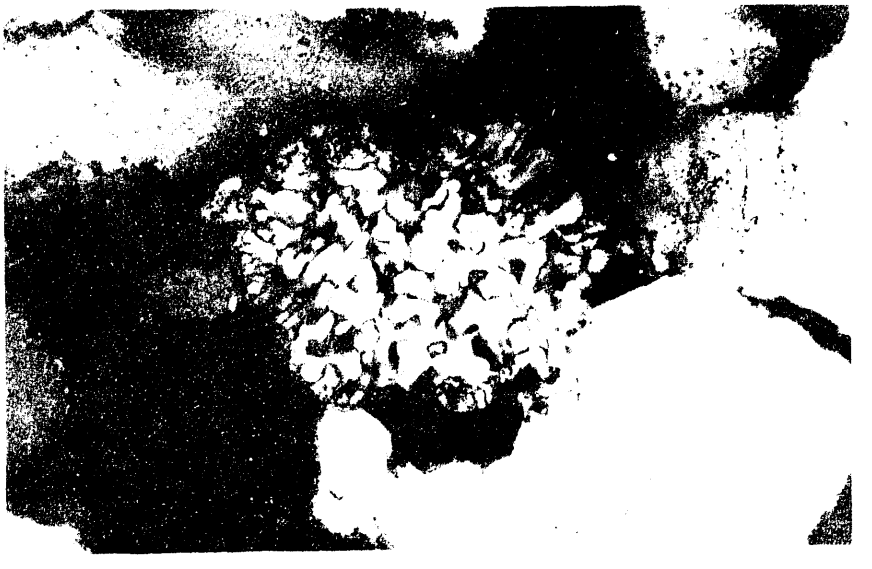

Figure 31.--Thin-section photomicrograph of polycrystalline quartz detrital framework grain (Carter sandstone, North Blowhorn Creek oil unit, well PN3058, 2,291 ft; crossed polars; field of view = 2.6 mm).

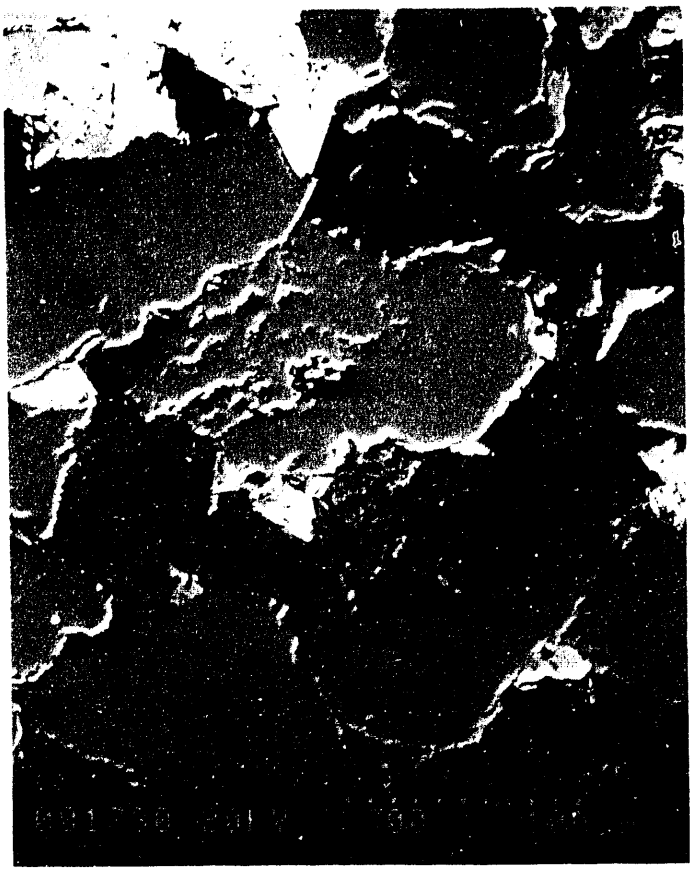

Figure 32.--Backscattered-electron micrograph of deformed intrabasinal shale fragments (Carter sandstone, North Blowhorn Creek oil unit, well PN3160, 2,311.7 ft, scale is on photograph). The mud fragments are the dark gray areas in the lower center of the photograph. Detrital quartz grains are medium gray; authigenic ferroan dolomite/ankerite are light gray; and pores are black.

replaced by ferroan calcite or ferroan dolomite/ankerite. Some fossil fragments have completely or partially dissolved to form moldic pores. Although fossil fragments are not abundant, they are an important control on heterogeneity in Carter and other Mississippian reservoirs in the Black Warrior basin because they serve as nucleation sites for pore-filling carbonate-mineral cement.

Micas are also minor framework constituents in Carter sandstone and are most abundant in very fine grained sandstone and nonreservoir siltstone. Most detrital mica in Carter sandstone is muscovite, but some bleached, bloated biotite is also present, as is detrital chlorite. Micas are typically bent around harder detrital framework grains due to compaction, and some have splayed ends. Some muscovite, biotite, and chlorite is partially to completely replaced by authigenic kaolinite.

The heavy mineral assemblage in Carter sandstone, as determined from thin-section observation, is ultrastable, consisting of tourmaline and zircon. The present composition of the heavy-mineral assemblage is due to sedimentary recycling and/or to burial diagenesis and is not diagnostic of provenance (Pettijohn, 1941; Morton, 1985; Milliken, 1988; Milliken and Mack, 1990).

Figure 33.--Secondary-electron micrograph of deformed intrabasinal shale fragments between detrital quartz grains (Carter sandstone, North Blowhorn Creek oil unit, well PN3160, 2,313.7 ft; scale is on photograph). Note the micropores within the mud fragments.

Figure 34.--Thin section of photomicrograph of pseudomatrix formed by deformation of dutile, intrabasinal mud clasts (Carter sandstone, North Blowhorn Creek oil unit, well PN3058, 2,291 ft; plane polarized light; field of view = 1.0 mm).

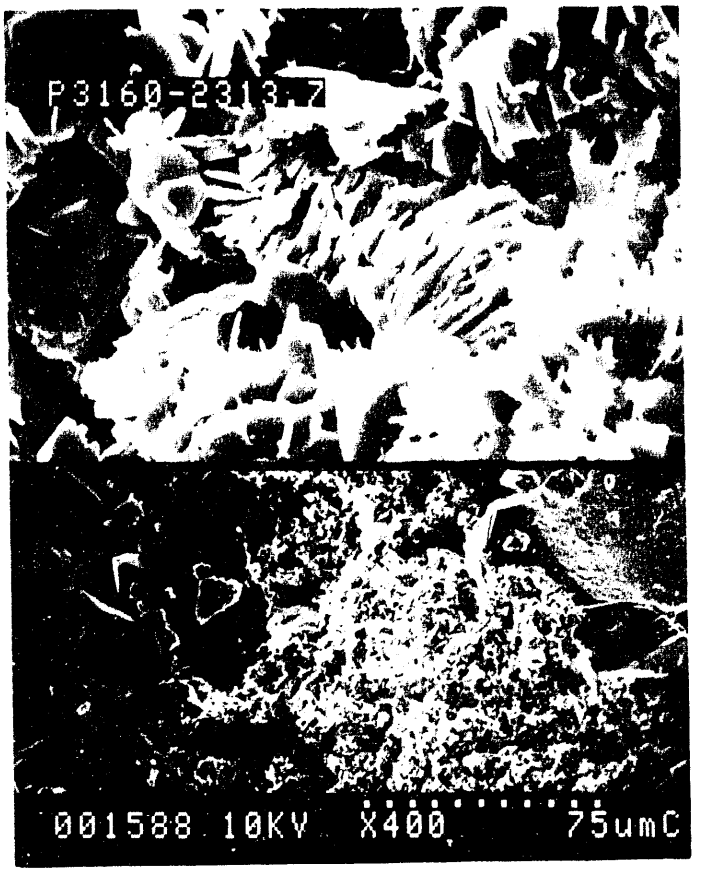

Figure 35.--Secondary-electron micrograph of kaolinite in an intrabasinal shale fragment (Carter sandstone, North Blowhorn Creek oil unit, well PN3160, 2,313.7 ft; scale for lower photograph is on the photograph). There is also a minor amount of illite within the field of view. The field of view in the upper photograph is outlined in the lower photograph.

PROVENANCE OF CARTER SANDSTONE

The geographic location of the source area for the Carter sandstone in North Blowhorn Creek oil unit, based on petrographic observation, is equivocal. The reason for this is that extracting provenance information from quartzarenite is difficult (Blatt, 1982). The presence of chert, the abundance of well-rounded quartz, and scarce abraded quartz overgrowths in Carter sandstone suggest recycling from older sedimentary source terranes. The presence of feldspars derived from plutonic rocks and of metamorphic rock fragments suggests that those rock types also were present in the source area. However, a major problem that has bearing on provenance determination is reconstruction of the original detrital framework composition, particularly with respect to feldspar.

Textural evidence such as oversize areas of carbonate cement clearly indicate that framework grains have dissolved. Although, some of these grains may have been intrabasinal shale clasts, some may have been chemically unstable feldspar. Much of the authigenic kaolinite that occupies detrital grain-size volumes in Carter sandstone probably replaced detrital feldspar. The present detrital framework composition of Carter sandstone in North Blowhorn Creek oil unit falls within the cratonic interior provenance field on the tectonic-provenance discriminate diagrams of Dickinson and coworkers (Dickinson and Suczek, 1979; Dickinson and others, 1983; Dickinson, 1985). However,

Figure 36.--Secondary-electron micrograph of face-to-face and face-to-edge flakes of chlorite in an intrabasinal mud fragment (Carter sandstone, North Blowhorn Creek oil unit, well PN3058, 2,287 ft, scale is on photograph).

without quantitative assessment of the magnitude of framework grain replacement and/or dissolution in Mississippian sandstone in the Black Warrior basin, interpretation of source area using tectonic-provenance discriminate diagrams is premature. The reason for this is that small variation in the amount of feldspar in quartzose sandstone can result in a change of field in which the composition of the sandstone plots on the tectonic discriminate diagrams. Milliken and others (1989) demonstrated the effects of feldspar alteration in interpretation of tectonic-provenance discriminate diagrams for Tertiary sandstone of the Texas Gulf Coast.

An additional problem elucidated by Mack (1984) as an exception to the relation between sandstone composition and plate tectonics concerns enrichment of quartz by reworking of detritus and degradation of labile minerals in shallow marine environments, such as that in which Carter sandstone was deposited. This enrichment of quartz in specific depositional settings could result in erroneous interpretation of tectonic setting from compositional data. Mack (1978) demonstrated this type of sedimentary fractionation in fluvial, eolian, and shallow-marine sandstones of the same provenance in the Cutler and Cedar Mesa formations in Utah. Mack (1984) suggested that Mississippian Hartselle Sandstone in the Black Warrior basin of Alabama is an example where the present detrital composition leads to erroneous tectonic-provenance interpretation. However, quartzarenite can be produced by processes other than sedimentary recycling and sedimentary reworking. First-cycle (Franzinelli and Potter, 1983) and diagenetic (McBride, 1987) quartzarenite also has been documented.

Until the effect of diagenesis on the framework composition of Carter and other Mississippian reservoir sandstone is better understood, provenance determinations for the Black Warrior basin

based on petrographic evidence will remain equivocal. In summary, the petrographic results of this study neither confirm nor reject the contention of Mack and others (1981, 1983) that Parkwood sandstone was derived from a Ouachita orogenic source. Similarly, the results of this study cannot be used to support a cratonic source, as suggested by Hughes and Meylan (1988) for Carter and Lewis sandstones from the Black Warrior basin of eastern Mississippi.

A technique which has not been used on Carter sandstone, but which may have promise in resolving problems of provenance, is cathodoluminescence petrography. Owen and Carozzi (1986) used cathodoluminescence petrography of detrital quartz to determine the provenance of Mississippian Jackfork quartzose sandstone in the Ouachita Mountains in Arkansas. Problems of provenance determination for Jackfork sandstone are similar to those for Carter and other Mississippian sandstones in the Black Warrior basin. Owen and Carozzi concluded that Jackfork sandstone was derived from the same southern source as the Parkwood Formation in the Black Warrior basin of Alabama. This conclusion directly conflicts with that of Cleaves and Broussard (1980) and Cleaves (1983), who suggest that Parkwood sandstone was derived from a northern cratonic source, based on subsurface mapping. Therefore, resolution of provenance of Mississippian sandstones in the Black Warrior basin will have implications for provenance studies in regions outside the Black Warrior basin, most notably the Ouachita trough.

MATRIX

The term matrix commonly has been used to describe any fine-grained material in a sandstone that is difficult to identify optically, regardless of its origin. If the goal of an investigation is to determine controls on reservoir heterogeneity in a predictive manner, the genetic origin of matrix must be determined. Jonas and McBride (1977) noted that, because of hydrodynamic considerations, only a minor amount of matrix-size material (particles <30 μm in diameter) can be transported with sand-size detrital grains. Therefore, an origin other than a detrital origin should be considered for sandstones with more than a few percent matrix-size material. Dickinson (1970) suggested that most matrix is authigenic in origin, resulting either from mechanical compaction of labile sand-size detrital grains (pseudomatrix) or from precipitation of finely crystalline, authigenic clay minerals. Other processes that result in mixtures of sand-, silt- and clay- size material include pedogenic infiltering of clay in soil zones, bioturbation, and slumping (Jonas and McBride, 1977). Prediction of the distribution of matrix in sandstone reservoirs requires detailed knowledge of both the depositional and the diagenetic evolution of the sandstone. An understanding of the origin and distribution of matrix-size particles is important, not only in interpretation of provenance and diagenesis, but also in interpretation of petrophysical properties (Neesham, 1977) and well-log response (Frost and Fertl, 1981). Previous research on Carter and Lewis sandstone in the Black Warrior basin suggests that matrix-size material is an important component (Shepard, 1979; Holmes, 1981; Bearden, 1984; Bat, 1987; Hughes and Meylan, 1988). Bearden (1984) noted an inverse relationship between thin-section porosity and the amount of matrix in Carter sandstone in North Blowhorn Creek and other Carter oil fields in Alabama. The results of the present study suggest that detrital matrix in the Carter sandstone generally composes less than one percent of total sandstone volume, as would be expected in sandstone deposited in a high-energy beach-barrier environment. Most detrital matrix in the Carter reservoir occurs as very small clay drapes or remnants of clay drapes, less than 1 mm in length, primarily in rippled sandstone. Despite the small volume of detrital matrix in the Carter, matrix-size material may account for 2 to more than 20 percent of the volume of some sandstones. In reservoir sandstone, matrix-size material has two origins. First, intrabasinally derived shale clasts deformed during burial to form pseudomatrix. Second, authigenic kaolinite replaced detrital feldspar grains during burial diagenesis. Matrix-size material of both origins results in increased tortuosity of fluid flow in reservoir sandstones. In some sandstone between closely spaced clay drapes within the reservoir interval, all intergranular areas are filled with kaolinite, formed by replacement of feldspar, micas, and intrabasinal shale fragments. This kaolinite is an authigenic mineral formed during burial diagenesis and, therefore, does not constitute matrix.

In nonreservoir sandstone and siltstone, matrix-size material is most commonly introduced by bioturbation. Matrix in these sandstones commonly occupies all intergranular areas. In nonreservoir backshore sandstone and siltstone above the reservoir interval, matrix is introduced locally by pedogenic processes.

DIAGENESIS

Diagenesis of Carter and Lewis reservoir sandstone in the Black Warrior basin of Alabama and Mississippi previously has been described by Shepard (1979), Holmes (1981), Bearden (1984), Bat (1987), and Hughes and Meylan (1988). Results of this study agree with these previous studies in general, but differ in detail. Specific differences include the origin of "matrix," the importance of authigenic clay minerals, and the composition of authigenic carbonate minerals. Volumetrically important authigenic minerals in Carter sandstone are quartz, kaolinite, and a variety of carbonate minerals, including siderite, nonferroan and ferroan calcite, and ferroan dolomite/ankerite (fig. 37). Chlorite and illite are minor authigenic clay minerals in a few samples, but do not affect reservoir properties. Mechanical and chemical compaction affect reservoir quality. Mechanical compaction resulted in plastic deformation of locally derived shale fragments around harder quartz detrital grains. Stylolites and areas of intergranular pressure solution are other important diagenetic features affecting reservoir quality in Carter sandstone.

CARBONATE MINERALS

Siderite

Authigenic siderite occurs both in Carter sandstone and in associated siltstone and shale. In cores, siderite can be recognized by its yellow-brown to red or red-brown color, which results from oxidation of the mineral. However, in some cores, ferroan dolomite/ankerite also has oxidized to a red color. In thin section, siderite commonly is brown in plane light, owing to oxidation. This oxidation typically obscures details of texture, but the mineral can be readily identified due to its high birefringence. Siderite occurs in several forms, including pervasive pore-occluding microcrystalline mosaics of 10 to 20 μm subhedral crystals in concretionary patches and horizons that may be several centimeters in thickness, as spherulitic patches (fig. 38) up to 0.5 mm in diameter, as thin isopachous coats on sand-size detrital framework grains (fig. 39), and as dispersed, "flattened" rhombic crystals ("wheatseed" siderite), up to 50 μm in length (fig. 39). Siderite concretions and spherulites are most abundant in siltstone and shale of nonreservoir shelf and backshore deposits. Bioturbation by burrowing organisms and roots localized siderite and resulted in color mottling in backshore deposits. Deflection of laminae around siderite concretions, open framework-grain packing and high minus-cement porosity (in excess of 40 percent) in shale and siltstone suggest that siderite precipitated prior to significant burial and compaction. Some siderite was partially to completely replaced by ferroan dolomite/ankerite during later burial diagenesis. In shoreface reservoir sandstone, siderite locally occurs as isopachous framework-grain coats and as dispersed rhombic crystals (fig. 39). Textural evidence indicates that the isopachous grain coats precipitated early in the diagenetic evolution of the sandstone. Isopachous siderite grain coats, however, are not well documented in the literature. Howard (1990) described isopachous siderite rims similar to those in Carter sandstone in Holocene and Pleistocene beach or nearshore environments on the Mississippi-Alabama-Florida continental shelf.

Within the reservoir interval, siderite may have been more abundant prior to late-stage burial diagenesis than it is at present. Some horizons that are pervasively cemented by ferroan dolomite/ankerite contain grains with isopachous siderite coats near their margins. These coats appear ragged due to partial replacement by ferroan dolomite/ankerite. Siderite coats are not present in the interiors of these cemented horizons. However, pristine isopachous siderite coats detrital grains in the porous sandstone immediately adjacent to the pervasively cemented zones. Ferroan dolomite/ankerite apparently replaced early siderite cement in these horizons. The nature of

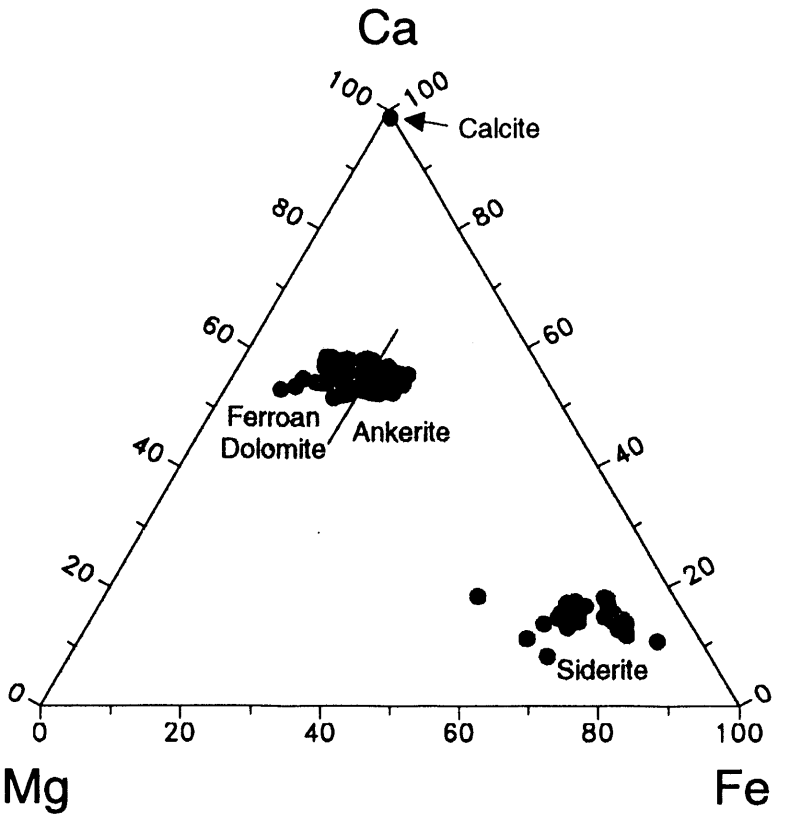

Figure 37.--Ca-Mg-Fe ternary diagram showing composition of authigenic carbonate minerals in Carter sandstone, based on electron microprobe analyses.

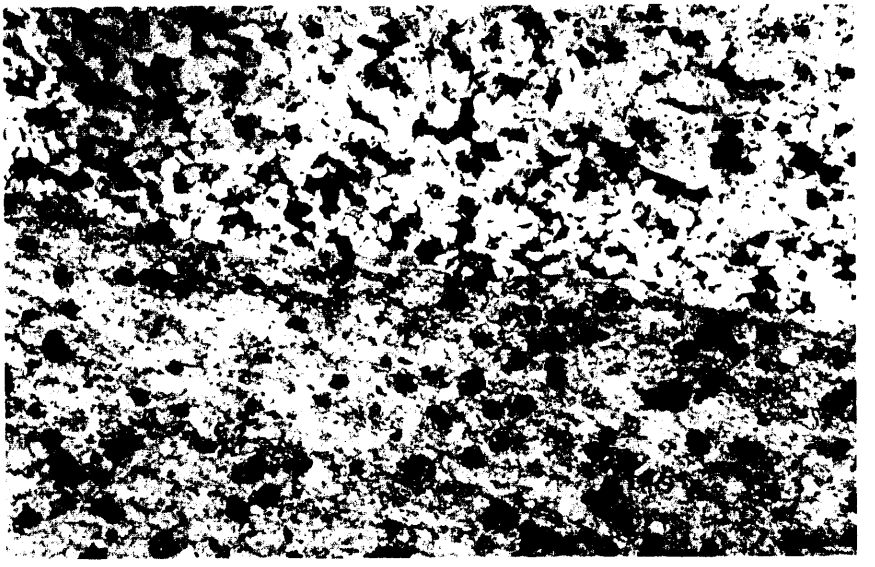

Figure 38.--Thin-section photomicrograph of spherulitic siderite in silty shale (Carter sandstone, North Blowhorn Creek oil unit, well PN3160, 2,293.4 ft; plane polarized light; field of view = 5.2 mm). The spherulites are the circular areas in the upper half of the photograph.

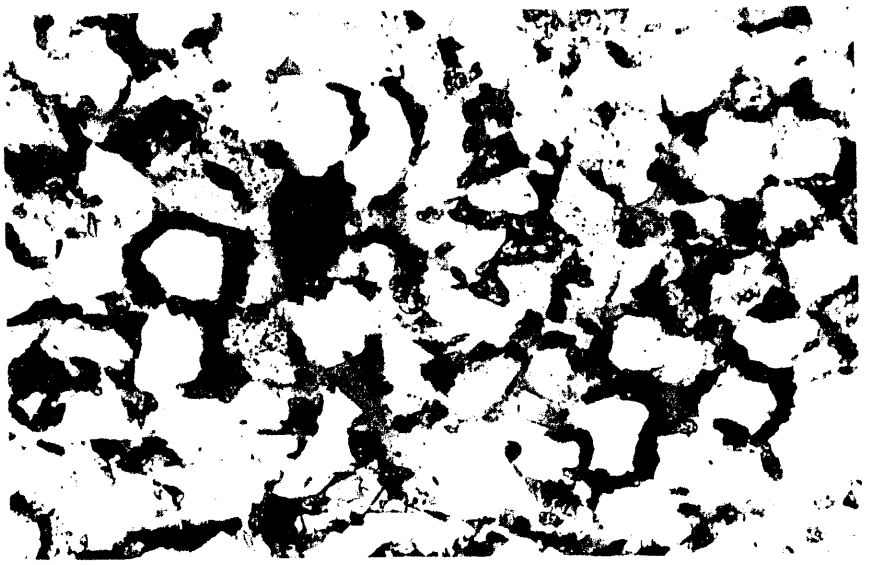

Figure 39.--Thin-section photomicrograph of isopachous and rhombic siderite (Carter sandstone, North Blowhorn Creek oil unit, well PN3314, 2,325 ft; plane polarized light; field of view = 1.0 mm).

siderite in the interior of the horizons is not known but perhaps was microcrystalline, mosaic siderite that occupied all pores. Isopachous siderite rims formed on detrital grains near the margins of these concretionary horizons. Ferroan dolomite/ankerite subsequently replaced siderite completely in the concretions, but only partially replaced the isopachous siderite near their margins.

Cement-stratigraphic relationships suggest that dispersed rhombic crystals also formed early but precipitated after the isopachous grain coats. Ultraviolet-light-induced fluorescence microscopy, using techniques described by Mozley (1989), and backscattered electron imaging show that the rhombic crystals are complexly chemically zoned, reflecting variations in Fe/(Ca + Mg) ratios. Generally, rhombic siderite crystals are more iron-rich on their outer margins than their cores. Electron microprobe analysis reveals the impure nature of the siderite (fig. 40) with extensive substitution of magnesium and calcium for iron in the crystal lattice. Siderite precipitates in reducing, anaerobic, sulfide-free environments, corresponding to zones of methanogenesis (Berner, 1981). The methanogenic zone is located below the oxic and sulfate-reduction zones. Pore water in the methanogenic zone is sulfide-free due to sulfate-reducing bacteria.

Nonferroan and Ferroan Calcite

Nonferroan and ferroan calcite are scarce in Carter reservoir sandstone but occlude all pores in intervals containing skeletal debris (figs. 41, 42). Concentrations of fossil debris occur in a variety of settings within the Carter depositional system at North Blowhorn Creek oil unit, including beach and shoreface deposits. These calcite-cemented intervals range from centimeters to decimeters in thickness; some are less than the width of a core, but most are laterally more extensive. Concentrations of skeletal debris cemented by calcite are significant level-4, and, perhaps, level-3, heterogeneities in shoreface sandstone in the central and southern parts of North Blowhorn Creek oil unit.

Nonferroan and ferroan calcite are present only in intervals containing fossil fragments; these minerals are absent throughout the rest of the Carter sandstone. Both minerals typically are replaced by ferroan dolomite/ankerite. Nonferroan calcite occurs as mosaics of crystals between framework grains and as poikilotopic crystals that encompass several framework grains (figs. 41, 42). Loose detrital grain packing and high minus-cement porosity indicate that calcite precipitated during early diagenesis, prior to significant compaction. Ferroan calcite has the same occurrence as nonferroan

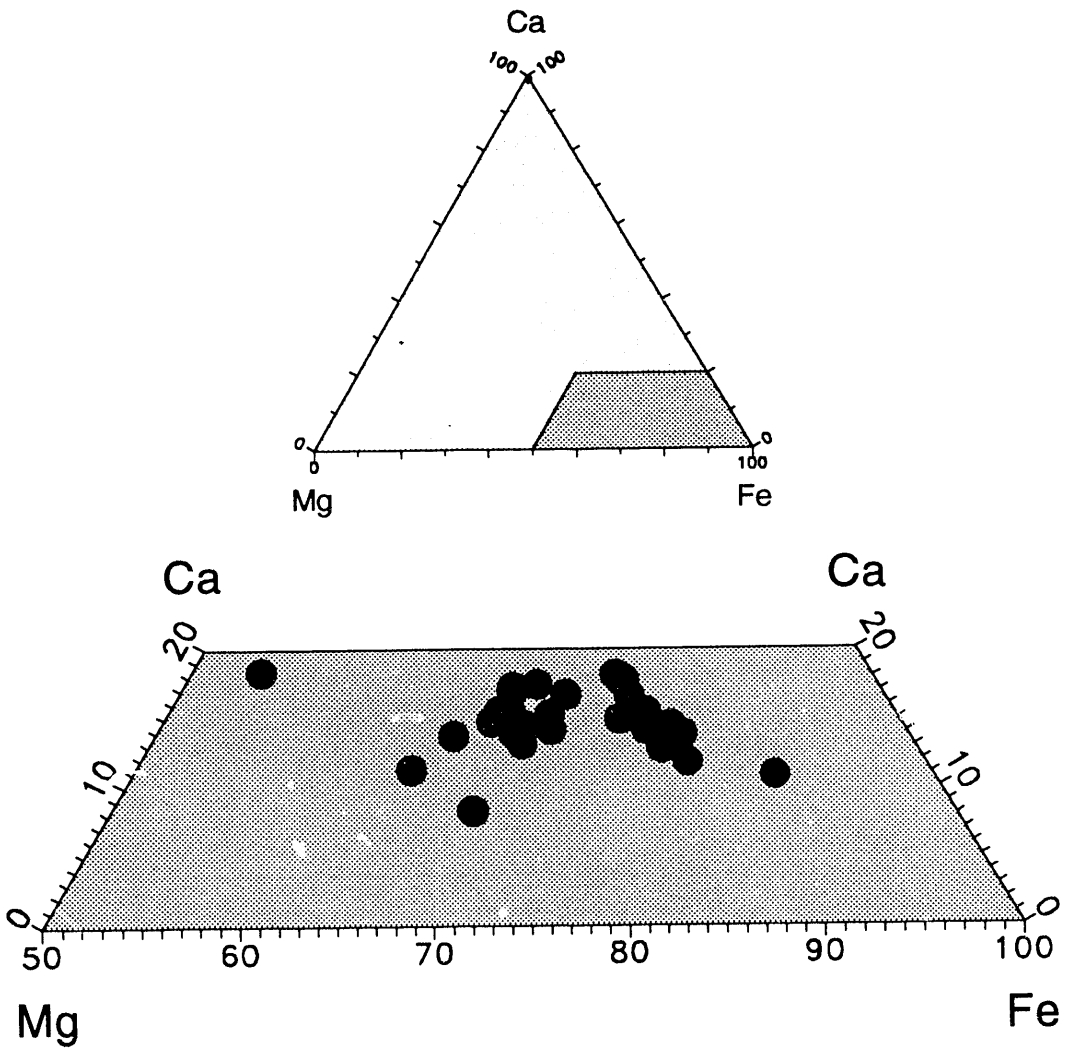

Figure 40.--Expanded corner of Ca-Mg-Fe ternary diagram showing chemical composition of authigenic siderite in Carter sandstone based on electron microprobe analyses.

calcite and therefore is limited in its distribution in Carter sandstone. Ferroan calcite was identified by its mauve to purple color after staining with alizarin red-S and potassium ferricyanide.

Fossil fragments in calcite-cemented intervals have been recrystallized and have lost their original internal structure. Chemically, calcite crystals that precipitated in dissolution pores in the interior of partially dissolved fossil fragments typically are concentrically zoned (fig. 43). Concentric zonation is due to variation in the abundance of iron. Most crystals are enriched in iron at their outer margins relative to the cores. Preservation of this zonation suggests that this calcite cement has not been recrystallized.

Ferroan Dolomite/Ankerite

Ferroan dolomite/ankerite is the most abundant authigenic carbonate-mineral in Carter sandstone in North Blowhorn Creek oil unit and occupies in excess of 40 percent of total rock volume

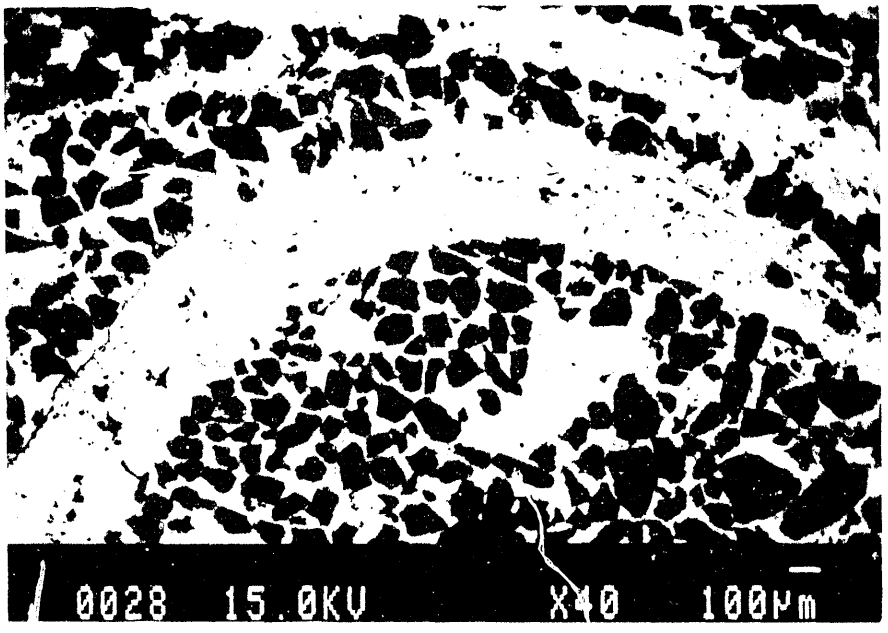

Figure 41.--Backscattered-electron micrograph of pervasive calcite cement (Carter sandstone, North Blowhorn Creek oil unit, well PN3160, 2,302.5 ft; scale is on photograph). The calcite is white. Note the open packing of quartz framework grains (dark gray). Light gray areas in the center of the fossil fragment are ferroan dolomite/ankerite.

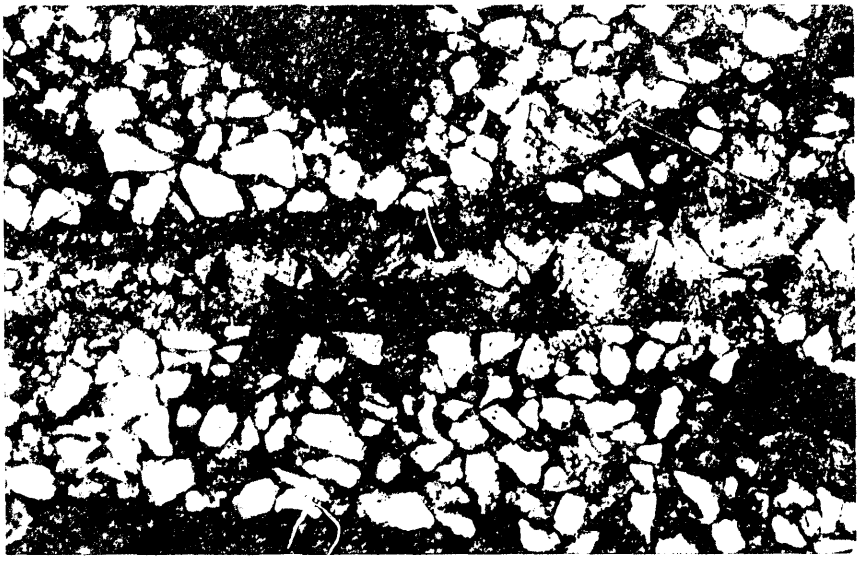

Figure 42.--Thin-section photomicrograph of sandstone pervasively cemented by nonferroan and ferroan calcite (Carter sandstone, North Blowhorn Creek oil unit, well PN3069, 2,263.5 ft; plane polarized light; field of view = 2.6 mm). Note ferroan dolomite/ankerite crystals replacing the central part of a fossil shell fragment in the center of the photograph.

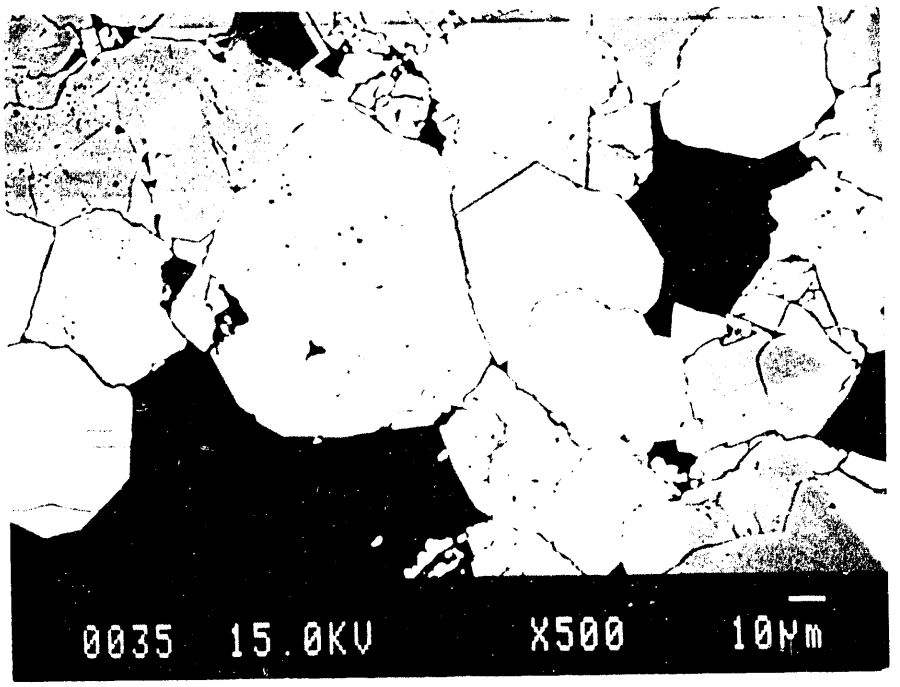

Figure 43.--Backscattered-electron micrograph of concentrically zoned calcite crystals in a dissolution void in a fossil fragment (Carter sandstone, North Blowhorn Creek oil unit, well PN3160, 2,302.5 ft; scale is on photograph).

in some sandstone with concentrations of fossil debris and in nonreservoir siltstone and very fine grained sandstone. Ferroan dolomite/ankerite cement is a major heterogeneity in Carter sandstone in North Blowhorn Creek oil unit that forms permeability barriers within the reservoir and partially to completely seals the margins of the reservoir. Ferroan dolomite/ankerite has not been reported previously in Carter sandstone reservoirs in Alabama but is readily identified by its blue color after staining with potassium ferricyanide and by its rhombic crystal habit.

In nonreservoir sandstone and siltstone, ferroan dolomite/ankerite partially to completely replaces matrix introduced by bioturbation. These intervals commonly have a patchy distribution of the cement due to incomplete replacement of matrix. Ferroan dolomite/ankerite is present throughout the reservoir interval, but typically accounts for less than 5 percent of total rock volume. In reservoir sandstone, ferroan dolomite/ankerite occurs as isolated rhombic crystals or as clusters of crystals that partially fill pores (fig. 44). Ferroan dolomite/ankerite also partially to completely replaces intrabasinal shale clasts (fig. 45) and fossil fragments (fig. 42). Individual crystals have long axes ranging from approximately 20 to 70 µm. Concentric chemical zonation from magnesium-rich cores to iron-rich rims in individual crystals was not commonly observed with backscattered-electron imaging, although complex chemical variation occurs within patches of closely spaced crystals (fig. 46). Electron microprobe analyses indicated ferroan dolomite/ankerite in Carter sandstone is nonstoichiometric, contains excess calcium, and has a highly variable iron-to-magnesium ratio (fig. 37). Individual samples contain the range of composition shown in figure 37.

Ferroan dolomite/ankerite is a late-stage diagenetic mineral in Carter sandstone that postdates precipitation of all other authigenic carbonate minerals and quartz. During burial diagenesis, ferroan dolomite/ankerite typically precipitates at temperatures of around 100°C. The Carter reservoir in North Blowhorn Creek oil unit presently is at a burial depth of around 2,300 feet. Thus, the presence of ferroan dolomite/ankerite in Carter sandstones suggests the unit was buried significantly deeper (perhaps more than 10,000 feet) and subsequently uplifted. In sandstone containing calcite cement, there is clear textural evidence for replacement of calcite by ferroan dolomite. Boles (1978) documented similar replacement of early calcite by late-stage ferroan dolomite/ankerite in Wilcox

Figure 44.--Secondary-electron micrograph of a cluster of rhombic, authigenic ferroan dolomite/ankerite crystals (Carter sandstone, North Blowhorn Creek oil unit, well PN3160, 2,297.3 ft, scale is on photograph).

sandstone in south Texas. Boles and Franks (1979) suggested that the source of iron for ferroan dolomite/ankerite in Tertiary sandstones in Texas was the smectite-to-illite reaction in associated shale. Land and others (1987) suggested that precipitation of ferroan dolomite/ankerite in sandstone is unrelated to clay-mineral reactions in adjacent shale and suggested sources for iron deeper in the basin. In Carter sandstone in North Blowhorn Creek oil unit, the intervals most intensely cemented by ferroan dolomite/ankerite are adjacent to shale enclosing the sandstone body.

QUARTZ

Authigenic quartz occurs as euhedral, syntaxial overgrowths on detrital quartz grains that partially fill pores (fig. 47) and locally, as a pervasive cement that occludes all pores. The first occurrence is prevalent in reservoir sandstone, whereas the second occurrence is more common in the adjacent nonreservoir siltstone and very fine grained sandstone. In reservoir sandstone, quartz overgrowths occupy up to 10, but typically less than 7, percent, of total rock volume. Quartz overgrowths are present throughout the reservoir interval and commonly result in polygonal pore outlines (fig. 48). Although authigenic quartz is ubiquitous in the Carter reservoir in North Blowhorn Creek oil unit and nearby oil fields, an effective, interconnected pore system remains intact (fig. 49). In nonreservoir siltstone and in the vicinity of some clay drapes, a spatial relationship exists between areas of extensive authigenic quartz and stylolites or areas of intergranular pressure solution.

Figure 45.--Backscattered-electron micrograph showing ferroan dolomite/ankerite replacement of an intrabasinal mud clast (Carter sandstone, North Blowhorn Creek oil unit, well PN3160, 2,311.7 ft; scale is on photograph). Light gray areas are ferroan dolomite/ankerite, medium gray grains are quartz, and black areas are pores.

KAOLINITE

Kaolinite is ubiquitous in Carter sandstone in minor amounts, but is volumetrically significant in some horizons within high-quality reservoir zones where almost all intergranular space is filled by the mineral. Kaolinite most commonly occurs as vermicular stacks of pseudohexagonal platelets that fill grain-size and grain-shape areas between detrital quartz (figs. 50 through 52). This occurrence differs from that in the Tertiary of the Texas Gulf Coast, where kaolinite typically fills primary but not secondary pores (Land and others, 1987). Individual platelets commonly are less than 10 μm in diameter. Less abundant kaolinite with similar morphology partially to completely fills intergranular pores and dissolution voids within fossil fragments (fig. 53).

An authigenic origin for kaolinite in primary intergranular pores and in dissolution voids within fossil fragments is evident. However, the origin of kaolinite in detrital-grain-size areas is less evident. Some of this kaolinite is colorless in plane-polarized light, occupies rectangular areas similar in shape to detrital feldspar grains, and consists of stacks containing perfectly hexagonal platelets with micropores between stacks. This kaolinite probably precipitated in areas once occupied by detrital feldspars. Other kaolinite that occupies grain-size areas appears murky in plane-polarized light. Scanning electron microscopy reveals that some of this kaolinite has textures indicative of detrital kaolinite and is intermixed with other clay minerals, such as illite or chlorite. This kaolinite most likely

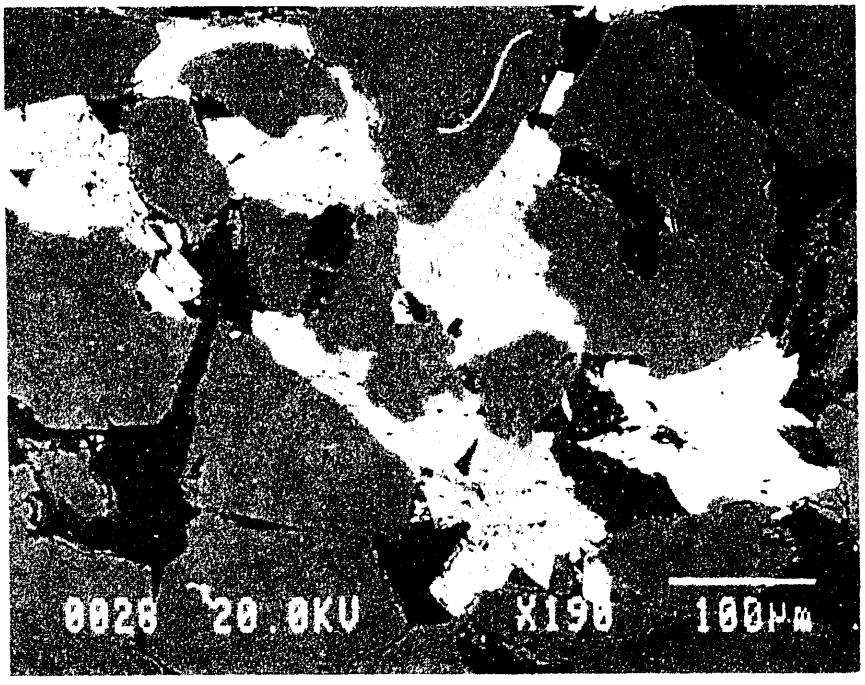

Figure 46.--Backscattered-electron micrograph showing chemical variation in authigenic ferroan dolomite/ankerite (Carter sandstone, North Blowhorn Creek oil unit, well PN2999, 2,194 ft; scale is on photograph). Light medium gray areas are ferroan dolomite/ankerite. Lighter areas are enriched in iron relative to the darker areas. White areas are siderite. Quartz detrital grains are medium gray and pores are black.

Figure 47.--Thin-section photomicrograph of hexagonal quartz overgrown on detrital quartz grain (Carter sandstone, North Blowhorn Creek oil unit, well PN3058, 2,295.5 ft; plane polarized light; field of view = 0.5 mm).

Figure 48.--Thin-section photomicrograph showing polygonal pore outlines formed by quartz overgrowths (Carter sandstone, North Blowhorn Creek oil unit, well PN3058, 2,295.5 ft; plane polarized light; field of view = 0.5 mm).

is a component of intrabasinal shale fragments or fecal pellets. An origin as a component in an intrabasinal shale clast or fecal pellet is clear in many cases because of the geometry of the grains. However, these types of fragments commonly partially dissolve. Where these fragments have dissolved so that only kaolinite remains, distinction between detrital and authigenic origins is difficult to determine.

Another type of kaolinite occurs as isolated, curved stacks of platelets that are typically larger than 10 μm in diameter (fig. 54). These platelets are not perfectly hexagonal but contain grooves that commonly extend the length of the stack. At least some of this kaolinite formed prior to the major phase of kaolinite precipitation in Carter sandstone because it is encased by quartz overgrowths. The morphology of some of this kaolinite resembles kaolinite formed in weathering environments (Keller, 1976a, b, c, 1977a, b). However, textural relationships indicate that much kaolinite with this morphology formed later, during burial diagenesis. This kaolinite is an example of "kopy-kat kaolinite" (D.R. Pevear, verbal communication, 1991), which replaces detrital mica. The kaolinite precipitates between sheets of detrital mica, using the mica as a template. The authigenic kaolinite further inherits surface irregularities in the mica template.

Formation of most authigenic kaolinite in Carter sandstone postdates precipitation of quartz overgrowths and ferroan dolomite/ankerite (fig. 55). Precipitation of ferroan dolomite/ankerite apparently did not overlap with that of kaolinite because authigenic kaolinite does not occur as inclusions in ferroan dolomite (fig. 56), as has been reported elsewhere (Loukes and others, 1984; Walton and others, 1986). Formation of kaolinite predates migration of hydrocarbons into the reservoir because hydrocarbon residue coats the surfaces of kaolinite patches but does not penetrate micropores within the patches.

Most kaolinite in Carter sandstone does not form permeability barriers but fills grain size volumes that enhance microporosity in the sandstone and increase tortuosity of fluid flow. However, in intervals with concentrations of clay drapes, particularly drapes spaced on the order of a centimeter apart and thicker than 1 or 2 mm, kaolinite occupies all intergranular space, resulting in a sandstone with only microporosity. This combination of this kaolinite and clay drapes results in formation of effective barriers to vertical fluid flow of indeterminate lateral extent that likely do not extend between adjacent wells. The effectiveness of kaolinite-cemented sandstone as permeability barriers is evident in thin section. Back-pressure impregnated blue-dyed epoxy used in thin section preparation

Figure 49.--Secondary-electron micrograph of a pore and pore throat surrounded by quartz overgrowths on detrital quartz grains (Carter sandstone, Wayside oil unit, well PN4591, 2,146 ft., scale is on photograph).

commonly penetrated micropores in kaolinite in reservoir sandstone. However, blue-dyed epoxy did not penetrate kaolinite in the horizons with clay drapes. Aside from the implications for reservoir heterogeneity, this lack of penetration of blue-dyed epoxy creates other problems in petrographic evaluation of the sandstones. Care should be taken so that unimpregnated kaolinite is not misidentified as chert.

OTHER CLAY MINERALS

Authigenic illite and chlorite are scarce in Carter reservoirs. Illite occurs as plates that precipitated perpendicular to detrital grain surfaces. Chlorite occurs as face-to-face and face-to-edge plates that partially fill pores and replace rip-up clasts (fig. 57). Formation of chlorite predates precipitation of quartz overgrowths (fig. 58). Because both minerals occur in trivial amounts, their impact on reservoir quality is insignificant.

COMPACTION

The effects of both mechanical and chemical compaction contribute to reservoir heterogeneity in Carter sandstone. The major detrimental effect of mechanical compaction is loss of porosity due to ductile deformation of intrabasinal shale clasts to form pseudomatrix. Pseudomatrix occludes pores disproportionately to the original abundance of the rip-up clasts and increases tortuosity of fluid

Figure 50.--Secondary-electron micrograph of vermicular stacks of authigenic kaolinite platelets (Carter sandstone, Armstrong Branch gas field, well PN3717, 2,185 ft; scale is on photograph).

flow. Intervals above scoured surfaces contain sufficient pseudomatrix to form permeability barriers of limited lateral extent. Porosity lost by ductile-grain deformation cannot be regenerated by subsequent diagenetic events (McBride, 1984).

Chemical compaction occurs by pressure solution and is evident at various scales in Carter sandstone. At the scale of an individual core, the most significant type of chemical compaction is due to development of stylolites (fig. 59) or pressure-solution seams along individual or anastamosing clay drapes that span the width of the core. Pressure-solution seams predominantly consist of birefringent micas, clay minerals, such as illite, and organic material. Quartz grains within pressure-solution seams have bizarre shapes due to dissolution. Because of the high-energy environment in which Carter sandstone was deposited, it is unlikely that these pressure-solution seams extend from well to well; most are probably of limited lateral extent. However, their effectiveness as permeability barriers is demonstrated in cores from several wells. The base of the oil-stained interval in these cores is a pressure-solution seam formed along a clay drape.

Wispy microstylolites formed along disrupted clay drapes associated with small-scale sedimentary structures, such as ripples, and along deformed rip-up clasts (fig. 60). These microstylolites range from less than 1 mm to several millimeters in length and rarely extend across the width of a thin section. Therefore, these microstylolites do not form extensive barriers to fluid flow but increase tortuosity. The presence of these small-scale clay drapes and microstylolites contributes to reduction of

Figure 51.--Backscattered-electron micrograph of authigenic kaolinite partially filling a detrital grain size area and intergranular pores (Carter sandstone, North Blowhorn Creek oil unit, well PN3160, 3,211.7 ft; scale is on photograph).

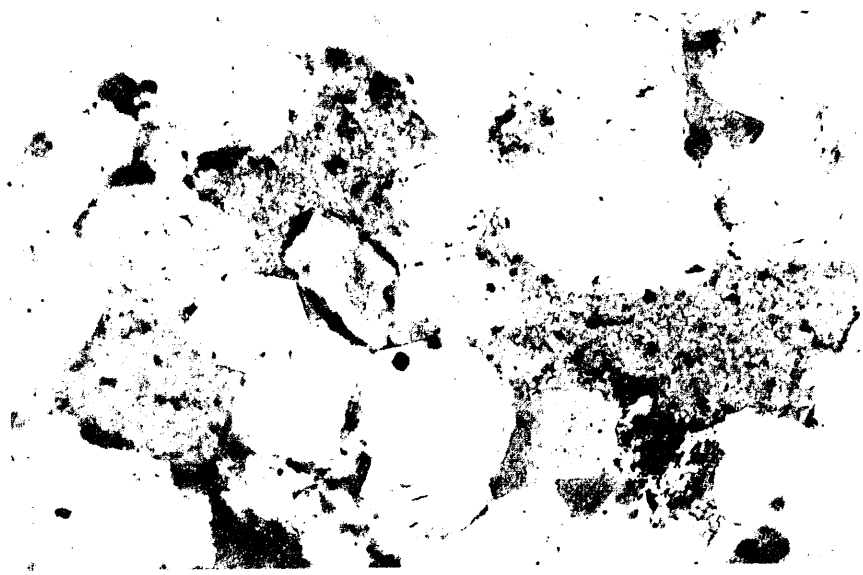

Figure 52.--Thin-section photomicrograph of three detrital grain size patches of kaolinite (Carter sandstone, North Blowhorn Creek oil unit, well PN3058, 2,291 ft; plane polarized light; field of view = 1.0 mm).

Figure 53.--Backscattered-electron micrograph of authigenic kaolinite filling dissolution voids in fossil shell fragments (Carter sandstone, North Blowhorn Creek oil unit, well PN3160, 2,302.5 ft; scale is on photograph). Medium gray areas are quartz. White areas are nonferroan and ferroan calcite. Light gray, rhombic crystals are ferroan dolomite/ankerite. Black areas are pores.

permeability in intervals containing these structures, which results in permeability contrasts within the productive reservoir interval.

The presence of stylolites and other pressure-solution features suggests that maximum depth of burial of the Carter sandstone was much greater than the present burial depths of 2,100 to 2,400 ft in North Blowhorn Creek oil unit. This contention also is supported by the abundant long and concavo-convex contacts between detrital framework grains and by the presence of ferroan dolomite/ankerite cement.

HYDROCARBON RESIDUE

Hydrocarbon residue occurs locally in Carter sandstone in North Blowhorn Creek oil unit, particularly in ripple-laminated sequences. This residue fills intergranular pores or coats surfaces surrounding macropores, but apparently does not penetrate micropores. The residue postdates precipitation of all major authigenic minerals in Carter sandstone, including quartz, ferroan dolomite/ankerite, and kaolinite (fig. 61). Similar localization of hydrocarbon residue and relative timing of introduction of hydrocarbons has been documented in outcrops of asphaltic Hartselle and Lewis sandstone in the Black Warrior basin of northeastern Alabama (Pashin and others, 1991).

Figure 54.--Secondary-electron micrograph of a single stack of authigenic "kopy-kat" kaolinite (Carter sandstone, North Blowhorn Creek oil unit, well PN3058, 2,287 ft; scale is on photograph). Note the groove that extends the length of the stack. The kaolinite is partially encased by a quartz overgrowth.

PARAGENETIC SEQUENCE

The generalized paragenetic sequence for Carter sandstone in North Blowhorn Creek oil unit is shown in figure 62. Not all minerals shown in the sequence occur in every sample. The sequence of precipitation of authigenic carbonate minerals and kaolinite commonly is well exhibited within altered fossil shell fragments (fig. 63).

The present diagenetic character of Carter sandstone is the product of both early and late-stage events, reflecting compaction and pore-water evolution during burial to depths in excess of 10,000 ft and subsequent uplift to present burial depths of approximately 2,300 ft. Early pore waters probably were seawater or perhaps a mixture of seawater and meteoric water in backshore regions. Calcite and siderite precipitated prior to significant mechanical compaction in different geochemical settings. Siderite is most abundant in the shale-and-sandstone facies and in the variegated facies where reducing, anaerobic, sulfide-free environments were prevalent during early burial. Calcite is restricted to the reservoir sandstone facies where more oxygenated pore waters were present during early burial. Skeletal debris in shoreface deposits localized sites of calcite precipitation. Concentric chemical zonation in both calcite and siderite crystals suggests rapidly changing pore-water chemistry in the early diagenetic environment.

Figure 55.--Thin-section photomicrograph showing paragenetic relationship between kaolinite and ferroan dolomite/ankerite (Carter sandstone, North Blowhorn Creek oil unit, well PN3204, 2,213 ft; plane polarized light; field of view = 1.0 mm). Kaolinite fills oversize area in lower half of photograph. Rhombic ferroan dolomite/ankerite crystals are in the upper part of the photograph. Kaolinite precipitated after ferroan dolomite/ankerite.

As burial continued, pore-water evolved due to mineral-water and organic reactions, both in reservoir sandstone and in adjacent shale. Rearrangement of detrital quartz grains during mechanical compaction deformed larger, intrabasinally derived shale clasts to locally form pore-occluding pseudomatrix. During burial, precipitation of quartz overgrowths was followed by ferroan dolomite/ankerite replacement of siderite, calcite, and intrabasinal shale clasts. Although quartz overgrowths are ubiquitous, they rarely occlude all pores. Ferroan dolomite/ankerite is volumetrically the most abundant authigenic carbonate mineral in the Carter sandstone reservoir. Shell accumulations in shoreface deposits are pervasively cemented by ferroan dolomite/ankerite to form permeability barriers within reservoir sandstone of indeterminate lateral extent. Within the reservoir, ferroan dolomite/ankerite partially replaces intrabasinal shale clasts and occurs as clusters of crystals that partially fill pores.

As Carter sandstone approached its maximum burial depth, pressure solution seams and microstylolites formed along clay laminae and fragmented clay drapes on ripple foresets. Kaolinite precipitated after ferroan dolomite/ankerite, perhaps as acidic meteoric water was introduced into the basin as Carter sandstone was uplifted to its present burial depth. Migration of hydrocarbons into the reservoir postdates precipitation of ferroan dolomite/ankerite and kaolinite.

The major diagenetic features in Carter sandstone that create permeability barriers and baffles, such as pervasive ferroan dolomite/ankerite cemented intervals, pressure-solution seams, and microstylolites are products of late-stage diagenesis. However, the occurrence of these features is directly related to depositional texture.

POROSITY

Pittman (1979) discussed four types of porosity that may be present in reservoir sandstone: intergranular porosity, intragranular porosity, microporosity, and fractures. Of these, intergranular and fracture porosity form the best interconnected pore system. Intragranular porosity, formed by framework-grain dissolution may or may not contribute to effective porosity; microporosity is not part of the effective pore system. The contribution of natural fractures in Carter sandstone to

Figure 56.--Backscattered-electron micrograph of authigenic kaolinite (Carter sandstone, North Blowhorn Creek oil unit, well PN3160, 2,303.4 ft; scale is on photograph). Note the lack of kaolinite inclusions in ferroan dolomite/ankerite (light gray). Also note the micropores (black) between stack of kaolinite platelets. Quartz detrital grains are medium gray.

effective porosity was not analyzed in this study. Based on petrographic observation, the pore system in Carter reservoir sandstone consists dominantly of interconnected, intergranular pores between detrital quartz grains (fig. 64). However, microporosity, although much less abundant than intergranular porosity, is abundant in the Carter reservoir in North Blowhorn Creek oil unit. Because of the compositional maturity of Carter sandstone, the contribution of intragranular porosity by partial dissolution of detrital feldspar is minimal, accounting for less than 1 percent of total porosity in most reservoir sandstone. More abundant intragranular pores occur within partially dissolved intrabasinal shale clasts and fossil fragments (fig. 65). The pores in these fragments do not contribute to the effective pore network because they are typically isolated and enclosed by pervasively carbonate-cemented sandstone.

Secondary porosity in sandstone consists of pores produced by dissolution of detrital framework grains and by dissolution of authigenic minerals that precipitated in intergranular pores or replaced framework grains. Although criteria have been established for recognition of secondary porosity in sandstones (Schmidt and McDonald, 1979), quantitative assessment of the contribution of secondary pores to the overall pore system remains difficult in practice. This is particularly true for recognition of carbonate-cement-dissolution pores because standard petrographic criteria used to assess and quantify this type of porosity are highly subjective (Larese and Pittman, 1987). Interpretation of the extent of carbonate-dissolution porosity is critical in assessing reservoir quality and heterogeneity

Figure 57.--Secondary electron micrograph of face-to-face and face-to-edge plates of authigenic chlorite (Carter sandstone, North Blowhorn Creek oil unit, well PN3069, 2,273.5 ft; scale is on photograph).

because approaches used to develop predictive models of porosity distribution heavily depend on the origin of the porosity (Bloch, 1991). The results of several studies have shown that dissolution of pervasive carbonate cement to produce secondary porosity is not feasible in many reservoirs. Attempts to identify sufficient sources of carbon dioxide produced from decarboxylation reactions related to hydrocarbon maturation commonly result in mass-balance problems (Lundegard and Land, 1987). Similar mass-balance problems are encountered during attempts to document sources for sufficient volumes of organic acid to dissolve carbonate minerals and detrital framework grains in pervasively or highly cemented sandstone. In addition, sandstone must retain some permeability in order for diagenetic fluids to gain access to carbonate cements. Bjørlykke (1984) noted that the highest primary porosity also has the highest potential for leaching carbonate-mineral cement.

Based on the above discussion, the importance of determining the extent of carbonate-cement dissolution porosity in Carter sandstone in North Blowhorn Creek oil unit is clear. Several lines of evidence indicate that the former extent of carbonate cement may not have been significantly different from the present distribution. Within the reservoir interval, pervasive carbonate cement occurs only in association with skeletal debris; calcite cement is entirely restricted to these intervals. Isolated clusters of rhombic ferroan dolomite/ankerite are sparsely distributed throughout the reservoir interval. Ferroan dolomite/ankerite commonly replaces a carbonate mineral precursor, such as calcite. Sparse distribution of carbonate cement may be due to extensive leaching of an abundant precursor or may be due to limited dissolution of a minor precursor (Giles, 1987). The most reliable evidence for carbonate-cement dissolution is characteristic textures on detrital quartz grain surfaces that were in contact with carbonate cement prior to dissolution (Burley and Kantorowicz, 1986).

Figure 58.--Secondary-electron micrograph of authigenic quartz crystals partially enclosing plates of authigenic chlorite (Carter sandstone, North Blowhorn Creek oil unit, well PN3058, 2,287 ft; scale is on photograph). This relationship shows that chlorite formed prior to quartz.

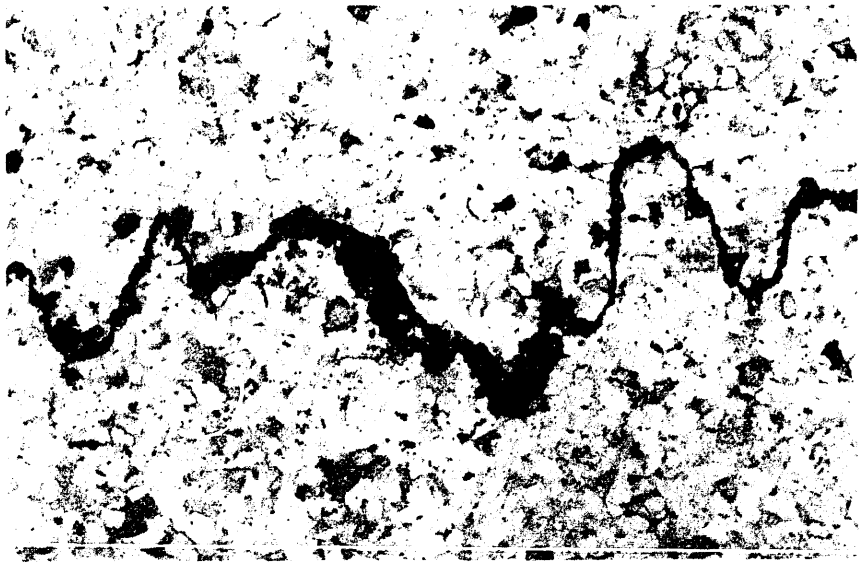

Figure 59.--Thin-section photomicrograph of a stylolite (Carter sandstone, North Blowhorn Creek oil unit, well PN3058, 2,295.5 ft; plane polarized light, field of view = 5.2 mm).

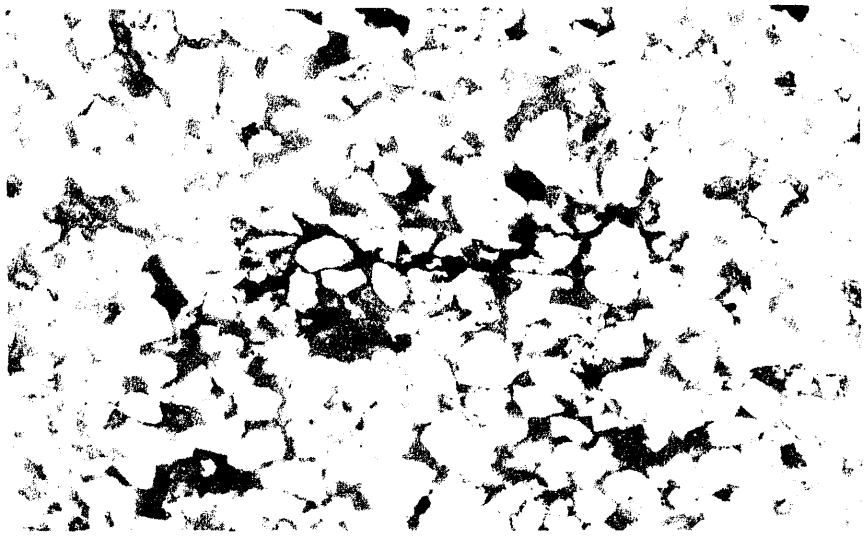

Figure 60.--Thin-section photomicrograph of a wispy microstylolite (Carter sandstone, North Blowhorn Creek oil unit, well PN3314, 2,301 ft; plane polarized light; field of view = 2.6 mm).

Figure 61.--Secondary-electron micrograph of hydrocarbon residue (Carter sandstone, North Blowhorn Creek oil unit, well PN3049, 2,353 ft; scale is on photograph). The hydrocarbon residue is the cylindrical object in the center of the photograph. The residue is attached to a quartz overgrowth. Note authigenic kaolinite in upper left half of photograph.

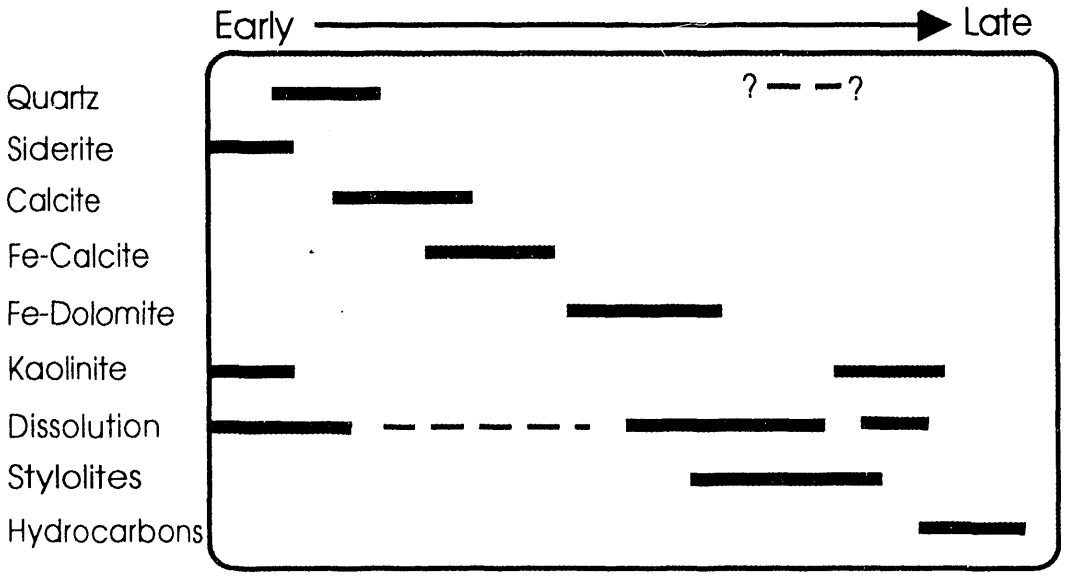

Figure 62.--Generalized paragenetic sequence for Carter sandstone in North Blowhorn Creek oil unit.

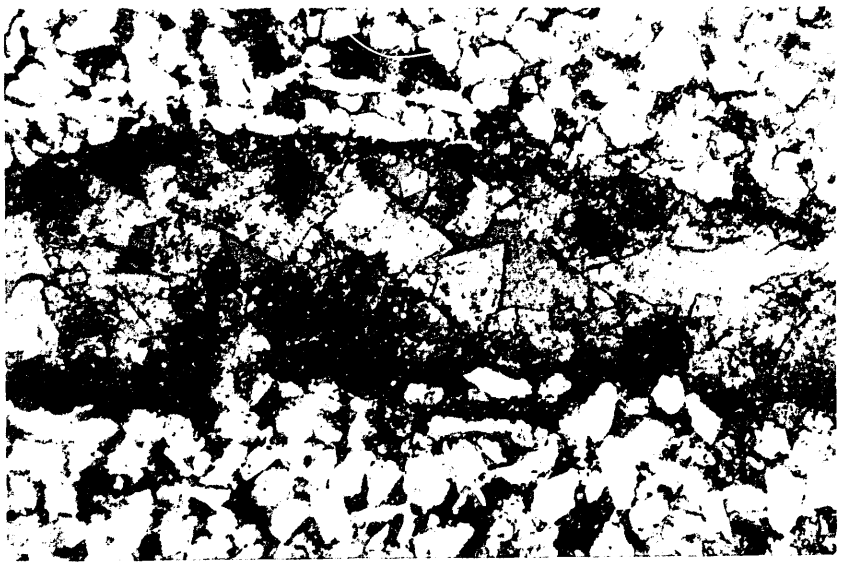

Figure 63.--Thin-section photomicrograph showing paragenetic sequence in replaced shell fragment (Carter sandstone, North Blowhorn Creek oil unit, well PN3204, 2,213 ft; plane polarized light; field of view = 2.6 mm). Authigenic minerals replacing the shell fragment are, in order of precipitation: (1) nonferroan and ferroan calcite at the outer margins; (2) rhombic ferroan dolomite/ankerite crystals in the interior of the fragment; and (3) kaolinite overlying ferroan dolomite/ankerite in the left-center part of the photograph. Also note the pores between ferroan dolomite/ankerite crystals in the right-center part of shell fragment.

Figure 64.--Secondary-electron micrograph of the pore network in Carter reservoir sandstone (Carter sandstone, North Blowhorn Creek oil unit, well PN3049, 2,355.5 ft, scale is on photograph). The fractured material in some pores is hydrocarbon residue.

These textures are best observed with the scanning electron microscope. The importance of calcite or other authigenic carbonate minerals in massively corroding detrital quartz in Carter sandstone may have been overemphasized by previous workers in the Carter sandstone (Hughes and Meylan, 1988) because in thin sections, overlap of calcite cement on detrital quartz grains gives the impression that replacement of quartz by calcite is extensive (McBride, 1987). Etched or corroded detrital quartz grains generally occur in porous sandstone only in areas immediately adjacent to clusters of ferroan dolomite/ankerite crystals (fig. 66), suggesting the original distribution of carbonate-mineral cement in Carter sandstone approximates the present distribution.

Although carbonate-dissolution appears to be limited in Carter sandstone, secondary porosity resulting from dissolution of aluminosilicate minerals in detrital framework grains is an important component of the present pore system. Feldspars and intrabasinal shale clasts have been partially to completely dissolved in Carter sandstone. This type of secondary porosity enhances the effective pore system only if dissolution products are removed from the system. Redistribution of reaction products near the site of dissolution may not result in a net increase in porosity. Therefore, it is important to distinguish redistributional secondary porosity from enhanced secondary porosity (Giles and de Boer, 1990). Most secondary porosity in Carter sandstone is redistributional porosity, resulting from dissolution of detrital feldspar and precipitation of kaolinite in the volumes originally occupied by the

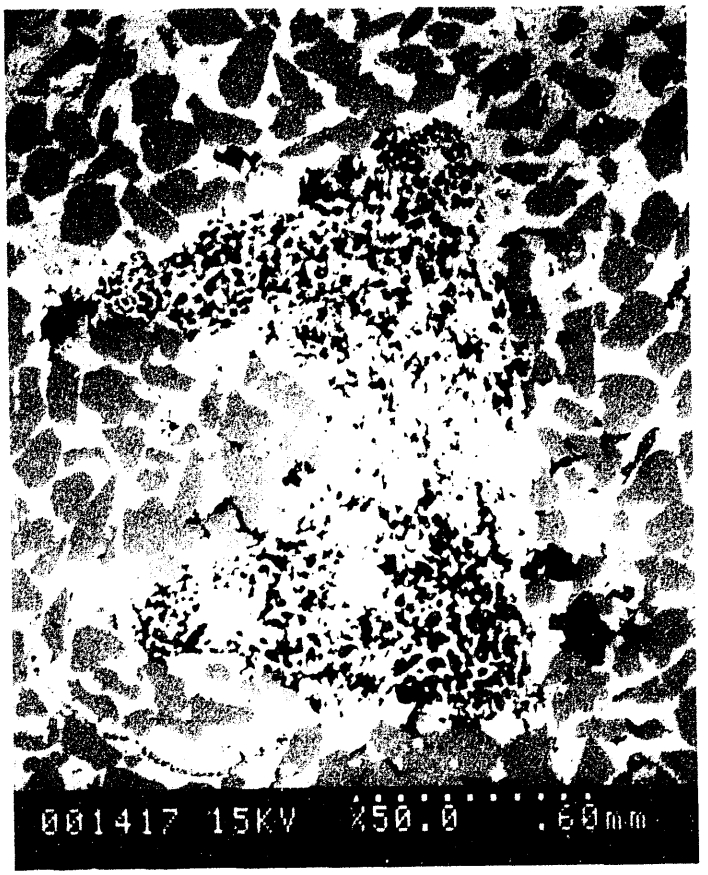

Figure 65.--Backscattered-electron micrograph of partially dissolved fossil fragments in pervasively calcite and ferroan dolomite/ankerite cemented sandstone (Carter sandstone North Blowhorn Creek oil unit, well PN3160, 2,302.5 ft; scale is on photograph).

detrital grains or in intergranular pores (fig. 51). Most of this redistributional porosity consists of micropores between stacks of kaolinite platelets.

In summary, the present pore system of Carter reservoir sandstone in North Blowhorn Creek oil unit consists of an effective, interconnected system of primary pores modified by mechanical and chemical compaction and by precipitation of carbonate minerals, quartz, and kaolinite and of ineffective micropores within clay laminae, fragmented clay drapes on ripple foresets, intrabasinal shale clasts, and authigenic kaolinite (fig. 67). Secondary porosity does not significantly enhance the effective pore system because reaction products of detrital-grain dissolution are redistributed within the sandstone as authigenic kaolinite. However, the effects of authigenic and detrital clay on the effective pore system in Carter quartzarenite merit further consideration. Methods such as X-ray diffraction are inadequate to quantify the effects of clay minerals on reservoir properties because the distribution of clay within the reservoir also must be known. The textural distribution of clays in reservoir sandstone commonly is described in terms of dispersed, structural, and laminated types (Frost and Fertl, 1981; Hurst and Archer, 1986) (fig. 68). Dispersed clay typically is authigenic. This type of clay occurs as discrete particles in pores, coats detrital grains, or bridges pore throats. Structural clay occurs in clay-mineral rich detrital clasts, whereas laminated clays occur in clay-mineral rich or micaceous laminae. Of these, dispersed clay is most detrimental to reservoir quality (figs. 68, 69) because it bridges pore throats or migrates to and blocks pore throats during production. Additionally, dispersed clay contains irreducible water that may affect calculation of water saturation from resistivity logs. If mechanical compaction is not significant, structural clay may be much more

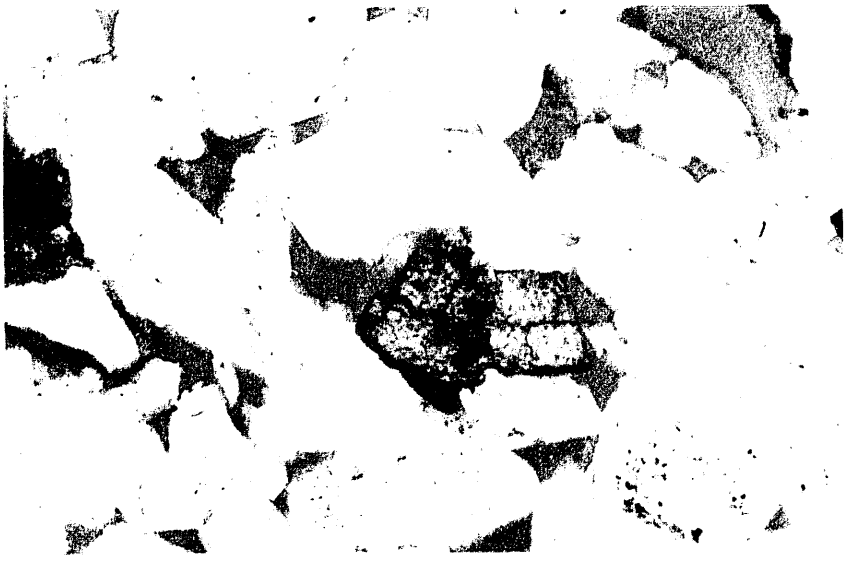

Figure 66.--Thin-section photomicrograph of isolated rhombic crystals of ferroan dolomite/ankerite (Carter sandstone, North Blowhorn Creek oil unit, well PN3314, 2,296 ft; plane polarized light; field of view = 1.0 mm). Note the rhombic embayment in the quartz detrital grain and overgrowth adjacent to the crystals, suggestive of dissolution of a precursor carbonate cement.

abundant in a reservoir than dispersed clays but have less influence on effective porosity (Frost and Fertl, 1981; Hurst and Archer, 1986) (figs. 68, 69). However, McBride (1984) noted that effective porosity may be destroyed completely by compaction in sandstone containing more than 20 percent ductile framework grains.

Carter reservoir sandstone in North Blowhorn Creek oil unit contains all three types of clay distributions discussed above. Structural clay is present as intrabasinal shale clasts throughout the reservoir interval. Dispersed clay is present as authigenic kaolinite in intergranular pores. Authigenic kaolinite in grain-size volumes formerly occupied by detrital feldspars apparently represents a hybrid between dispersed and structural clay. Laminated clay occurs in individual to anastomosing clay laminae that span the width of a core and as millimeter-scale fragmented clay drapes on ripple foresets. All three types of clay may be present in a single permeability plug or thin section.

PETROPHYSICS

Two types of petrophysical data for Carter sandstone from North Blowhorn Creek oil unit were evaluated during the course of this study: commercial core analyses and capillary-pressure data derived from high-pressure mercury porosimetry. Data obtained from high-pressure (20,000 psia) mercury porosimetry were used to define pore-throat-size distributions in Carter reservoir sandstone and associated nonreservoir rocks. These data provide important information regarding level-5 heterogeneity. When integrated with core descriptions and petrologic analyses, these data define controls on the nature of the pore system in Carter reservoir sandstone.

COMMERCIAL CORE ANALYSES

On the basis of all available data from commercial core analyses for North Blowhorn Creek oil unit, the average porosity of Carter reservoir sandstone, using a cutoff of 6 percent, is 12 percent and average permeability, using a cutoff of 0.1 millidarcy, is 6.82 millidarcies. Maximum porosity and permeability are 22 percent and 440 millidarcies, respectively. Average permeability of Carter

Figure 67.--Backscattered-electron micrograph of pore system in Carter sandstone (Carter sandstone, North Blowhorn Creek oil unit, well PN3160, 2,303.4 ft; scale is on photograph). Pores are black. Note intergranular pores and microporosity within kaolinite (center) and partially dissolved intrabasinal shale fragments (upper right). Light gray crystals are ferroan dolomite/ankerite.

sandstone in North Blowhorn Creek oil unit is three orders of magnitude lower than that of barrier-island reservoir sandstone in Bell Creek field, Montana (Sharma and others, 1990a).

A crossplot of porosity versus air permeability for all data from North Blowhorn Creek oil unit shows a roughly linear trend with wide scatter (fig. 70). The coefficient of determination (R^2) is 0.52. Similar plots for individual wells have R^2 values ranging from 0.09 to 0.83, but most are less than 0.5, indicating a poor relationship between porosity and permeability and a wide range of variation in these relationships among wells. Part of this variation owes to sampling bias. Wells from which nonreservoir siltstone and sandstone were sampled typically exhibit better porosity-permeability relationships (fig. 71) than those for which measurements were taken only from reservoir sandstone (fig. 72). In addition to between-well variation in porosity and permeability, permeability in reservoir sandstone within a single well in North Blowhorn Creek oil unit may vary by two orders of magnitude (fig. 72).

Plots of porosity and permeability versus depth also reveal both between-well heterogeneity and stratigraphic variation within single wells. In well PN2999 (fig. 73), permeability generally tracks porosity. However, in well PN3314 (fig. 74), porosity is relatively constant throughout the sampled interval, but permeability is an order of magnitude or more lower in the lower part of the interval. The interval from which measurements were made is entirely within the productive reservoir, so this permeability contrast represents a significant heterogeneity that could influence sweep efficiency. In

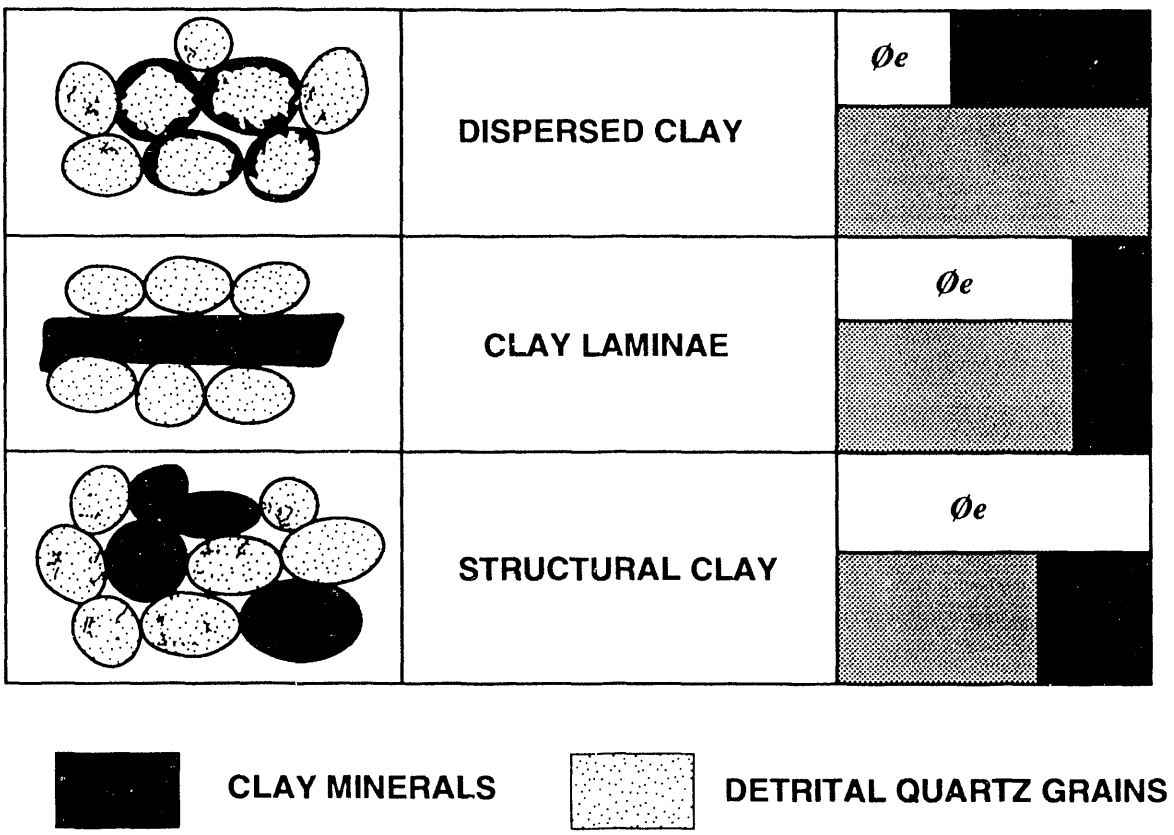

Figure 68.--Influence of clay-mineral distribution on effective porosity ($\varnothing_e$) (modified from Frost and Fertl, 1981).

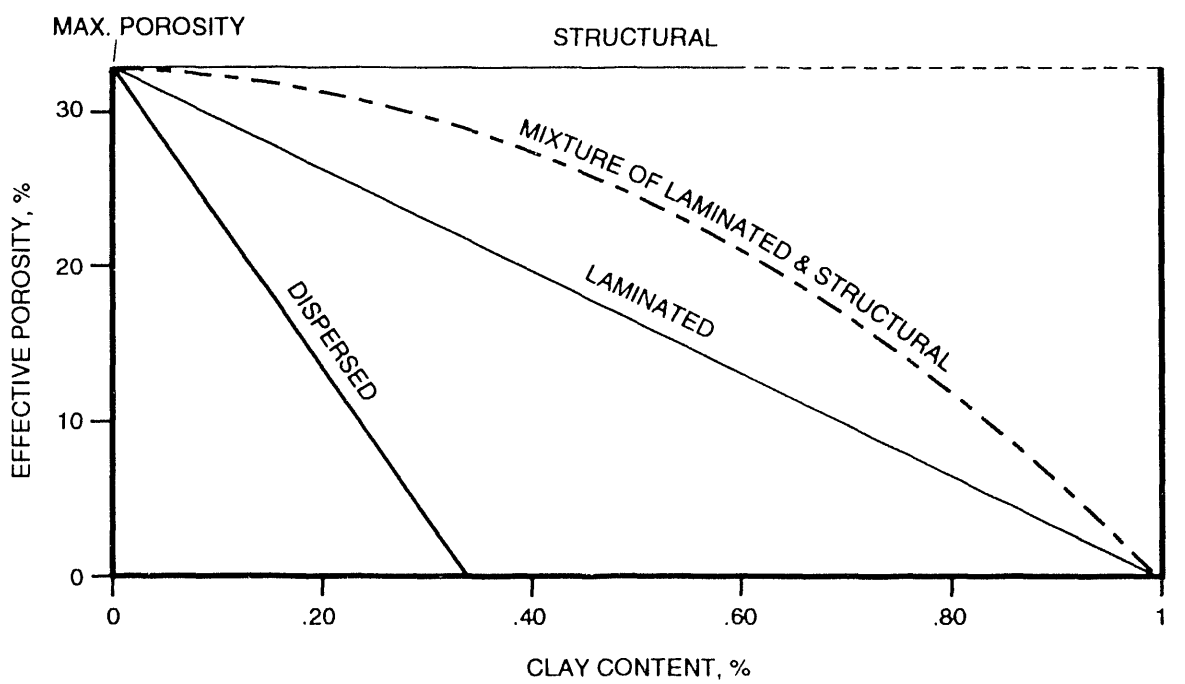

Figure 69.--Plot of clay content versus effective porosity demonstrating the influence of clay distribution (modified from Frost and Fertl, 1981).

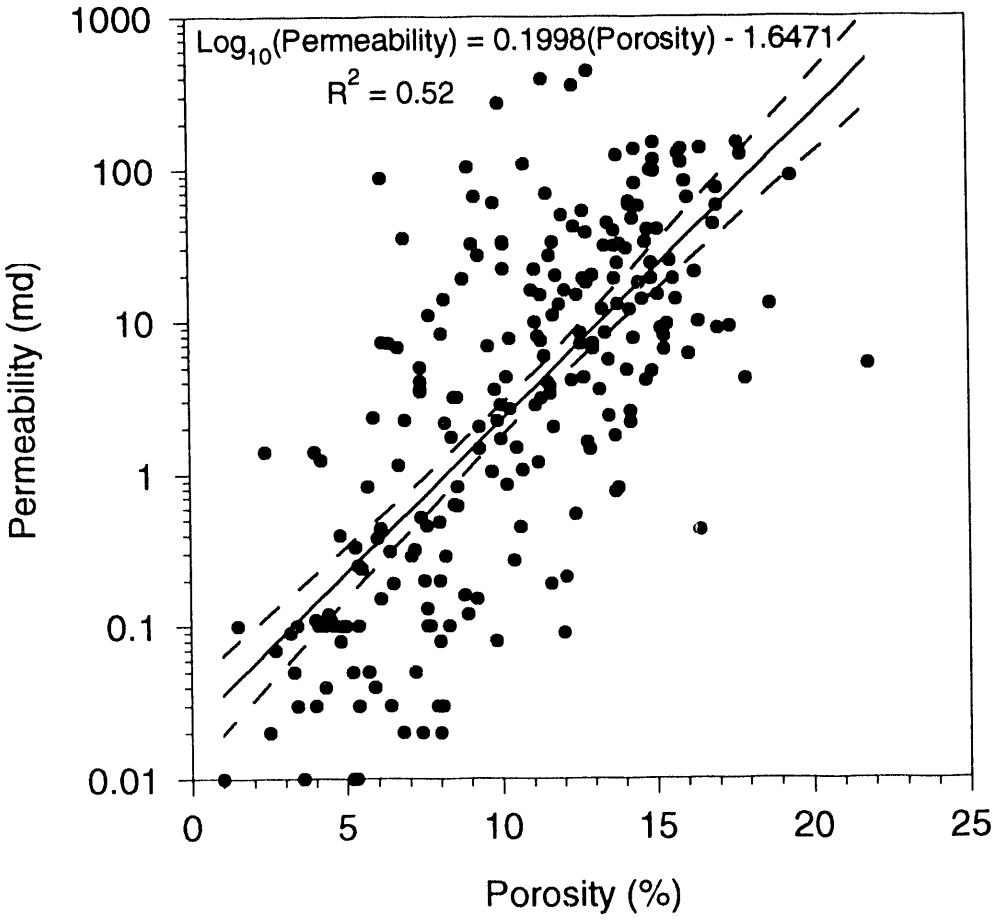

Figure 70.--Plot of porosity versus permeability for all commercial core analyses from North Blowhorn Creek oil unit. The solid line is a linear regression line, and the dashed lines encase the 95 percent confidence interval. The regression equation and the coefficient of determination are at the top of the diagram.

core, the change from the lower permeability to the higher permeability zone corresponds to a transition from very fine-grained, ripple-laminated lower shoreface deposits to fine-grained upper shoreface or foreshore deposits containing more abundant horizontal to low-angle planar lamination near the top of the reservoir. This change is subtle. Because porosity is constant throughout the reservoir interval, the change in permeability is due to factors other than variation in amount of pore-filling cement. Several possibilities could explain the difference in permeability. The larger detrital grains in the more permeable zone have larger throats between detrital framework grains if pore throats are not clogged with cement or clay. A greater abundance of wispy clay drapes in the ripple-laminated sequence than in the horizontal to low-angle planar laminated sequence would reduce permeability. Finally, an increase in abundance of microporous authigenic kaolinite could reduce permeability without significantly affecting total porosity. Routine core analyses are insufficient to distinguish among these factors. However, pore-throat size distributions derived from high-pressure mercury porosimetry provide evidence to distinguish among the possibilities listed above.

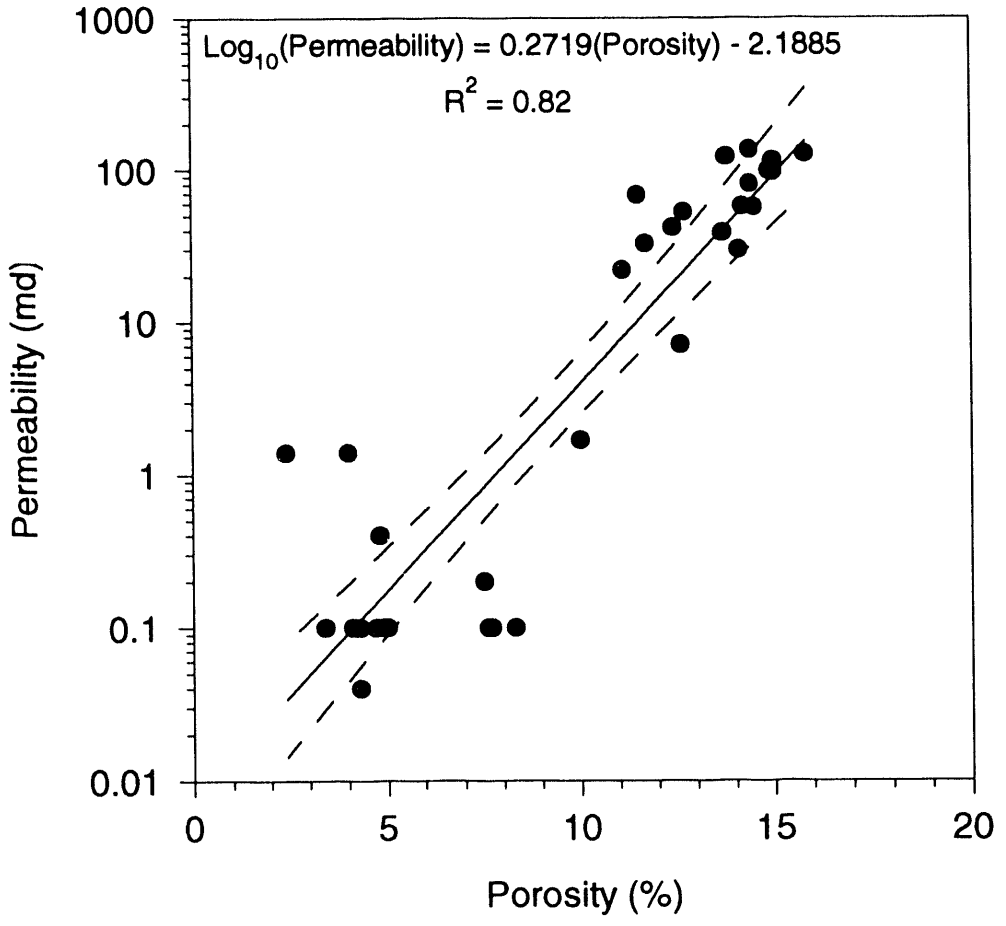

Figure 71.--Plot of porosity versus permeability for all commercial core analyses from well PN2999, North Blowhorn Creek oil unit. The solid line is a linear regression line, and the dashed lines encase the 95 percent confidence interval. The regression equation and the coefficient of determination are at the top of the diagram.

HIGH-PRESSURE MERCURY POROSIMETRY

The pore system in any sandstone reservoir consists of large spaces (pores) and small channels between the pores (pore throats). These pore throats constrict fluid flow. Critical capillary pressure must be attained before fluid can enter a pore through a pore throat. Therefore, pore-throat size and distribution is a critical control on the distribution and producibility of hydrocarbons in a reservoir. High-pressure mercury porosimetry is the only effective means quantitatively evaluating pore throats (Kopaska-Merkel and Friedman, 1989). In addition, high-pressure mercury porosimetry is capable of measuring porosity that is not detectable by standard commercial porosimetry methods. Capillary-pressure curves derived from mercury porosimetry can be used to determine several petrophysical parameters, including pore-throat size distribution, relationships between surface area and volume, porosity, recovery efficiency and oil-column height (Purcell, 1949; Dullien and Dhawan, 1974: Wardlaw, 1976; Jennings, 1987; Wardlaw and others, 1988; Kopaska-Merkel and Friedman, 1989).

High-pressure mercury porosimetry is well suited to analysis of heterogeneity at levels 4 and 5. The size of samples used in this study typically was about 0.5 x 1 cm or less than one-quarter of the volume commonly used in standard commercial core analysis. Several measurements can be made from adjacent samples cut from a single permeability plug, allowing assessment of homogeneity on

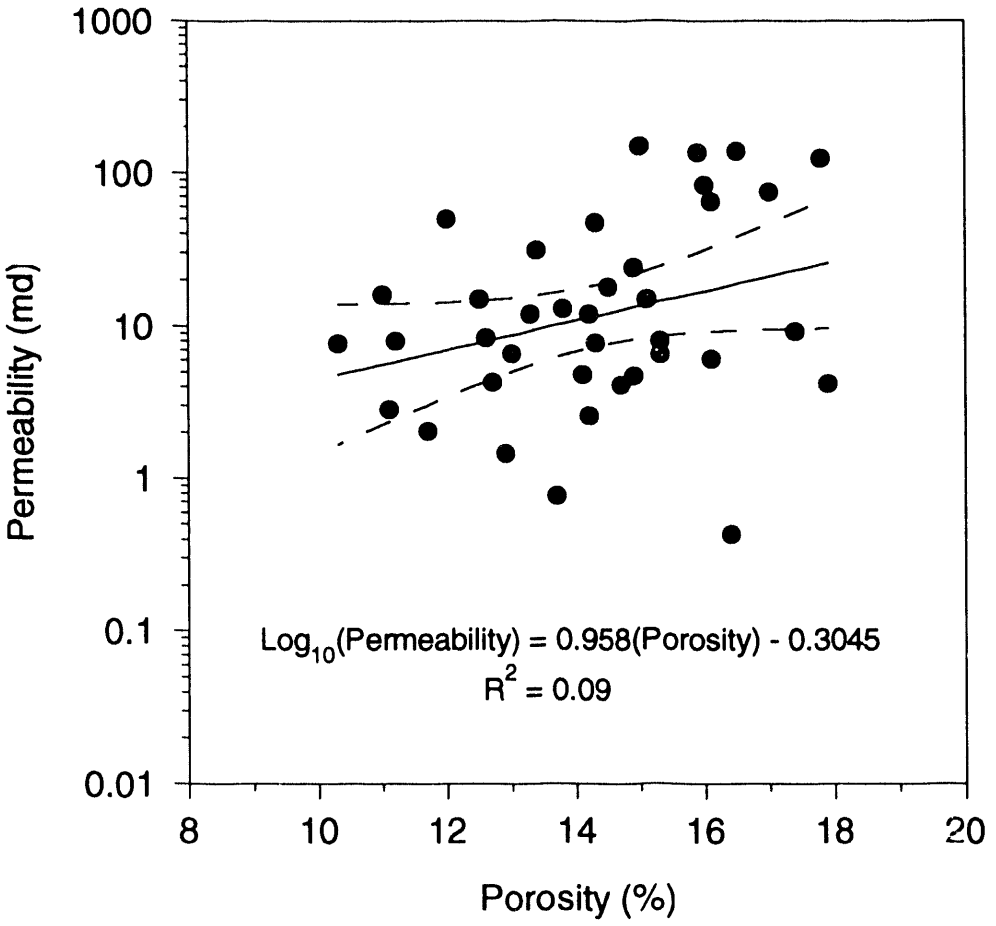

Figure 72.--Plot of porosity versus permeability for all commercial core analyses from well PN3314, North Blowhorn Creek oil unit. The solid line is a linear regression line, and the dashed lines enclose the 95 percent confidence interval. The regression equation and the coefficient of determination are at the top of the diagram.

the scale of centimeters. Thus, measurements can be made at about the scale sampled by minipermeameters. Unfortunately, in contrast to minipermeameter measurement , mercury porosimetry is destructive, and repetitive measurements cannot be made on the same sample. Kopaska-Merkel (1991) has shown that well cuttings are also suitable for analysis by high-pressure mercury porosimetry. However, cuttings of friable reservoir sandstone would not be suitable for this technique.

In mercury porosimetry, the volume of mercury intruded at a specific pressure is precisely related to the number of pore throats of corresponding size. Because of this relationship, plots of cumulative mercury-intrusion volume versus capillary pressure are equivalent to cumulative-mercury intrusion volume versus pore-throat size. Thus, a distribution of pore-throat sizes is readily obtainable. In addition, porosity can be calculated readily because bulk density is determined as part of the measurement procedure. Because pressure is increased incrementally, with mercury-intrusion volume being measured at each increment, porosity at several pressures can be determined. The range of pressures used in this study was 1.5 to 20,000 psia, following procedures outlined by Kopaska-Merkel (1991). This maximum pressure is considerably higher than that used in most previously published work. However, Kopaska-Merkel and Friedman (1989) successfully used these pressures without damaging carbonate reservoir-rock samples; likewise, these very high pressures apparently do not damage sandstone reservoir rocks (D.M. Kopaska-Merkel, verbal communication, 1990). High-

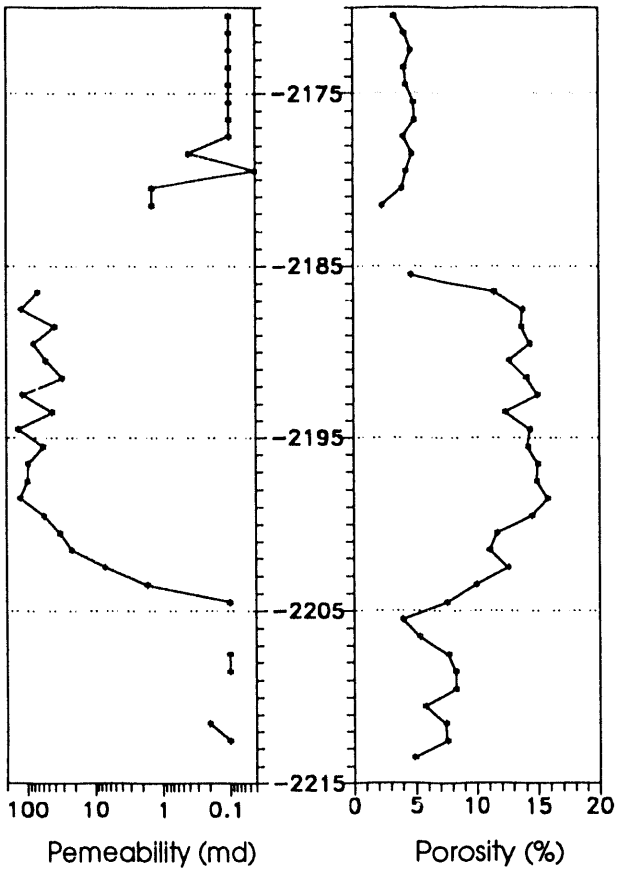

Figure 73.--Plot of permeability and porosity versus depth for well PN2999, North Blowhorn Creek oil unit.

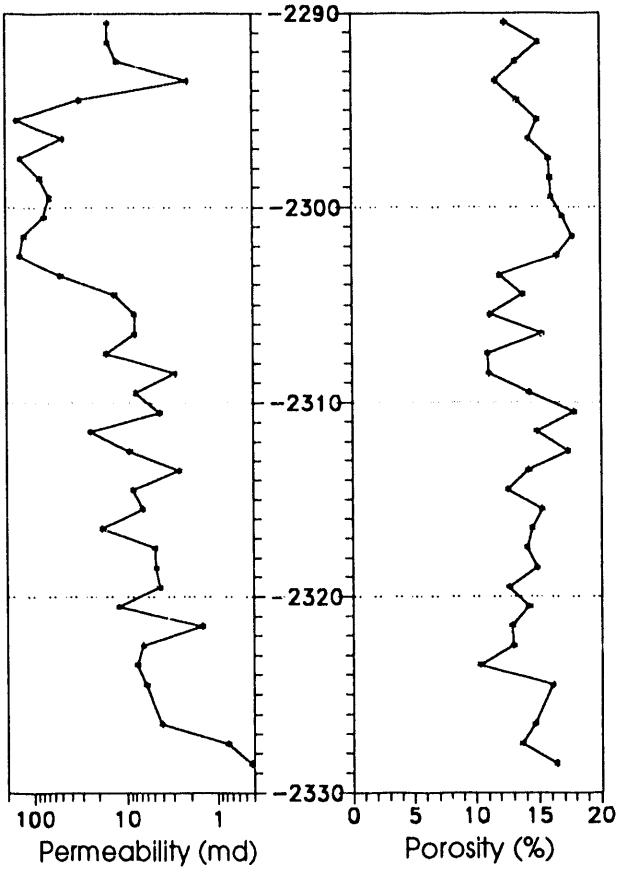

Figure 74.--Plot of permeability and porosity versus depth for well PN3314, North Blowhorn Creek oil unit.

pressure mercury porosimetry has application to reservoir sandstones, such as the Carter, that contain micropores in authigenic kaolinite, intrabasinal shale fragments, and wispy clay drapes on ripple foresets, which would remain undetected if substantially lower pressures were used. Figure 75 shows the amount of mercury intrusion volume (milliliters per gram of sample) at pressures typically used in routine commercial porosimetry as a percentage of maximum intrusion volume obtained at an intrusion pressure of 20,000 psia for Carter sandstone in well PN3160 in North Blowhorn Creek oil unit. Major differences in intrusion volume between low- and high-pressure measurements are most notable for low-permeability, nonreservoir siltstone and very fine grained sandstone below and above the reservoir interval where most pores are micropores. Large differences in intrusion volume within the reservoir interval in this well are associated with thin carbonate-cemented horizons.

Figure 76 shows porosity calculated from mercury intrusion volumes at 1,000, 2,000, 5,000, and 20,000 psia as a function of depth in well PN3160. The most obvious differences between porosity calculated from low- and high-pressure data are for samples from nonreservoir siltstones bounding the reservoir interval. Within the reservoir interval, porosity values calculated for low pressures are typically close to those calculated for the maximum intrusion pressure. However, the difference between porosity determined at low and high pressure is significant because it reflects variation in microporosity due to detrital and authigenic clay minerals. The relative importance of microporosity in the overall pore system can be better understood by examining the distribution of pore-throat sizes calculated from mercury-intrusion data.

The most notable aspect of pore-throat radius versus incremental mercury-intrusion curves for Carter reservoir sandstone in North Blowhorn Creek oil unit is the polymodal distribution of pore-throat sizes (fig. 77). Typical Carter reservoir sandstone has a dominant pore-throat-radius mode of 2

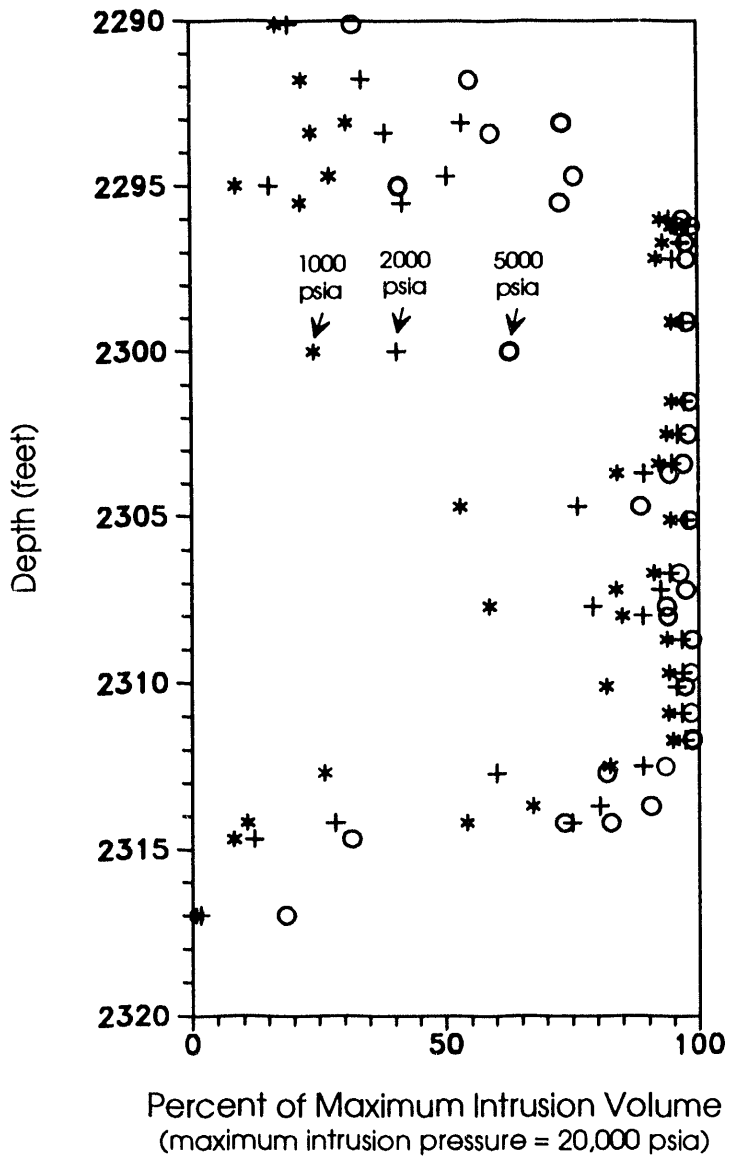

Figure 75.--Plot of percent of maximum intrusion volume versus depth for well PN3160. Asterisks represent intrusion of 1,000 psia, crosses at 2,000 psia, and open circles at 5,000 psia. The maximum mercury intrusion pressure is 20,000 psia.

μm or more and several lesser modes at smaller pore-throat sizes. The dominant mode represents the size of pore throats between sand-size detrital grains. The other pore-throat-size modes represent the range of variation in smaller pore throats between detrital grains, between clay particles in intrabasinal shale clasts, between dissolution pores in mud clasts, and between stacks of authigenic kaolinite crystals. Unimodal pore-throat-size distributions are scarce in Carter reservoir sandstone but are typical of some nonreservoir siltstone bounding the unit and some carbonate-cemented intervals within the reservoir, where the dominant mode is less than 0.1 μm.

The shapes of curves of pore-throat radius plotted against cumulative mercury-intrusion volume normalized to maximum intrusion volume are directly related to the distribution of pore-throat sizes shown on incremental intrusion plots. Four distinct shapes of cumulative-intrusion curves can be

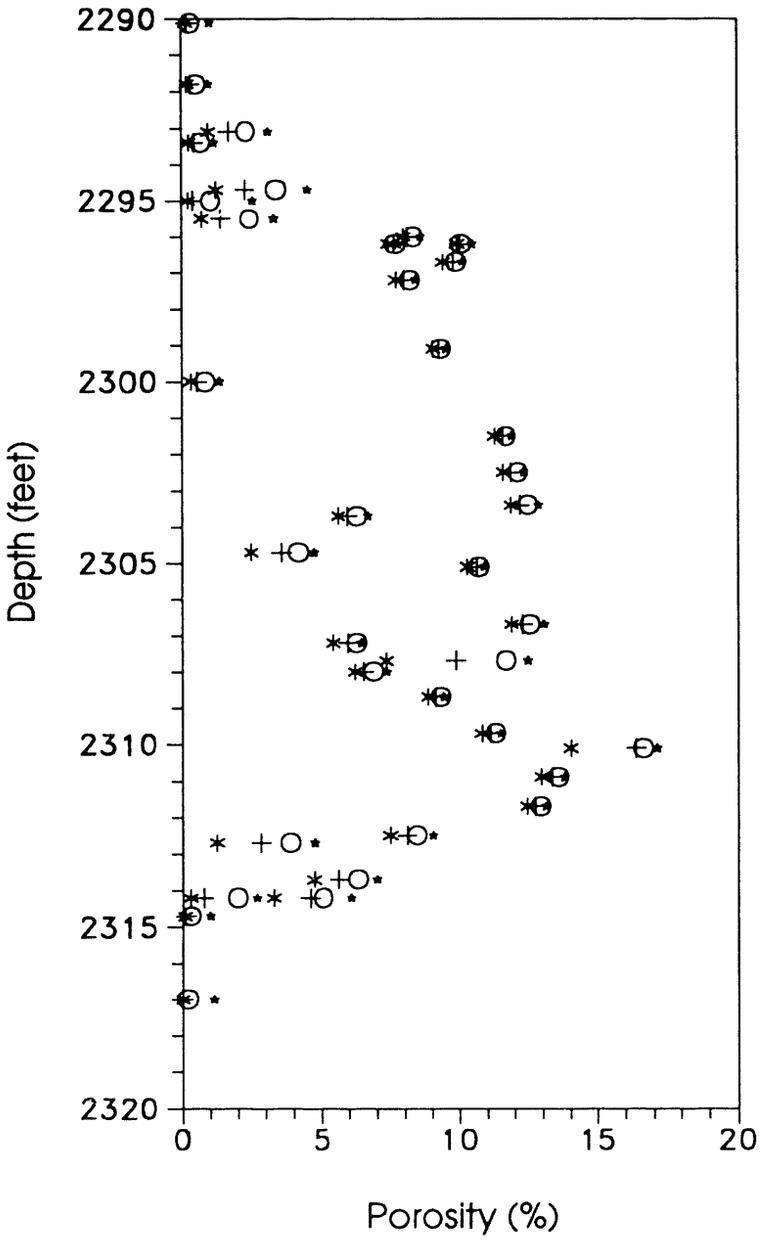

Figure 76.--Plot of porosity at various mercury-intrusion pressures versus depth for well PN3160. Asterisks represent intrusion of 1,000 psia, crosses at 2,000 psia, and open circles at 5,000 psia. The maximum mercury intrusion pressure is 20,000 psia.

recognized for Carter sandstone and associated sedimentary rocks (fig. 78). Curve A, which is convex with the steepest slope of the curve at a large pore-throat radius, is representative of the best quality reservoir in North Blowhorn Creek oil unit (figs. 78, 79). Curve B is also convex, but the steepest slope is at a smaller pore-throat radius and the overall slope is gentler (figs. 78, 80).The gentler slope indicates a polymodal distribution of pore-throat sizes. This curve shape is also representative of Carter reservoir sandstone. A gradation exists between curves A and B in the Carter reservoir at North Blowhorn Creek, due to variation in detrital grain size and variation in abundance of components

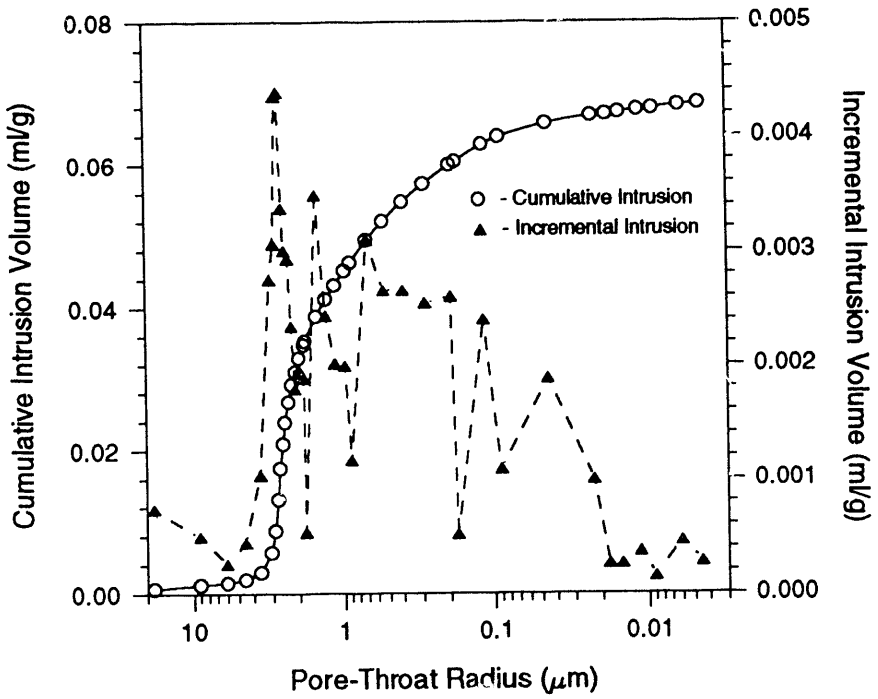

Figure 77.--Plot of pore-throat radius versus cumulative-intrusion volume and incremental-intrusion volume showing polymodal pore-throat-size distribution for well PN3150, 2,371 ft, North Blowhorn Creek oil unit.

that contribute to microporosity. The bimodal shape shown in curve C (figs. 78, 81) is rare and generally indicates partially cemented transitional zones between pervasively carbonate-cemented sandstone and porous reservoir sandstone. Curve D is convex with the steepest slope at a small pore-throat size radius (figs. 78, 82). This type of cumulative-intrusion curve is representative of nonreservoir siltstone, pervasively carbonate-cemented zones, and sandstone in which all pores are filled with pseudomatrix.

Plots of cumulative-intrusion curves for all samples from a single well are useful for demonstrating the range of variation in pore-throat-size distribution within a reservoir and for deciphering controls on reservoir properties. Figure 83 is a cumulative-intrusion plot for all data from well PN3314. The convex curve shapes are representative of the gradation between curves A and B shown on figure 78. The solid lines in the darkly shaded area on the plot are data for samples from the zone of high permeability in the upper part of the reservoir interval shown in figure 74, whereas the dashed lines in the lightly shaded area are from the less permeable zone in the lower part of the interval; porosity is constant throughout the interval (fig. 74). When the data shown in figure 83 are integrated with core descriptions and petrographic observations, two controls on permeability are evident. Sandstone in the upper, more permeable interval is fine grained, in contrast to the very fine grained sandstone in the lower, less permeable interval. Coarser grained sandstone would be expected to have larger pore throats than fine-grained sandstone, barring diagenetic factors, and thus, higher permeability. Grain-size control of pore-throat size contributes to the permeability variation observed in well PN3314 because the dominant pore-throat size mode is larger for samples from the more permeable zone than for samples from the less permeable zone (fig. 83). However, another factor contributes to lower permeability in the lower zone. The lower, less permeable sandstone has more microporosity than sandstone in the upper zone, as indicated by gentler slopes on cumulative-intrusion curves (fig. 83) and pore-throat-size distributions on incremental-intrusion curves. The difference between porosity calculated for maximum intrusion pressure (20,000 psia) and

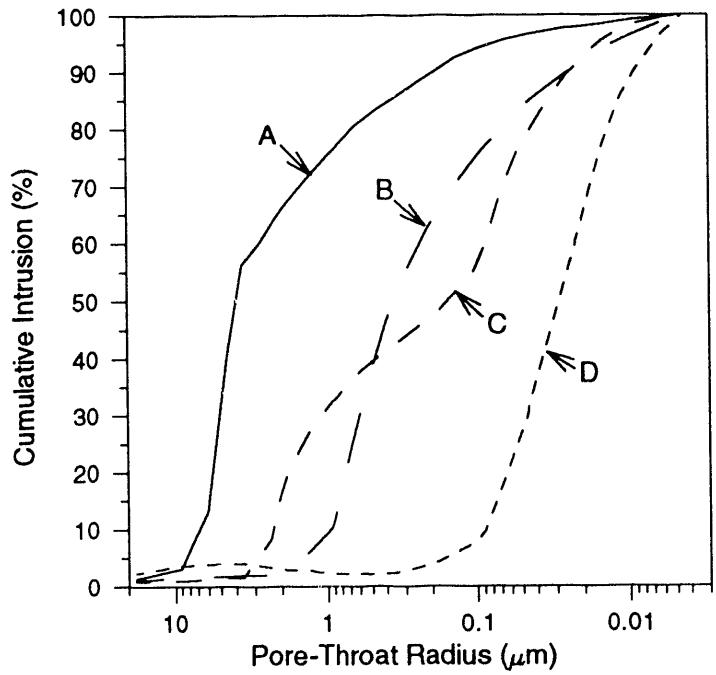

Figure 78.--Plot of pore-throat radius versus cumulative intrusion showing typical shapes of cumulative-intrusion curves for Carter sandstone: (A) Convex curve with large maximum pore-throat-size mode (well PN3314, 2,297 ft). (B) Convex curve with smaller maximum pore-throat-size mode (well PN3150, 2,364.5 ft). (D) Concave curve with small pore-throat-size mode (well PN3150, 2,350 ft).

porosity at 1,000 psia also suggests that microporosity is a factor related to lower permeability (fig. 84). Differential porosity is highest in the lower permeability zone.

The variation is subtle, but differential porosity for samples from the more permeable zone is consistently less than one percent, in contrast to the lower permeability zone where differential porosity is greater than one percent. The lower zone consists of very fine-grained, ripple-laminated, lower shoreface deposits. The additional microporosity in these sandstones most likely is contained in fragmented clay drapes on ripple foresets that create very small scale permeability barriers and baffles. The combination of variations in pore-throat size and in the abundance of micropores, as total porosity remains constant throughout the reservoir interval in well PN3314, accounts for the poor correlation between porosity and permeability shown in figure 72. Although the higher and lower permeability zones in well PN3314 are discernible from commercial core analyses, high-pressure mercury porosimetry provides a means of documenting factors controlling the permeability variation and of characterizing the pore-throat distribution in flow units.

Median pore-throat size is a useful parameter that can easily be used to show stratigraphic variation of reservoir properties. Median pore-throat size has been shown to have at least some degree of correlation with several other petrophysical parameters, including recovery efficiency and porosity (Kopaska-Merkel and Friedman, 1989). In well PN3160 in North Blowhorn Creek oil unit, median pore-throat size does not correlate with recovery efficiency or permeability where analyses were available but correlates well with porosity calculated from the maximum mercury intrusion volume at 20,000 psia (fig. 85). Few permeability measurements are currently available for Carter sandstone from the samples used for high-pressure mercury porosimetry.

Median pore-throat size can be calculated directly from the raw data output of the porosimeter or can be determined graphically from normalized cumulative-intrusion curves. However, median pore-throat size alone does not give information regarding the distribution of pore-throat sizes in a

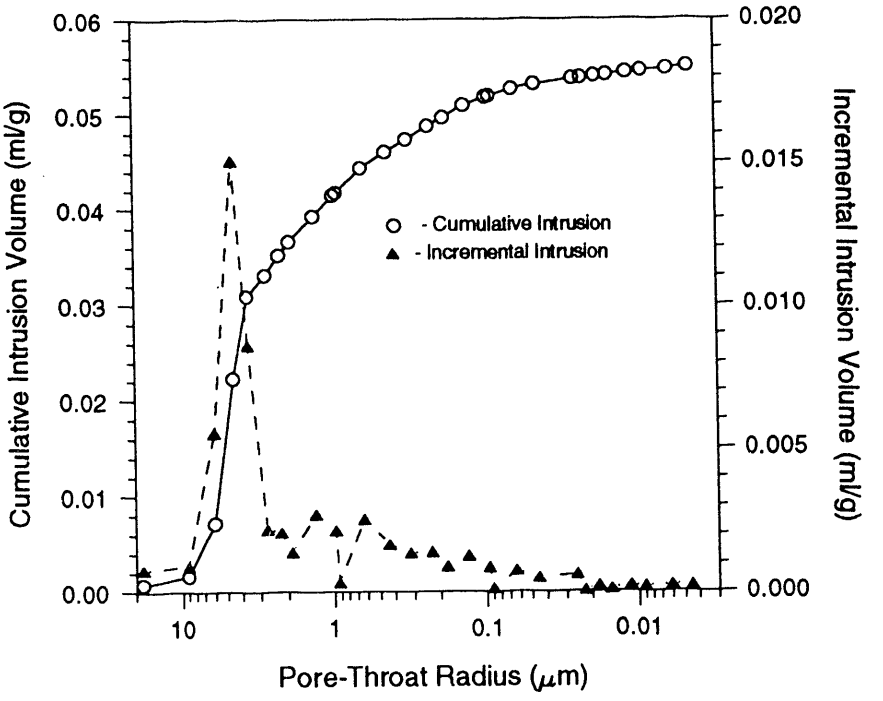

Figure 79.--Plot of pore-throat radius versus cumulative-intrusion volume and incremental-intrusion volume for well PN3314, 2,297 ft, North Blowhorn Creek oil unit.

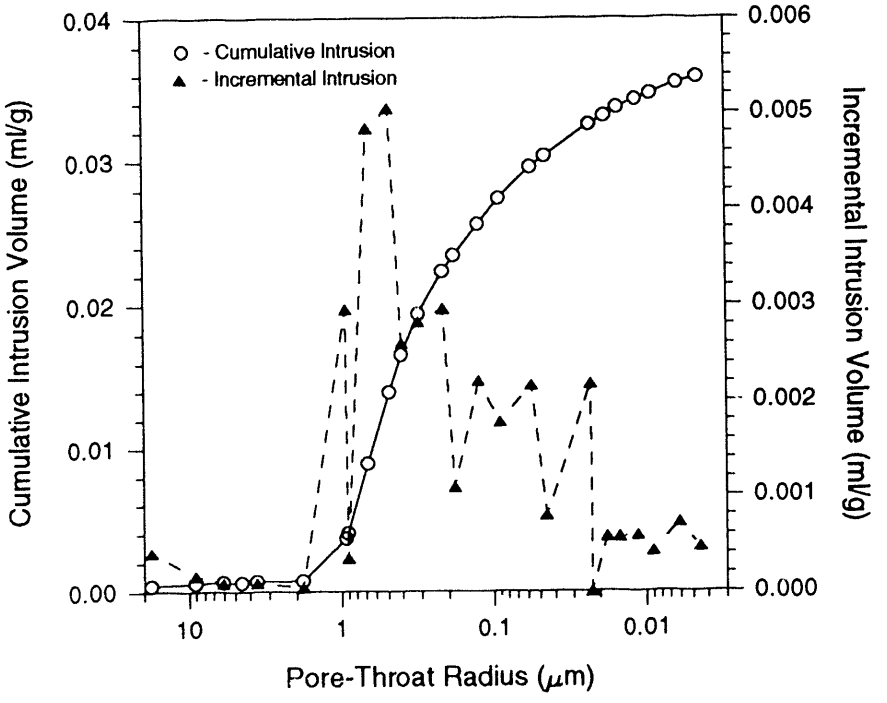

Figure 80.--Plot of pore-throat radius versus cumulative intrusion volume and incremental-intrusion volume for well PN3150, 2,364.5 ft, North Blowhorn Creek oil unit.

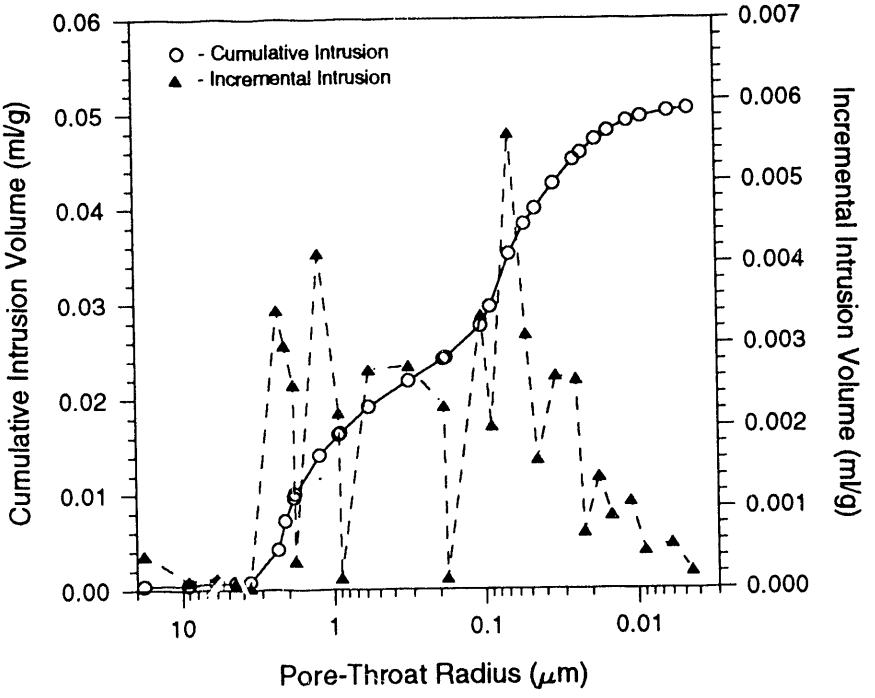

Figure 81.--Plot of pore-throat radius versus cumulative-intrusion volume and incremental-intrusion volume for well PN3160, 2,307.7 ft, North Blowhorn Creek oil unit.

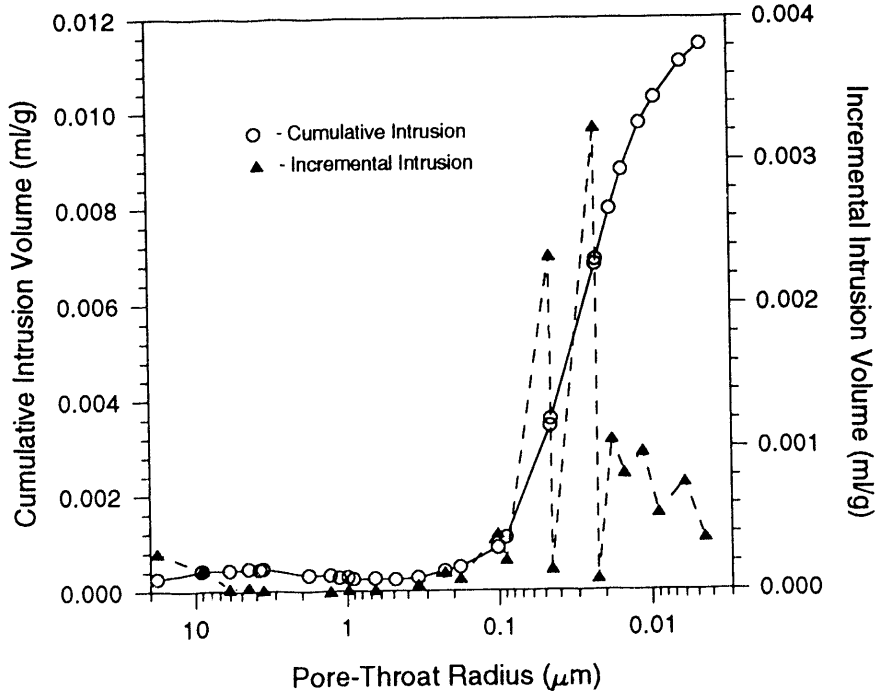

Figure 82.--Plot of pore-throat radius versus cumulative-intrusion volume and incremental-intrusion volume for well PN3150, 2,350 ft, North Blowhorn Creek oil unit.

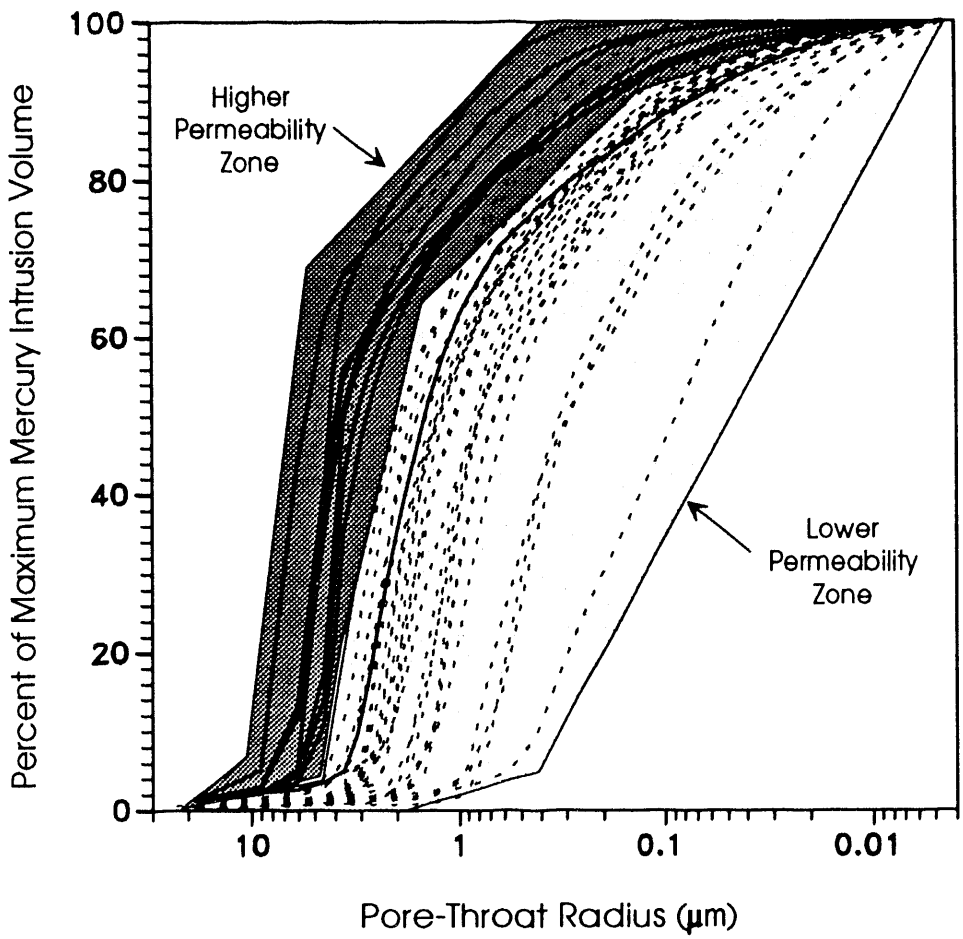

Figure 83.--Plot of pore-throat radius versus cumulative intrusion as a percent of maximum mercury intrusion volume for all data from well PN3314. Darkly shaded area encases curves for samples from the high-permeability zone at the top of the reservoir. Lightly shaded area encases curves for samples from the underlying lower permeability zone.

sample. A simple method of conveying this information on depth plots is to show a percentile range, derived from normalized cumulative-intrusion curves (fig. 86), about the median pore-throat size. Pore-throat sizes at the 16th and 84th percentiles of normalized cumulative intrusion were used in this study. Plots of this percentile range about the median pore-throat radius versus depth are shown for three wells, PN3314, PN3160, and PN3150, along the axis of the Carter beach-barrier system in North Blowhorn Creek oil unit in figures 87 through 89. Several aspects of the pore-throat system in Carter reservoir sandstone and associated nonreservoir rocks in North Blowhorn Creek oil unit are apparent in these diagrams. Nonreservoir siltstone and very fine-grained sandstone typically have median pore-throat sizes less than 0.1 μm. Replicate samples cut from the same core chip and stratigraphically closely spaced samples commonly exhibit wide variation in median pore-throat size and in the position of the median pore-throat size relative to the 16th and 84th percentiles of cumulative-intrusion volume. Petrographic data show this variation results from a complex combination of microporosity in clay filling interstitial volumes between detrital grains, patchy to pervasive carbonate-mineral cement, and poorly interconnected macropores.

Median pore-throat sizes and pore-throat size distributions are much more uniform within the Carter reservoir interval than in nonreservoir intervals (figs. 87 through 89). The median pore-throat radius of reservoir sandstone commonly is between 1 and 2 μm. This median pore-throat size is typical of shoreface and foreshore sandstone in the Carter reservoir. The larger median pore-throat sizes in

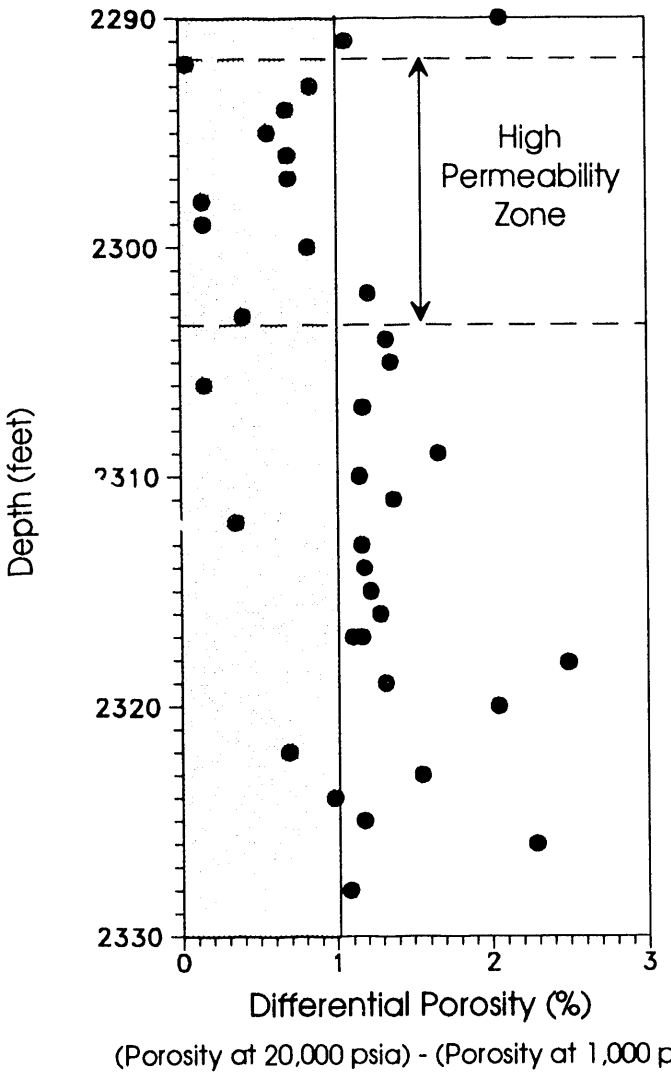

Figure 84.--Plot of differential porosity versus depth for well PN3314. Shaded area represents a difference of less than one percent between porosity calculated from the mercury intrusion volume at 20,000 psia and that calculated for the intrusion volume at 1,000 psia. Note that samples from the high-permeability zone have differential porosity of less than one percent.

the high-permeability zone in well PN3314 (fig. 87) are not common in the cored reservoir sandstone but are important in this well because sweep efficiency during waterflooding would be affected by this zone, perhaps resulting in bypassing of oil in the lower, less permeable zone, which is not separated from the upper zone by a permeability barrier. Pore-throat size distribution for replicate and stratigraphically closely spaced samples from reservoir sandstone are remarkably uniform (figs. 87 through 89). Thus, Carter reservoir sandstone in North Blowhorn Creek oil unit is relatively homogeneous in terms of median pore-throat size. Although pore-throat size distributions indicate the pore system consists of macropores connected by larger pore throats and micropores connected by small pore throats, petrographic data show that much of the micropo[illegible]in reservoir sandstone is within aggregates of authigenic and detrital clay that occupy detrital grain-size volumes (structural clay), rather than block pore throats. This structural clay may not reduce effective porosity significantly. However, anastomosing and fragmented clay drapes on ripple foresets in shoreface sequences disrupt the continuity of the interconnected pore system at the scale of heterogeneity levels 4 and 5. Figures 87 through 89 show horizons within the reservoir interval with pore-throat sizes less than 1 μm and variable pore-throat size distributions. These intervals with small pore-throat sizes have a variety of origins. Most are thin ferroan dolomite/ankerite-cemented zones, but ot[illegible]rs are within sandstone with concentrations of intrabasinal shale clasts and thin horizontal or anastomosing clay laminae. These intervals give a false impression of segmentation of the reservoir on the median pore-throat size versus depth plots. These permeability barriers typically are level- 3 to

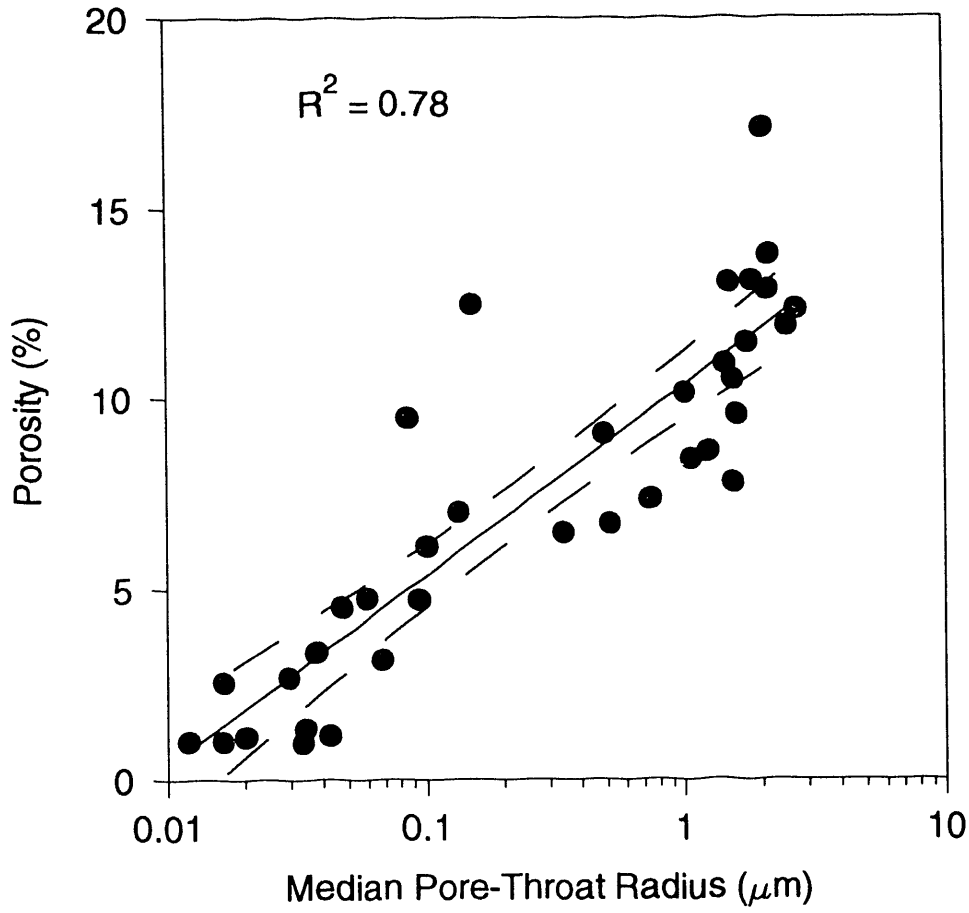

Figure 85.--Plot of median pore-throat radius versus porosity calculated from intrusion volume at 20,000 psia for well PN3160. This solid line is a linear regression line. The dashed lines enclose the 95 percent confidence interval.

4 heterogeneities that do not extend between adjacent wells; many likely extend only a few feet laterally from the well bore. Therefore, the lower permeability zones shown on the plots in figures 87 through 89 commonly are not permeability barriers that divide the reservoir into flow units. Rather, they are stratigraphically and areally localized barriers of limited lateral extent that increase tortuosity of vertical flow. However, thicker shale-siltstone intervals with small median pore-throat sizes, such as that at the top of the reservoir interval in well PN3150 (fig. 89), are barriers that may extend among wells. This backshore shale-siltstone sequence separates shoreface reservoir sandstone from an upper washover sandstone with pore-throat size distributions similar to those of the reservoir interval. Sandstone such as this is most common on the backshore or southwest side of the reservoir sandstone body in North Blowhorn Creek oil unit. The shale bodies separating these sandstones are more extensive than the thin clay laminae within the shoreface sequence and may compartmentalize or segregate the reservoir into more than one flow unit.

In summary, high-pressure mercury porosimetry shows that Carter reservoir sandstone along the axis of the spit complex in North Blowhorn Creek oil unit has a characteristic median pore-throat size of 1 to 2 μm and a uniform distribution of pore-throat sizes. High-pressure mercury porosimetry has proven to be a useful tool for characterizing the nature of the pore system in the Carter reservoir. The technique assists in characterizing the relative importance of microporosity and in determining controls on permeability contrasts within the reservoir interval. Although high-pressure mercury porosimetry is the only way to quantify pore-throat size distributions, quantifying of the spatial

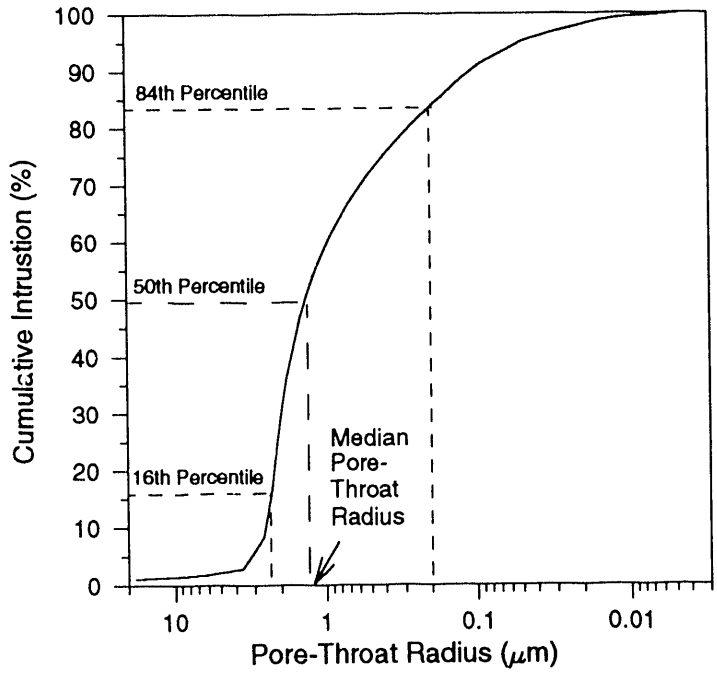

Figure 86.--Plot of pore-throat radius versus cumulative intrusion illustrating graphical method for determination of median pore-throat radius and percentile range. Cumulative intrusion is percent of total mercury-intrusion volume

distribution of pore types within individual samples requires other types of analysis. The spatial configuration of components containing microporosity can be determined by routine thin-section petrography. However, quantification of microporosity is difficult because criteria are subjective due to the small size of the pores relative to the thickness of a thin section. Quantitative image-analysis, using backscattered electron microscopy or blue-light-induced fluorescence microscopy, of pore systems shows promise for documenting the spatial distribution of pore types in reservoir sandstone and for determining their effect on reservoir properties.

HETEROGENEITY IN THE CARTER SANDSTONE RESERVOIR OF NORTH BLOWHORN CREEK OIL UNIT: IMPLICATIONS FOR IMPROVED OIL RECOVERY

Although the Carter sandstone reservoir in North Blowhorn Creek oil unit is a quartzarenite deposited in a high-energy spit complex, internal depositional and diagenetic characteristics influence the effectiveness of various improved recovery strategies, such as waterflooding, injection, strategic well placement, and infill drilling in the oil unit and have implications for recovery of hydrocarbons from similar Carter sandstone reservoirs in the Black Warrior foreland basin. Models of heterogeneity in barrier-island sandstone reservoirs are available (Sharma and others, 1990a, b), but many aspects of those models are not applicable to the localized, lensoid beach deposits of the Black Warrior basin of Alabama. In the following sections, the sedimentological, petrological, and petrophysical characteristics of the Carter sandstone reservoir in North Blowhorn Creek oil unit are synthesized with the five-level classification of heterogeneity discussed earlier in this report (fig. 3).

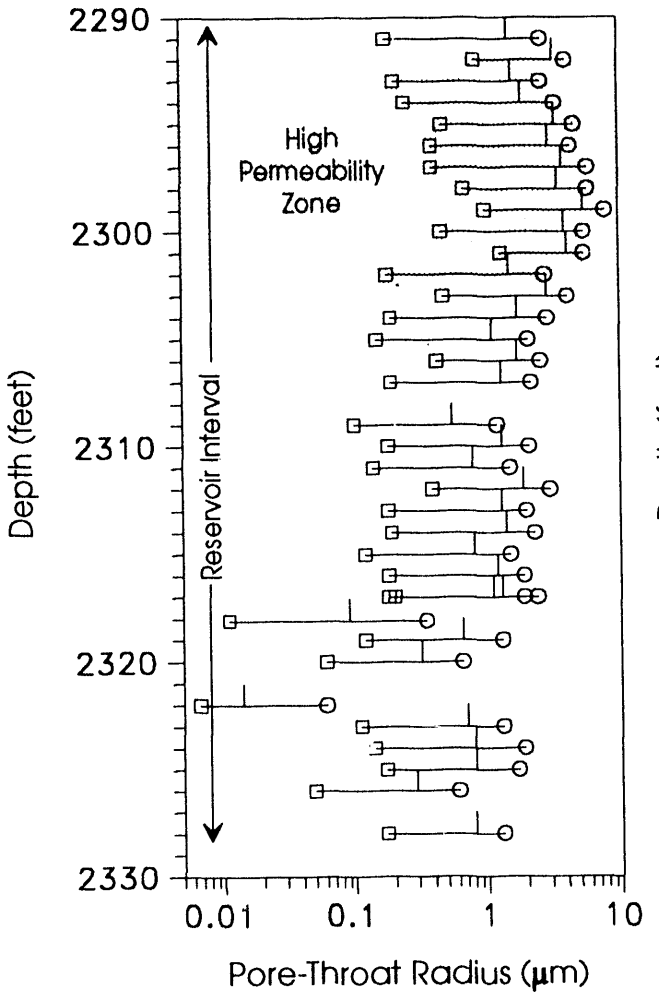

Figure 87.--Plot of pore-throat radius versus depth for well PN3314. Vertical lines represent median pore-throat radius, open circles represent the pore-throat radius at the 16th percentile, and open boxes .epresent the pore-throat radius at the 84th percentile. The high-permeability zone near the top of the reservoir is shaded.

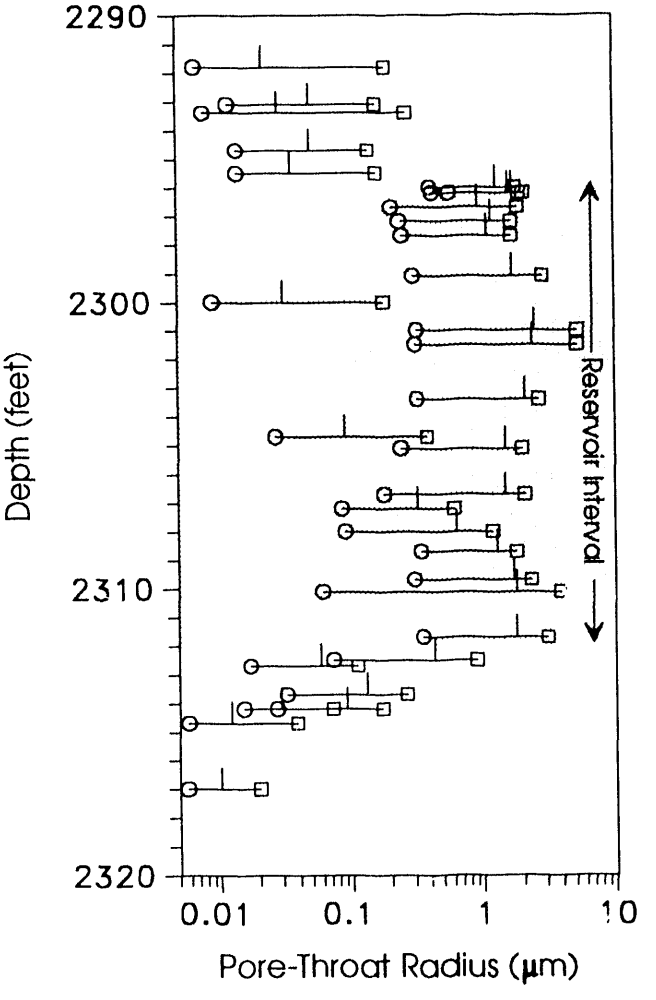

Figure 88.--Plot of pore-throat radius versus depth for well PN3160. Vertical lines represent median pore-throat radius, open circles represent the pore-throat radius at the 16th percentile, and open boxes represent the pore-throat radius at the 84th percentile. The reservoir interval is shaded.

LEVEL-1 HETEROGENEITY

In the Carter sandstone of North Blowhorn Creek oil unit, level-1 heterogeneity is a primary control on producibility of oil because the reservoir is a small, isolated body of reservoir rock composed of imbricate sandstone lenses. Thus, the Carter reservoir is vertically and laterally confined by impermeable shale. Other Carter sandstone reservoirs northeast of the Bangor platform margin are similarly isolated and confined by shale (Moore and Kugler, 1990). At the scale of level-1 heterogeneity, improved recovery operations, such as injection, can utilize the margins or reservoir sandstone bodies to confine flow and to direct migration of oil toward desired extraction points.

LEVEL-2 HETEROGENEITY

Level-2 heterogeneity, which comprises features that restrict flow and occur at the scale of a few wells, is an important and predictable component of the Carter sandstone reservoir in North Blowhorn Creek oil unit. At this scale, the Carter sandstone is not a homogeneous reservoir, but

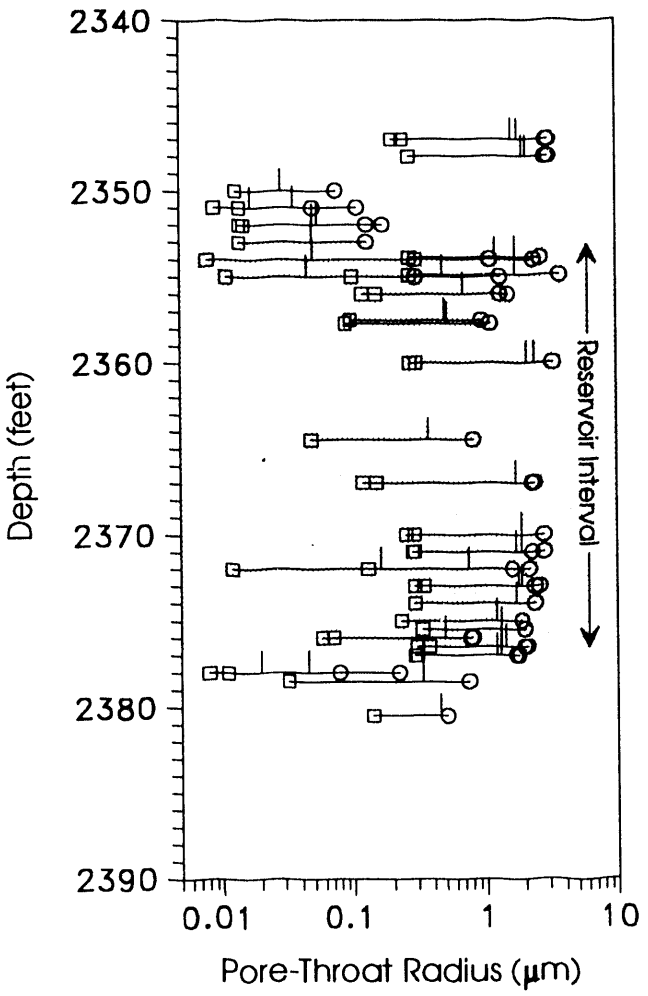

Figure 89.--Plot of pore-throat radius versus depth for well PN3150. Vertical lines represent median pore-throat radius, open circles represent the pore-throat radius at the 16th percentile, and open boxes represent the pore-throat radius at the 84th percentile. The reservoir interval is shaded.

comprises numerous sandstone lenses (figs. 12, 13). Near the depositionally downdip margin of the reservoir, amalgamated sandstone lenses are clearly joined to form a single strike-oriented flow unit with the thickest, highest quality reservoir sandstone. Depositionally updip, where facies changes are most pronounced, reservoir quality decreases as separate lenses of reservoir sandstone merge into nonreservoir facies. Thus, the Carter sandstone has a fundamental facies anisotropy that favors flow along the axis of the sandstone body.

LEVEL-3 HETEROGENEITY

In North Blowhorn Creek oil unit, level-3 or interwell heterogeneity is largely a product of facies anisotropy. Parallel to the sandstone body axis, facies generally extend among wells, thus interwell heterogeneity is of limited concern (fig. 12). Perpendicular to the axis, however, shoreface and foreshore reservoir sandstone commonly does not extend between wells (figs. 12, 13, 18). For this reason, fluids may be easier to transmit along the sandstone body axis than perpendicular to the axis. Only in the southeastern part of the oil unit where numerous spit arms were developed (figs. 12,13, 27) is interwell heterogeneity pronounced parallel to the sandstone body axis. Even bedform

distribution within the reservoir sandstone was affected by facies anisotropy. For example, shoreface and foreshore bars represented by high-angle crossbeds in the sandstone facies probably prograded shoreward only tens of feet. Along depositional strike, however, these bars may have extended for hundreds or thousands of feet.

In contrast to large-scale facies variation, subtle interwell heterogeneity exists in North Blowhorn Creek. Fine-grained, low-angle planar, crossbedded sandstone is sparse and likely is not laterally extensive. However, this sandstone is more permeable than surrounding very fine- grained sandstone because clay is less abundant and pore throats between detrital grains are larger than those in adjacent very fine-grained sandstone. Lenses of fine-grained sandstone form permeability contrasts within the reservoir rather than permeability barriers. These contrasts affect sweep efficiency by focusing flow into the most permeable lenses.

Shell accumulations localize pervasive calcite and ferroan dolomite/ankerite cement, forming permeability barriers up to 4 ft thick but with lateral extent less than the well spacing in the oil unit. These tightly cemented zones increase tortuosity of vertical flow and locally segregate horizontal flow. Stylolitized clay laminae and carbonate and kaolinite cement are common at the base of the sandstone facies. These cemented zones and pressure-solution seams prevented introduction of hydrocarbons into the lowest part of the sandstone. Thus, the base of the reservoir does not necessarily coincide with the base of the sandstone facies. Kaolinite-cemented sandstone of indeterminate lateral extent also occurs within horizons containing abundant clay laminae and shale clasts near the depositionally updip margin of the reservoir body. These kaolinite-cemented horizons increase tortuosity of vertical fluid flow.

LEVEL-4 HETEROGENEITY

Features resulting in heterogeneity at the wellbore or core scale include thin, individual to anastomosing groups of stylolitized clay laminae, lunate-ripple cross laminae, grain-size variations within laminae, intrabasinal shale chips, and kaolinite- and carbonate-cemented horizons. Within the reservoir interval, the contribution of bioturbation to heterogeneity is insignificant because burrows are sparse. Convergence of anastomosing clay laminae and clay drapes on ripple foresets increases tortuosity of flow and impounds minor amounts of oil in ripple-laminated sandstone during enhanced recovery operations. Grain-size variations within individual laminae in low-angle planar-crossbedded sandstone may result in slight differences in permeability, similar to those in eolian reservoirs (Goggin and others, 1989; Chandler and others, 1989). However, results of high-pressure mercury porosimetry indicate median pore-throat size is relatively uniform throughout the reservoir, suggesting these differences have minimal effect on recovery. Calcite and ferroan dolomite/ankerite pervasively cement thin intervals surrounding dispersed shell fragments. These intervals likely do not extend much beyond the wellbore and slightly increase tortuosity of vertical fluid flow. However, detrital grain-size clay and larger shale rip-up clasts, which are dispersed throughout the reservoir, decrease permeability disproportionately to their abundance in Carter quartzarenite.

LEVEL-5 HETEROGENEITY

Level-5 heterogeneity occurs at the scale of pores and pore throats. Although Carter reservoir sandstone is quartzarenite deposited in high-energy environments, the quality of the reservoir is affected by detrital and authigenic clay minerals. These clays are present throughout the reservoir and contribute to polymodal pore and pore-throat size distributions.

The pore system consists of diagenetically modified, effective, interconnected macropores between detrital framework grains and ineffective micropores among detrital and authigenic clays. Secondary pores formed by carbonate-cement dissolution did not enhance the effective pore system significantly. Dissolution of aluminosilicate framework grains also contributed little to the effective pore system because reaction products of dissolution of detrital feldspar were redistributed as authigenic kaolinite.

Clay minerals in Carter sandstone have high surface area to volume ratios and likely contain immobile water, which affects calculation of water saturation from resistivity logs. Well log based interpretations of reservoir parameters should acknowledge the presence of both structural and dispersed clay in the sandstone. X-ray diffraction analysis alone is inadequate to characterize the influence of kaolinite on the effective pore system in the Carter reservoir because kaolinite occurs both as a dispersed and as a structural clay. The distribution of kaolinite in Carter sandstone poses a potential migration-of-fines problem during production. Individual kaolinite plates are larger than pore throats in Carter sandstone. If these plates dislodge during production and migrate to pore throats, permeability would be reduced substantially.

SUMMARY AND CONCLUSIONS

Additional oil remains to be produced from the Black Warrior basin using improved recovery strategies, such as waterflooding, injection, strategic well placement, and infill drilling. Characterizing heterogeneity provides information regarding how those strategies may be applied effectively. This report presents accomplishments made during Task 3 of this project, which characterizes heterogeneity in the Upper Mississippian Carter sandstone reservoir in North Blowhorn Creek oil unit in Lamar County, Alabama, through sedimentologic, petrologic, and petrophysical analysis. In the first part of the report, a subsurface cross-section network is synthesized with lithofacies descriptions of cores to develop a depositional model for Carter sandstone in North Blowhorn Creek oil unit. In the second part, the detrital and diagenetic framework of the Carter reservoir is described and interpreted. This is followed by an evaluation of commercial porosity and permeability data and of the results of high-pressure mercury porosimetry. In the final part, results are synthesized with a five-level classification of reservoir heterogeneity in order to assess heterogeneities that may affect recoverability of oil in the Black Warrior basin.

North Blowhorn Creek oil unit currently is under waterflood and has 31 producing wells and 18 water-injection wells. Cumulative production through December 1990 was 4,832,247 bbls of oil, 2,781,598 Mcf of gas, and 4,488,217 bbls of water. This production represents 33 percent of the original oil in place and 67 percent of the total oil produced from the Black Warrior basin of Alabama. The Carter sandstone in North Blowhorn Creek oil unit is part of an isolated, northwest-southeast trending sandstone body that is enclosed in shale. The Carter oil reservoir in North Blowhorn Creek oil unit is contiguous with the Carter gas reservoir in the adjacent Armstrong Branch gas field to the northwest. The trapping mechanism for hydrocarbons in the combined North Blowhorn Creek oil unit/Armstrong branch gas field is stratigraphic, defined by pinchout of Carter sandstone.

Resistivity-log cross sections show that the Carter reservoir is internally complex, but varies systematically and predictably. The sandstone body has a sublinear northeast margin and an irregular southwest margin and is locally thicker than 40 ft along the axis of the body, near the northeast margin. The sandstone is not a single, homogeneous reservoir, but comprises a series of imbricate, clinoformal lenses that dip southeast and decrease in size toward the southeastern terminus of the sandstone body. Depositionally downdip parts of the reservoir have a blocky signature with high resistivity, reflecting the highest quality reservoir. Along the axis of the sandstone body, near the depositionally downdip margin, lenses are commonly amalgamated. Depositionally updip, lenses have a serrate pattern and resistivity decreases toward the southwest, reflecting decreased reservoir quality.

Cores of Carter sandstone typically have a tripartite sequence, including from bottom to top, (1) a shale-and-siltstone facies, (2) a sandstone facies, and (3) a variegated facies. The shale-and-siltstone facies, is interpreted to represent a storm-dominated shelf mud blanket that prograded across the Bangor carbonate platform. The sandstone facies, which is the principal Carter oil reservoir, represents a spectrum of beach and shoreface environments. The variegated facies, which contains lenticular sandstone, siltstone, and shale, was deposited in a suite of backshore environments which were dominated by storm surges. Sandstone-body geometry and depositional sequences indicate that the Carter sandstone in North Blowhorn Creek oil unit represents a southwestward-accreting spit

complex that was part of a muddy strand plain that developed on a former carbonate platform, just beyond the limit of major delta progradation.

Carter sandstone dominantly is very fine-grained quartzarenite, containing locally abundant, intrabasinally derived shale fragments and skeletal debris. Because of the quartzose nature of the sandstone, provenance, based on petrographic criteria, is equivocal. Authigenic minerals in Carter sandstone include, in approximate order of formation, siderite, calcite, ferroan calcite, quartz, ferroan dolomite/ankerite, and kaolinite. Pressure-solution features include stylolites along shale laminae and wispy microstylolites on foresets of ripple laminae. Hydrocarbon migration postdated precipitation of kaolinite. Authigenic minerals in Carter sandstone reflect a diagenetic evolution that began shortly after burial and continued through deep burial (>10,000 ft) and subsequent uplift to present burial depths of about 2,300 feet.

The pore system of Carter sandstone consists of effective, intergranular macropores and ineffective micropores among detrital and authigenic clay particles. Authigenic carbonate minerals occlude all pores only in the vicinity of accumulations of skeletal debris in shoreface sandstone; and calcite cement is restricted to these accumulations, suggesting that carbonate-dissolution porosity is not widespread in the reservoir. Similarly, secondary pores formed by dissolution of aluminosilicate framework grains did not enhance effective porosity because products of dissolution were redistributed locally as kaolinite.

Commercial core analyses reveal poor correlations between porosity and permeability in Carter reservoir sandstone. Average porosity of reservoir sandstone is 12 percent, and average permeability is 6.82 millidarcies. Capillary-pressure data derived from high-pressure mercury porosimetry show that pore-throat distributions in Carter sandstone are polymodal owing to a mixture of pore types. Median pore-throat size and pore-throat size distributions are highly variable in nonreservoir sandstone and siltstone, but are relatively uniform in very fine-grained reservoir sandstone, where the median pore-throat radius typically is between 0.7 to 2 μm. Fine-grained sandstone is not common, but occurs in some foreshore deposits, where median pore-throat radius is between 3 and 7 μm. Fine-grained sandstone is more permeable, by an order of magnitude or more, than very fine-grained sandstone, even though porosity is similar. Petrographic observations and pore-throat size distributions indicate that fine-grained sandstone have fewer clays than very fine-grained sandstone, in addition to having larger pore throats.

Synthesis of sedimentologic, petrologic, and petrophysical observations with heterogeneity models indicates several levels of heterogeneity in the Carter sandstone reservoir in North Blowhorn Creek oil unit. At the highest level, the reservoir is vertically and laterally confined by impermeable shale, suggesting that improved recovery operations, such as injection, could utilize the margins of the reservoir to confine flow and direct migration of oil toward desired extraction points. Near the depositionally downdip margin of the sandstone body, amalgamated shoreface and foreshore sandstone lenses clearly join to form a single flow unit that is continuous among wells along the axis of the reservoir. Depositionally updip, where facies changes are most pronounced, separate lenses of reservoir sandstone typically do not extend between wells and merge into nonreservoir, backshore siltstone and shale. This fundamental facies anisotropy suggests fluids may be transmitted more easily along the axis of the sandstone body than perpendicular to the axis. Bedform distribution within reservoir sandstone is also affected by facies anisotropy. Shoreface and foreshore bars probably prograded shoreward only tens of feet, but extended hundreds or thousands of feet along depositional strike.

Lenses of fine-grained sandstone, although sparse and not laterally extensive, are more permeable than adjacent very fine-grained sandstone. These lenses form permeability contrasts that affect sweep efficiency by focusing flow into the most permeable intervals. Accumulations of skeletal debris localize zones of pervasive calcite and ferroan dolomite/ankerite cement that form barriers to vertical fluid flow and do not extend between wells. Within shoreface sandstone, convergence of anastomosing clay laminae and clay drapes on ripple foresets increases tortuosity of flow and impounds minor amounts of oil during enhanced recovery operations. Clay minerals in Carter sandstone have high surface area to volume ratios and likely contain immobile water, which affects calculation of water saturation from resistivity logs. Well-log based interpretations of reservoir parameters should acknowledge the presence of both structural and dispersed clays in the sandstone.

The distribution of kaolinite in Carter sandstone poses a potential migration-of-fines problem during improved-recovery operations.

The localized, lensoid nature of Carter sandstone reservoirs differs greatly from the widespread beach-barrier sandstone bodies that have formed the basis of previous sandstone-heterogeneity models. Therefore, results of this study provide a template for recognizing heterogeneity that will be useful in implementing improved-recovery strategies, not only for oil reservoirs in the Black Warrior basin, but in other sedimentary basins as well.

REFERENCES CITED

Aigner, Thomas, and Reineck, H.-E., 1982, Proximality trends in modern storm sands from the Helgoland Bight (North Sea) and their implications for basin analysis: Senckenbergiana Maritima, v. 14, p. 183-215.

Almon, W.R., and Davies, D.K., 1981, Formation damage and the crystal chemistry of clays, *in* Longstaffe, F.J., ed., Clays and the resource geologist: Mineralogical Association of Canada, p. 81-103.

Bat, D.T., 1987, A subsurface facies analysis of the distribution, depositional environments, and diagenetic overprint of the Evans and Lewis sandstone units in north Mississippi and northwestern Alabama: Stillwater, Oklahoma State University, unpublished Master's thesis, 225 p.

Bearden, B.L., 1984, Hydrocarbon trapping mechanisms in the Carter sandstone (Upper Mississippian) in the Black Warrior basin, Fayette and Lamar Counties, Alabama: Tuscaloosa, University of Alabama, unpublished Master's thesis, 195 p.

_____ 1985, Hydrocarbon trapping mechanisms in the Carter sandstone (Upper Mississippian) in the Black Warrior basin of Alabama: Alabama State Oil and Gas Board Oil and Gas Report 9, 50 p.

Bearden, B.L., and Mancini, E.A., 1985, Petroleum geology of the Carter sandstone (Upper Mississippian) in the Black Warrior basin of Alabama: American Association of Petroleum Geologists Bulletin, v. 69, p. 361-377.

Beaumont, Christopher, Quinlan, G.M., and Hamilton, Juliet, 1987, The Alleghanian orogeny and its relationship to the evolution of the eastern interior, North America: Canadian Society of Petroleum Geologists Memoir 12, p. 425-445.

_____ 1988, Orogeny and stratigraphy: numerical models of the Paleozoic in the eastern interior of North America: Tectonics, v. 7, p. 389-416.

Berner, R.A., 1981, A new geochemical classification of sedimentary environments: Journal of Sedimentary Petrology, v. 51, p. 359-365.

Bjørlykke, Knut, 1984, Formation of secondary porosity: how important is it? *in* McDonald, D.A., and Surdam, R.C., eds., Clastic diagenesis: American Association of Petroleum Geologists Memoir 37, p. 277-286.

Blatt, Harvey, 1982, Sedimentary petrology: New York, W.H. Freeman and Company, 564 p.

Bloch, Salman, 1991, Empirical prediction of porosity and permeability in sandstones: American Association of Petroleum Geologists Bulletin, v. 75, p. 1145-1160.

Boles, J.R., 1978, Active ankerite cementation in the subsurface Eocene of southwest Texas: Contributions to Mineralogy and Petrology, v. 68, p. 13-22.

Boles, J.R., and Franks, S.G., 1979, Clay diagenesis in Wilcox sandstones of southwest Texas: Journal of Sedimentary Petrology, v. 49, p. 55-70.

Boothroyd, J.C., 1985, Tidal inlets and tidal deltas, *in* Davis, R.A., Jr., ed., Coastal sedimentary environments (2nd ed.): New York, Springer-Verlag, p. 445-532.

Burley, S.D., and Kantorowicz, J.D., 1986, Thin section and S.E.M. textural criteria for the recognition of cement-dissolution porosity in sandstones: Sedimentology, v. 33, p. 587-604.

Chandler, M.A., Kocurek, Gary, Goggin, D.J., and Lake, L.W., 1989, Effects of stratigraphic heterogeneity on permeability in an eolian sandstone sequence, Page Sandstone, north Arizona: American Association of Petroleum Geologists Bulletin, v. 73, p. 658-668.

Cleaves, A. W., 1981, Resource evaluation of Lower Pennsylvanian (Pottsville) depositional systems of the western Warrior coal field, Alabama and Mississippi: Mississippi Mineral Resources Institute Final Technical Report no. 81-1, 125 p.

_____ 1983, Carboniferous terrigenous clastic facies, hydrocarbon producing zones, and sandstone provenance, northern shelf of Black Warrior basin: Gulf Coast Association of Geological Societies Transactions, v. 33, p. 41-53.

Cleaves, A.W., and Bat, D.T., 1988, Terrigenous clastic facies distribution and sandstone diagenesis, subsurface Lewis and Evans format units (Chester series), on the northern shelf of the Black Warrior basin: Gulf Coast Association of Geological Societies Transactions, v. 38, p. 177-186.

Cleaves, A.W., and Broussard, M.C., 1980, Chester and Pottsville depositional systems, outcrop and subsurface, in the Black Warrior basin of Mississippi and Alabama: Gulf Coast Association of Geological Societies Transactions, v. 33, p. 41-53.

Clifton, H.E., 1976, Wave-formed sedimentary structures -- a conceptual model: Society of Economic Paleontologists and Mineralogists Special Publication 24, p. 126-148.

Davidson-Arnott, R.G.D., and Greenwood, Brian, 1976, Facies relationships on a barred coast, Kouchibougac Bay, New Brunswick, Canada: Society of Economic Paleontologists and Mineralogists Special Publication 24, p. 149-168.

Davis, R.A., Fox, W.T., Hayes, M.O., and Boothroyd, J.C., 1972, Comparison of ridge and runnel systems in tidal and non-tidal environments: Journal of Sedimentary Petrology, v. 42, p. 413-421.

Dickinson, W.R., 1970, Interpreting detrital modes of graywacke and arkose: Journal of Sedimentary Petrology, v. 40, p. 695-707.

_____ 1985, Interpreting provenance relations from detrital modes of sandstone, *in* Zuffa, G.G., ed., Provenance of arenites: Boston, D. Reidel Publishing Company, p. 333-361.

Dickinson, W.R., and Suczek, C.A., 1979, Plate tectonics and sandstone compositions: American Association of Petroleum Geologists Bulletin, v. 63, p. 2164-2182.

Dickinson, W.R., Beard, L.S., Brakenridge, G.R., Erjavec, J.L., Ferguson, R.C., Inman, K.F., Knepp, R.A., Lindberg, F.A., and Ryberg, P.T., 1983, Provenance of North American Phanerozoic sandstone in relation to tectonic setting: Geological Society of America Bulletin, v. 94, p. 222-235.

Dullien, F.A.L., and Dhawan, G.K., 1974, Characterization of pore structure by a combination of quantitative photomicrography and mercury porosimetry: Journal of Colloid and Interface Science, v. 47, p. 337-349.

Elliott, Trevor, 1986, Siliciclastic shorelines, *in* Reading, H.G., ed., Sedimentary environments and facies (2nd ed.): Oxford, Blackwell Scientific Publications, p. 155-188.

Epsman, M.L., 1987, Subsurface geology of selected oil and gas fields in the Black Warrior basin of Alabama: Alabama Geological Survey Atlas 21, 255 p.

Evamy, B.D., 1963, The application of a chemical staining technique to a study of dedolomitization; Sedimentology, v. 2, p. 164-170.

Fairbridge, R.W., 1980, The estuary: its definition and geodynamic cycle, *in* Olausson, E., and Cato, I., eds., Chemistry and biogeochemistry of estuaries, p. 1-36.

Folk, R.L., 1980, Petrology of sedimentary rocks: Austin, Texas, Hemphill Publishing Company, 182 p.

Franzinelli, Elena, and Potter, P.E., 1983, Petrology, chemistry, and texture of modern river sands, Amazon River system: Journal of Geology, v. 91, p. 23-39.

Frost, Elton, and Fertl, W.H., 1981, Integrated core and log analysis concepts in shaly clastic reservoirs: The Log Analyst, v. 32, no. 2, p. 3-16.

Giles, M.R., 1987, Mass transfer and problems of secondary porosity creation in deeply buried hydrocarbon reservoirs: Marine and Petroleum Geology, v. 4, p. 188-204.

Giles, M.R., and de Boer, R.B., 1990, Origin and significance of redistributional secondary porosity: Marine and Petroleum Geology, v. 7, p. 378-397.

Goggin, D.J., Chandler, M.A., Kocurek, Gary, and Lake, L.W., 1989, Permeability transects in eolian sands and their use in generating random permeability trends: Society of Petroleum Engineers, v. 64, p. 149-164.

Gould, H.R., and McFarlan, E., 1959, Geological history of the chenier plain, southwestern Louisiana: Gulf Coast Association of Geological Societies Transactions, v. 9, p. 261-270.

Harper, T.R., and Buller, D.C., 1986, Formation damage and remedial stimulation: Clay Minerals, v. 21, p. 735-751.

Hayes, M.O., 1967, Hurricanes as geological agents: case studies of Hurricane Carla, 1961, and Cindy, 1963: Texas Bureau of Economic Geology Report of Investigations 61, 54 p.

Hines, R.A., Jr., 1988, Carboniferous evolution of the Black Warrior foreland basin, Alabama and Mississippi: Tuscaloosa, University of Alabama, unpublished Doctoral dissertation, 231 p.

Holmes, J.W., 1981, The depositional environment of the Mississippian Lewis sandstone in the Black Warrior basin of Alabama: Tuscaloosa, University of Alabama, unpublished Master's thesis, 172 p.

Howard, R.O., Jr., 1990, Petrology of hardbottom rocks, Mississippi-Alabama-Florida continental shelf: Tuscaloosa, University of Alabama, unpublished Master's thesis, 122 p.

Hughes, S.B., and Meylan, M.A., 1988, Petrology and hydrocarbon reservoir potential of Mississippian (Chesterian) sandstones, Black Warrior basin, Mississippi: Gulf Coast Association of Geological Societies Transactions, v. 38, p. 167-176.

Hurst, Andrew, and Archer, J.S., 1986, Sandstone reservoir description: An overview of the role of geology and mineralogy: Clay Minerals, v. 21, p. 791-809.

Jennings, J.B., 1987, Capillary.pressure techniques: application to exploration and development geology: American Association of Petroleum Geologists Bulletin, v. 71, p. 1196-1209.

Jonas, E.D., and McBride, E.F., 1977, Diagenesis of sandstone and shale: application to exploration for hydrocarbons: Austin, University of Texas Continuing Education Program Publication Number 1, 120 p.

Kantorowicz, J.D., Lievaart, L., Eylander, J.G.R., and Eigner, M.R.P., 1986, The role of diagenetic studies in production operations: Clay Minerals, v. 21, p. 769-780.

Keller, W.D., 1976a, Scan electron micrographs of kaolins collected from diverse environments of origin, Pt I: Clays and Clay Minerals, v. 24, p. 107-113.

_____ 1976b, Scan electron micrographs of kaolins collected from diverse environments of origin, Pt. II: Clays and Clay Minerals, v. 24, p. 114-117.

_____ 1976c, Scan electron micrographs of kaolins collected from diverse environments of origin, Pt. III: Clays and Clay Minerals, v. 24, p. 262-264.

_____ 1977a, Scan electron micrographs of kaolins collected from diverse environments of origin, Pt. IV: Clays and Clay Minerals, v. 25, p. 311-346.

_____ 1977b, Scan electron micrographs of kaolins collected from diverse environments of origin, Pt. V: Clays and Clay Minerals, v. 25, p. 347-364.

Kidd, J.T., 1976, Configuration of the top of the Pottsville Formation in west-central Alabama: Alabama State Oil and Gas Board Oil and Gas Map 1.

Klitgord, K.D., Dillon, W.P., and Popenoe, Peter, 1983, Mesozoic tectonics of the southeastern United States coastal plain and continental margin: U.S. Geological Survey Professional Paper 1313-P, 15 p.

Kopaska-Merkel, D.C., 1991, Analytical procedure and experimental design for geological analysis of reservoir heterogeneity using mercury porosimetry: Alabama Geological Survey Circular 153, 29 p.

Kopaska-Merkel, D.C., and Friedman, G.M., 1989, Petrofacies analysis of carbonate rocks; example from Lower Paleozoic Hunton Group of Oklahoma and Texas: American Association of Petroleum Geologists Bulletin, v. 73, p. 1289-1306.

Krueger, R.F., 1986, An overview of formation damage and well productivity in oilfield operations: Journal of Petroleum Technology, v. 38, p. 131-152.

Lake, L.W., Carroll, H.B., Jr., and Wesson, T.C., eds., 1991, Reservoir characterization II: Orlando, Florida, Academic Press, Inc., 726 p.

Land, L.S., Milliken, K.L., and McBride, E.F., 1987, Diagenetic evolution of Cenozoic sandstones, Gulf of Mexico sedimentary basin: Sedimentary Geology, v. 50, p. 195-225.

Larese, R.E., and Pittman, E.D., 1987, Indirect evidence of secondary porosity in sandstones [abs.]: American Association of Petroleum Geologists Bulletin, v. 71, p. 581.

Loukes, R.G., Dodge, M.M., and Galloway, W.E., 1984, Regional controls on diagenesis and reservoir quality in Lower Tertiary sandstones along the Texas Gulf Coast, *in* McDonald, D.A., and Surdam, R.C., eds., Clastic Diagenesis, American Association of Petroleum Geologists Memoir 37, p. 15-45.

Lundegard, P.D., and Land, L.S., 1986, Carbon dioxide and organic acids: their role in porosity enhancement and cementation, Paleogene of the Texas Gulf Coast, *in* Gautier, D.L., ed., Roles of organic matter in sediment diagenesis: Society of Economic Paleontologists and Mineralogists Special Publication 38, p. 129-146.

Mack, G.H., 1978, The survivability of labile light-mineral grains in fluvial, aeolian, and littoral marine environments in the Permian Cutler and Cedar Mesa formations, Moab, Utah: Sedimentology, v. 25, p. 587-604.

Mack, G.H., 1984, Exceptions to the relationship between plate tectonics and sandstone composition: Journal of Sedimentary Petrology, v. 54, p. 212-220.

Mack, G.H., James, W.C., and Thomas, W.A., 1981, Orogenic provenance of Mississippian sandstones associated with southern Appalachian-Ouachita orogen: American Association of Petroleum Geologists, v. 65, p. 1444-1456.

Mack, G.H., Thomas, W.A., and Horsey, C.A., 1983, Composition of Carboniferous sandstones and tectonic framework of southern Appalachian-Ouachita orogen: Journal of Sedimentary Petrology, v. 53, p. 931-946.

McBride, E.F., 1984, Rules of sandstone diagenesis related to reservoir quality: Gulf Coast Association of Geological Societies Transactions, v. 34, p. 137-139.

——1987, Diagenesis of the Maxon sandstone (Early Cretaceous), Marathon region, Texas: a diagenetic quartzarenite: Journal of Sedimentary Petrology, v. 57, p. 98-107.

McCubbin, D.G., 1982, Barrier-island and strand-plain facies: American Association of Petroleum Geologists Memoir 31, p. 247-279.

Mellen, F.F., 1947, Black Warrior basin, Alabama and Mississippi: American Association of Petroleum Geologists Bulletin, v. 31, p. 1801-1816.

Miller, J.A., 1975, Facies characteristics of Laguna Madre wind-tidal flats, *in* Ginsburg, R.N., ed., Tidal deposits; a casebook of recent examples and fossil counterparts: New York, Springer-Verlag, p. 67-73.

Milliken, K.L., 1988, Loss of provenance information through subsurface diagenesis in Plio-Pleistocene sandstones, northern Gulf of Mexico: Journal of Sedimentary Petrology, v. 58, p. 992-1002.

Milliken, K.L., McBride, E.F., and Land, L.S., 1989, Numerical assessment of dissolution versus replacement in the subsurface destruction of detrital feldspars, Oligocene Frio Formation, south Texas: Journal of Sedimentary Petrology, v. 59, p. 740-757.

Milliken, K.L., and Mack, L.E., 1990, Subsurface dissolution of heavy minerals, Frio Formation sandstones of the ancestral Rio Grande Province, south Texas; Sedimentary Geology, v. 68, p. 187-199.

Moore, H.E., and Kugler, R.L., 1990, Determination of reservoir heterogeneity in the Mississippian Carter sandstone to improve hydrocarbon recovery in oil fields in the Black Warrior basin: Alabama Department of Economic and Community Affairs, Contract 1STE89 06, 291 p.

Morton, A.C., 1985, Heavy minerals in provenance studies *in* Zuffa, G.G., ed., Provenance of arenites: Boston, D. Reidel Publishing Company, p. 249-277.

Mozley, P.S., 1989, Complex compositional zonation in concretionary siderite: Implications for geochemical studies: Journal of Sedimentary Petrology, v. 59, p. 815-818.

Neesham, J.W., 1977, The morphology of dispersed clay in sandstone reservoirs and its effect on sandstone shaliness, pore space, and fluid flow properties: Society of Petroleum Engineers 6858, 52nd American Institute of Mining Engineers Fall Symposium, Denver, Colorado.

Nix, M.A., 1986, Facies within the lower part of the Parkwood Formation in the Black Warrior basin of Mississippi and Alabama: Appalachian Basin Industrial Associates Fall Program, v. 11, p. 93-107.

——1991, Facies and facies relationships of the lower part of the Parkwood Formation in the Black Warrior basin of Mississippi and Alabama: Tuscaloosa, University of Alabama, unpublished Master's thesis, 362 p.

Owen, M.R., and Carozzi, A.V., 1986, Southern provenance of upper Jackfork Sandstone, southern Ouachita Mountains, cathodoluminescence petrology: Geological Society of America Bulletin, v. 97, p. 110-115.

Pashin, J.C., 1991, Regional analysis of the Black Creek-Cobb coalbed-methane target interval, Black Warrior basin, Alabama: Alabama Geological Survey Bulletin 145, 127p.

Pashin, J.C., and Ettensohn, F.R., 1987, An epeiric shelf-to-basin transition: Bedford-Berea sequence, northeastern Kentucky and south-central Ohio: American Journal of Science, v. 287, p. 893-926.

Pashin, J.C., Osborne, W.E., and Rindsberg, A.K., 1991, Outcrop characterization of sandstone heterogeneity in Carboniferous reservoirs, Black Warrior basin, Alabama: U.S. Department of Energy, Contract Report DOE/BC/14448-6, 126 p.

Penland, Shea, and Boyd, Ron, 1985, Barrier island arcs along abandoned Mississippi River deltas: Marine Geology, v. 63, p. 197-233.

Pettijohn, F.J., 1941, Persistence of heavy minerals with geologic age: Journal of Geology, v. 49, p. 612-625.

Pittman, E.D., 1979, Porosity, diagenesis and productive capability of sandstone reservoirs, *in* Scholle, P.A., and Schluger, P.R., eds., Aspects of diagenesis: Society of Economic Paleontologists and Mineralogists Special Publication No. 26, p. 159-173.

Purcell, W.R., 1949, Capillary-pressures -- their measurement using mercury and the calculation of permeability therefrom: Petroleum Transactions, American Institute of Mining, Metallurgical, and Petroleum Engineers, v. 186, p. 39-48.

Raymond, D.E., 1990, Petrography of sandstones of the Pottsville Formation in the Jasper Quadrangle, Black Warrior basin, Alabama: Alabama Geological Survey Circular 144, 48 p.

Reineck, H-.E., and Singh, I.B., 1980, Depositional sedimentary environments, with reference to terrigenous clastics (2nd ed.); New York, Springer-Verlag, 549 p.

Rheams, K.F., and Neathery, T.L., 1988, Characterization and geochemistry of Devonian oil shale, north Alabama, northwest Georgia, and south-central Tennessee (a resource evaluation): Alabama Geological Survey Bulletin 128, 214 p.

Robertson Research (U.S.), Inc., 1985, Oil generation in the Black Warrior basin, Alabama: a geochemical study: Kingwood, Texas, 328 p.

Ryder, R.T., 1987, Oil and gas resources of the Black Warrior basin, Alabama and Mississippi: United States Geological Survey Open-file report 87-450, 23 p.

Scherer, M., 1987, Parameters influencing porosity in sandstone: a model for sandstone porosity prediction: American Association of Petroleum Geologists Bulletin, v. 71, p. 485-491.

Schmidt, Volkmar, and McDonald, D.A., 1979, Texture and recognition of secondary porosity in sandstones, *in* Scholle, P.A., and Schluger, P.R., eds., Aspects of diagenesis: Society of Economic Paleontologists and Mineralogists Special Publication no. 26, p. 209-225.

Selley, R.C., 1978, Porosity gradients in North Sea oil-bearing sandstone: Journal of the Geological Society of London, v. 135, p. 119-132.

Sharma, Bijon, Honarpour, M.M., Szpakiewicz, M.J., and Schatzinger, R.A., 1990a, Critical heterogeneities in a barrier island deposit and their influence on various recovery processes: Society of Professional Engineers Formation Evaluation, v. 5, p. 103-112.

Sharma, Bijon., Honarpour, M.M., Jackson, S.R., Schatzinger, R.A., and Tomutsa, Liviu, 1990b, Determining the productivity of a barrier island sandstone deposit from integrated facies analysis: Society of Professional Engineers Formation Evaluation, v. 5, p. 413-420.

Shepard, B.K., 1979, Petrography and environment of deposition of the Carter sandstone (Mississippian) in the Black Warrior basin of Alabama and Mississippi: Tuscaloosa, University of Alabama, unpublished Master's thesis, 196 p.

Smith, W.E., 1986, Geomorphology of coastal Baldwin County, Alabama: Alabama Geological Survey Bulletin 124, 86 p.

Thomas, W.A., 1972, Mississippian stratigraphy of Alabama: Alabama Geological Survey Monograph 12, 121 p.

_____ 1976, Evolution of the Appalachian-Ouachita continental margin: Journal of Geology, v. 84, p. 323-342.

_____ 1977, Evolution of the Appalachian-Ouachita salients and recesses from reentrants and promontories in the continental margin: American Journal of Science, v. 277, p. 1233-1278.

_____ 1985, The Appalachian-Ouachita connection: Paleozoic orogenic belt at the southern margin of North America: Annual Review of Earth and Planetary Sciences, v. 13, p. 175-199.

_____ 1988a, The Black Warrior basin, *in* Sloss, L.L., ed., Sedimentary cover -- North American craton: Geological Society of America, The Geology of North America, v. D-2, p. 471-476.

_____ 1988b, Early Mesozoic faults of the northern Gulf Coastal Plain in the context of opening the Atlantic Ocean, *in* Manspeizer, W., ed., Triassic-Jurassic Rifting: New York, Elsevier, p. 463-476.

_____ 1991, The Appalachian-Ouachita rifted margin of southeastern North America: Geological Society of America Bulletin, v. 103, p. 415-431.

Thompson, W.O., 1937, Original structures of beaches, bars, and dunes: Geological Society of America Bulletin, v. 48, p. 723-752.

Walton, A.W., Bouquet, D.J., Evenson, R.A., Rofheart, D.H., and Woody, M.D., 1986, Characterization of sandstone reservoirs in the Cherokee Group (Pennsylvanian, Desmoinsian) of southeastern Kansas, *in* Lake, L.W., and Carroll, H.B., Jr., eds., Reservoir characterization: Orlando, Florida, Academic Press, Inc., p. 39-61.

Wardlaw, N.C., 1976, Pore geometry of carbonate rocks as revealed by pore casts and capillary pressure: American Association of Petroleum Geologists Bulletin, v. 60, p. 245-257.

Wardlaw, N.C., McKellar, Malcolm, and Yu, Li, 1988, Pore and throat size distributions determined by mercury porosimetry and by direct observation: Carbonates and Evaporites, v. 3, p. 1-16.

Weber, K.J., 1986, How heterogeneity affects oil recovery, *in* Lake, L.W., and Carroll, H.B., Jr., eds., Reservoir characterization: Orlando, Florida, Academic Press, Inc., p. 181-222.

Welch, S.W., ed., 1978, Mississippian rocks of the Black Warrior basin -- a field guide: Mississippi Geological Society, 17th Annual Field Trip Guidebook, 79 p.

Wells, J.T., and Coleman, J.M., 1981, Physical processes and fine-grained sediment dynamics, coast of Surinam, South America: Journal of Sedimentary Petrology, v. 51, p. 1053-1068.

Wilson, G.V., 1987, Characteristics and resource evaluation of the asphalt and bitumen deposits of northern Alabama: Alabama Geological Survey Bulletin 111, 110 p.

Young, S.W., 1976, Petrographic textures of detrital polycrystalline quartz as an aid to interpreting crystalline source rocks: Journal of Sedimentary Petrology, v. 46, p. 595-603.

Zuffa, G.G., 1985, Optical analyses of arenites: Influence of methodology on compositional results, *in* Zuffa, G.G., ed., Provenance of Arenites: Boston, D. Reidel Publishing Company, p. 165-189.

*U.S.GPO:1992-661-026/60026

DATE
FILMED
07/8/92